

Electronic Thesis and Dissertation Repository

---

8-13-2014 12:00 AM

## ILK modulates stress-induced apoptosis in epidermal keratinocytes

Michelle Im, *The University of Western Ontario*

Supervisor: Dr. Lina Dagnino, *The University of Western Ontario*

A thesis submitted in partial fulfillment of the requirements for the Master of Science degree in Physiology

© Michelle Im 2014

Follow this and additional works at: <https://ir.lib.uwo.ca/etd>



Part of the [Cellular and Molecular Physiology Commons](#), and the [Laboratory and Basic Science Research Commons](#)

---

### Recommended Citation

Im, Michelle, "ILK modulates stress-induced apoptosis in epidermal keratinocytes" (2014). *Electronic Thesis and Dissertation Repository*. 2208.  
<https://ir.lib.uwo.ca/etd/2208>

This Dissertation/Thesis is brought to you for free and open access by Scholarship@Western. It has been accepted for inclusion in Electronic Thesis and Dissertation Repository by an authorized administrator of Scholarship@Western. For more information, please contact [wlsadmin@uwo.ca](mailto:wlsadmin@uwo.ca).

ILK modulates stress-induced apoptosis in epidermal keratinocytes

(Thesis format: Monograph)

by

Michelle Im

Graduate Program in Physiology and Pharmacology

A thesis submitted in partial fulfillment  
of the requirements for the degree of  
Master of Science

The School of Graduate and Postdoctoral Studies  
The University of Western Ontario  
London, Ontario, Canada

© Michelle Im, August 2014

## **Abstract**

Integrin-linked kinase (ILK) is a ubiquitous scaffold protein that mediates cellular responses to integrin stimulation by extracellular matrix proteins. Mice with inactivation of the *Ilk* gene in squamous epithelia display defects in skin regeneration after injury, failure to thrive, and perinatal death. ILK-deficient epidermis exhibits reduced adhesion to the basement membrane and impaired hair follicle morphogenesis. In culture, ILK-deficient keratinocytes fail to attach and spread efficiently, and demonstrate decreased survival. We now show that ILK-deficient keratinocytes exhibit a lower proliferative capacity and increased apoptosis in the absence or presence of growth factors. This reduced viability appears to be independent of the Akt pathway, as ILK-deficient cells exhibit normal levels of active, phosphorylated Akt. They do, however, display higher levels of cleaved caspase-3 and PARP, both associated with caspase-dependent programmed cell death. We have also observed an increase in  $\gamma$ H2A.X, a marker of DNA double-strand breaks, which is also associated with increased levels of reactive oxygen species (ROS) in these cells. Thus, increased susceptibility to DNA damage due an increase in ROS may lead to decreased cell survival. Our findings underline a distinct, novel role for ILK in promoting keratinocyte survival and a normal redox state.

## **Keywords**

Integrin-linked kinase, epidermis, keratinocytes, caspases, DNA damage, apoptosis, intrinsic pathway, reactive oxygen species, cell survival, proliferation

## **Co-Authorship Statement**

All experiments were completed by me throughout my graduate degree except for the measurement of apoptosis, which was performed by T.S. Irvine.

## **Acknowledgments**

I would like to, first and foremost, thank Dr. Lina Dagnino for her constant support and understanding throughout my time in her laboratory. From having zero knowledge on skin physiology and minimal encounters with pipettes, her patience and guidance have helped me grow immensely, both as a student and a researcher. Thank you for pushing me to learn the merits of critical thinking and teaching me that there is no such thing as failure in experimental findings. It was through your advice and direction that I have found my graduate experience so rewarding.

Next, I would like to thank all members of my advisory committee, Dr. Sean Cregan and Dr. Moshmi Bhattacharya, for their helpful suggestions and supervision. Their constructive feedback and proposals at each committee meeting allowed me to design new experiments and ideas that only strengthened the final outcome of my project.

I would also like to thank the very core of my research experience – present and former members of the Dagnino laboratory. Thank you to my big sister, Randeep Singh for calming me down before committee meetings and knocking some sense into me during my debilitating times of stress. Thank you to my other big sister, Stellar Boo, for her guidance, encouragement, and at times, unrelenting sass that made my time in the laboratory thoroughly entertaining. I would also like to thank Samar Sayedyahosseini for teaching me that the sky is always high and never to give up. You are ah-mazing. Thank you to Dr. Alena Rudkouskaya for always challenging me to stay positive and scolding me to live life without stress and to always stay in the moment. I cannot forget my lab mom, Meera Karajgikar, for having the most contagious laugh and always accompanying me on those long trips to

Robert's. Maria Doubova, thank you for always brightening my gloomy days in the lab with your laughter and sarcasm. Ladies, our tea times together will always remain my best memories of the lab. I would also like to thank big brother Tames for teaching me everything I know about laboratory technique and laughing at my snowy blots. Your constant advice and experience helped me brave my fear of experimental design and allowed me to finally detach that umbilical cord. Thank you to my clutter-free benchmate, Bradley Jackson, for your constant jokes and laughter and honouring me with the occasional presence of your gangster alter ego. Uncle Kevin, thank you for bringing back such an overwhelming source of humour, wit, and (at times, terrible) impressions and accents into my life.

And last but certainly not least, I would like to thank my family. My parents, grandparents, Wephanie, Davey Boy, Johnny and Julie – I cannot begin to express my appreciation for your endless support and encouragement throughout my highs and lows of this experience. Thank you for always just knowing what to say. You have been such a blessing in my life and I could not have done this without you.

# Table of Contents

<b>Abstract</b> .....	ii
<b>Co-Authorship Statement</b> .....	iii
<b>Acknowledgments</b> .....	iv
<b>Table of Contents</b> .....	vi
<b>List of Tables</b> .....	ix
<b>List of Figures</b> .....	x
<b>Chapter 1 – Introduction</b> .....	1
<b>1.1 Architecture of the skin</b> .....	1
<b>1.1.1 The epidermis</b> .....	1
<b>1.2 Keratinocyte survival and programmed cell death</b> .....	4
<b>1.2.1 Types of cell death</b> .....	4
<b>1.2.2 Apoptosis in the epidermis</b> .....	6
<b>1.2.3 Extrinsic vs. intrinsic apoptosis pathway</b> .....	6
<b>1.3 Reactive oxygen species</b> .....	11
<b>1.3.1 Sources of ROS</b> .....	13
<b>1.3.2 ROS in keratinocytes</b> .....	13
<b>1.3.3 Stress-induced apoptosis</b> .....	15
<b>1.4 Integrins</b> .....	16
<b>1.4.1 Integrins and epidermal homeostasis</b> .....	18
<b>1.5 Integrin-linked kinase</b> .....	18
<b>1.5.1 ILK as a pseudokinase</b> .....	19
<b>1.5.2 ILK in different cell types</b> .....	25
<b>1.5.3 ILK in the epidermis</b> .....	25
<b>1.5.4 The role of ILK in cell survival</b> .....	26

<b>1.6 Rationale and hypothesis</b> .....	27
<b>Chapter 2 – Materials and Methods</b> .....	29
<b>2.1 Reagents</b> .....	29
<b>2.2 Antibodies</b> .....	31
<b>2.3 Mouse strains and genotyping</b> .....	32
<b>2.4 Isolation and culture of primary mouse epidermal keratinocytes</b> .....	34
<b>2.5 Measurement of cell proliferation</b> .....	36
<b>2.6 Measurement of DNA synthesis</b> .....	36
<b>2.7 Apoptosis measurements</b> .....	37
<b>2.8 Preparation of cell lysates for protein analysis</b> .....	38
<b>2.9 Denaturing polyacrylamide gel electrophoresis and immunoblotting</b> .....	39
<b>2.10 Preparation of glass coverslips</b> .....	40
<b>2.11 Confocal and immunofluorescence microscopy</b> .....	41
<b>2.12 Quantification of reactive oxygen species (ROS)</b> .....	42
<b>2.13 Statistical analysis</b> .....	43
<b>Chapter 3 – Results</b> .....	44
<b>3.1 Proliferation of ILK-deficient keratinocytes</b> .....	44
<b>3.2 Apoptosis in cultured ILK-deficient keratinocytes</b> .....	50
<b>3.2.1 Role of the Akt pathway in increased apoptosis in ILK-deficient keratinocytes</b> .....	53
<b>3.3 Role of the mitochondrial localization of Bax in apoptosis of ILK-deficient keratinocytes</b> .....	56
<b>3.3.1 Activation of the MAPK pathway in ILK-deficient keratinocytes</b> .....	59
<b>3.3.2 Activation of Bax-caspase pathway in apoptosis in ILK-deficient keratinocytes</b> .....	59
<b>3.4 Reactive oxygen species in ILK-deficient cells</b> .....	69
<b>3.5 DNA damage markers in ILK-deficient keratinocytes</b> .....	77



<b>Chapter 4 - Discussion</b> .....	80
<b>4.1 Summary and general discussion</b> .....	80
<b>4.1.1 Modulatory role of ILK on keratinocyte viability</b> .....	80
<b>4.1.2 Modulatory role of ILK on ROS-induced apoptosis</b> .....	82
<b>4.2 Significance</b> .....	89
<b>4.3 Future Directions</b> .....	91
<b>References</b> .....	95
<b>Curriculum Vitae</b> .....	112

## List of Tables

Table 1: Reagents.....	29
Table 2: Antibodies.....	31

## List of Figures

Figure 1.1. Layers of the epidermis .....	3
Figure 1.2. The extrinsic and intrinsic apoptosis pathway .....	8
Figure 1.3. ILK protein domains .....	21
Figure 1.4. ILK signalling pathway .....	23
Figure 3.1. Proliferation of ILK-deficient keratinocytes .....	46
Figure 3.2. Proportion of BrdU-positive cells in ILK-deficient epidermis .....	49
Figure 3.3. Effect of <i>Ilk</i> gene inactivation on apoptosis .....	52
Figure 3.4. Effect of <i>Ilk</i> gene inactivation on Akt phosphorylation .....	55
Figure 3.5. Bax mitochondrial localization in ILK-deficient keratinocytes .....	58
Figure 3.6. ILK-deficiency is associated with JNK phosphorylation .....	61
Figure 3.7. ILK-deficiency is associated with ERK phosphorylation .....	63
Figure 3.8. Effect of <i>Ilk</i> gene inactivation on cleavage of caspase-3 .....	66
Figure 3.9. ILK-deficiency is associated with PARP inactivation .....	68
Figure 3.10. Effect of <i>Ilk</i> gene inactivation on cellular ROS levels .....	72
Figure 3.11. ROS in ILK-deficient keratinocytes .....	74
Figure 3.12. Effect of NAC on ROS in ILK-deficient keratinocytes .....	76
Figure 3.13. Effect of <i>Ilk</i> gene inactivation on $\gamma$ H2A.X levels .....	79
Figure 4.1. Proposed model of stress-induced apoptosis modulation by ILK .....	88

## **Chapter 1 – Introduction**

### **1.1 Architecture of the skin**

The largest organ in the body is the skin and it serves a critical function as a protective barrier from external harm and environmental stress (Jensen and Proksch, 2009). The skin is composed of 3 main layers: the outer epidermis, the dermis, and the underlying subcutaneous tissue (Macneal, 2006). The epidermis is a stratified, squamous epithelium, which acts as the first line of defense against environmental insults, and regulates the diffusion of water and electrolytes (reviewed in Indra and Leid, 2011). The dermis is mainly comprised of fibroblasts and connective tissue that cushions the body from mechanical strain, and provides elasticity (reviewed in Haake et al., 2001). Finally, the inner subcutaneous tissue, or hypodermis, consists of a thick layer of adipose and connective tissues. The hypodermis is essential for the proper regulation of body temperature, energy storage, and can act as a shock absorber (Walters and Roberts, 2002).

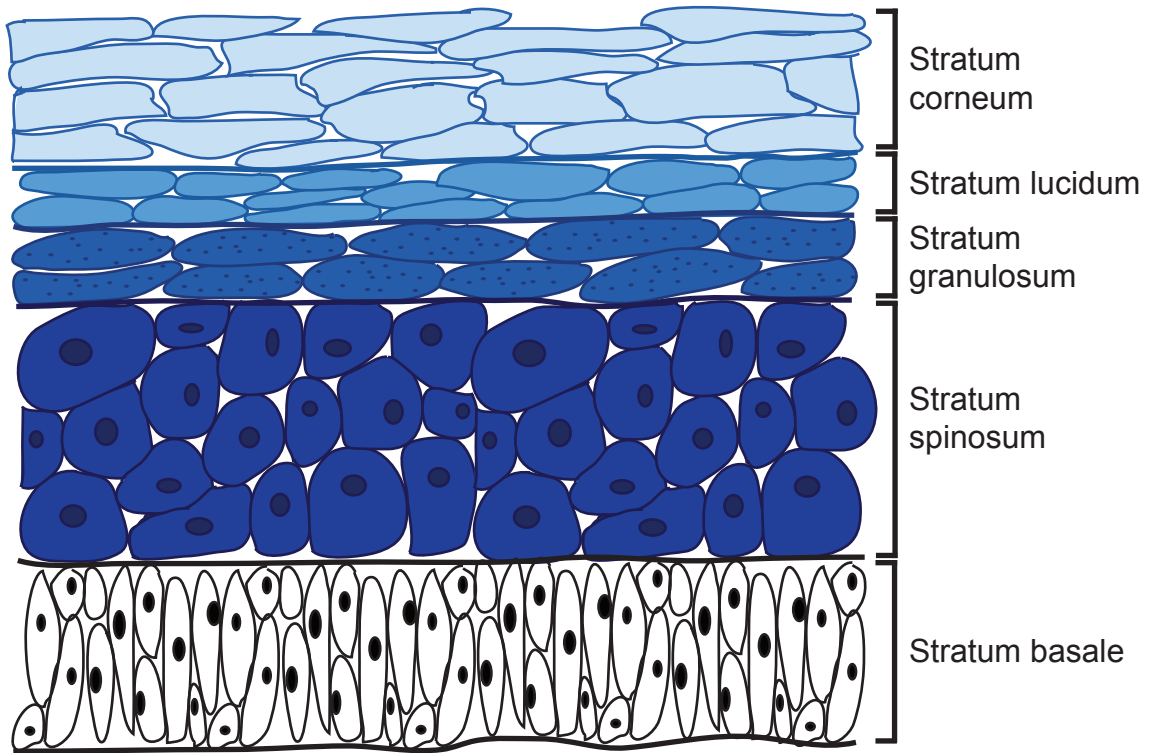
#### **1.1.1 The epidermis**

In humans, the epidermis is composed of 5 cell layers (reviewed in Haake et al., 2001; Figure 1.1). The innermost basal layer consists of basal keratinocytes that have a high proliferative capacity (Grinnel, 1992; Adams and Watt, 1989). Basal keratinocytes can be multipotent, epidermal stem cells that are responsible for the renewal capability of the epidermis (Elias, 2007). There is a concentration gradient of extracellular  $\text{Ca}^{2+}$  across the



**Figure 1.1. Layers of the epidermis.**

The epidermis is composed of 5 cell layers. The innermost layer, termed stratum basale, mainly consists of proliferating basal keratinocytes. These multipotent stem cells differentiate and move towards the outer layers of the skin to give rise to suprabasal layers termed spinous, granular, and clear cornified epidermal layers (Ivanova et al., 2005).



epidermal layers, which induces basal keratinocytes to differentiate and move towards the outer layers of the epidermis, giving rise to suprabasal layers termed spinous, granular, and cornified epidermal layers (Ivanova et al, 2005; Figure 1.1). The stratum spinosum is immediately above the basal layer, and contains keratinocytes, as well as immunologically active Langerhans cells that, in the case of pathogen invasion, trigger immune responses at the site of infection (Elias, 2007). Next, the stratum granulosum and stratum lucidum reside over the spinous layer (Méhul et al., 2003). The stratum granulosum is a thin, flattened layer in which cells begin to lose their nuclei, whereas the stratum lucidum is an extra epidermal layer present only on the thick skins of the palms and soles of feet (reviewed in Siegenthaler, 2006). Finally, the outermost stratum corneum is mainly comprised of dead keratinocytes that are continuously shedding and being replaced (Méhul et al., 2003).

## **1.2 Keratinocyte survival and programmed cell death**

A proper balance between keratinocyte survival and programmed cell death is necessary to maintain epidermal homeostasis (Raj et al., 2006). Older or damaged cells along the apical surface are constantly replaced (Pellettieri and Sanchez, 2007).

### **1.2.1 Types of cell death**

According to the Nomenclature Committee on Cell Death (NCCD), various forms of cell death exist, which can be defined by a number of characteristics, including morphological appearance (apoptotic vs. necrotic), enzymatic activity (presence or absence of nucleases



and/or proteases), functional components (accidental or systematic), or immunological features (Kroemer et al., 2009). Until recently, criteria accepted in a “dying” cell included activation of cysteine-aspartic proteases (caspases), loss of mitochondrial transmembrane potential, and/or phosphatidylserine (PS) exposure in the outer leaflet of the plasma membrane (reviewed in Kroemer et al., 2009). The currently accepted criteria to distinguish a cell undergoing death from a viable one are: (1) the structural integrity of the plasma membrane has been lost, (2) the cell has been fragmented into apoptotic bodies, (3) the fragmented pieces have been phagocytosed by neighbouring cells (reviewed in Kroemer et al., 2009).

Cell death can occur through a number of different processes based on the morphological properties of the dying cell (reviewed in Kroemer et al., 2009). Necrosis, more commonly known as death by cell injury or disease, is accompanied by a growth in cell volume, organelle swelling, and a loss of intracellular components due to rupturing of the cell membrane (reviewed in Kroemer et al., 2009). Apoptosis, on the other hand, is characterized by a reduction in cell volume, plasma membrane blebbing, chromatin condensation, DNA fragmentation, and rounding of the cell (reviewed in Kroemer et al., 2009). In contrast to necrotic cell death, the integrity of cytoplasmic organelles is preserved in apoptotic cells, until they are engulfed by adjacent cells (reviewed in Kroemer et al., 2009). Thus, the features of a cell undergoing necrosis differ from those of a cell undergoing apoptosis. In the epidermis, cornification is yet another form of programmed cell that exclusively occurs in keratinocytes (Candi et al., 2005). Keratinocytes of the basal layer become differentiated as they move towards the cornified layer of the epidermis. This cornified envelope is comprised of dead keratinocytes, called

corneocytes, which have reached the terminal stage of epidermal differentiation (Candi et al., 2005). The amalgam of proteins, including keratins, loricrin, and involucrin, as well as lipids, present in corneocytes, allow the cornified layer to fulfill its function for water retention and the formation of an impermeable barrier (reviewed in Kroemer et al., 2009).

### **1.2.2 Apoptosis in the epidermis**

Apoptosis, a highly regulated form of programmed cell death, is necessary for proper development and epidermal homeostasis (Raj et al., 2006). The dysregulation of apoptosis is a critical aspect of carcinogenesis (reviewed in Scatena et al., 2012). In the epidermis, apoptosis regulates tissue thickness, facilitates the turnover of newly synthesized tissue, and eliminates damaged or infected cells (Raj et al., 2006). As the first line of defense from the external environment, the epidermis is exposed to many insults, including ultraviolet (UV) radiation, oxidative stress, mechanical and chemical damage, and microbial infection (reviewed in Haake et al., 2001). Therefore, apoptosis is a key mechanism to eliminate damaged cells.

### **1.2.3 Extrinsic vs. intrinsic apoptosis pathway**

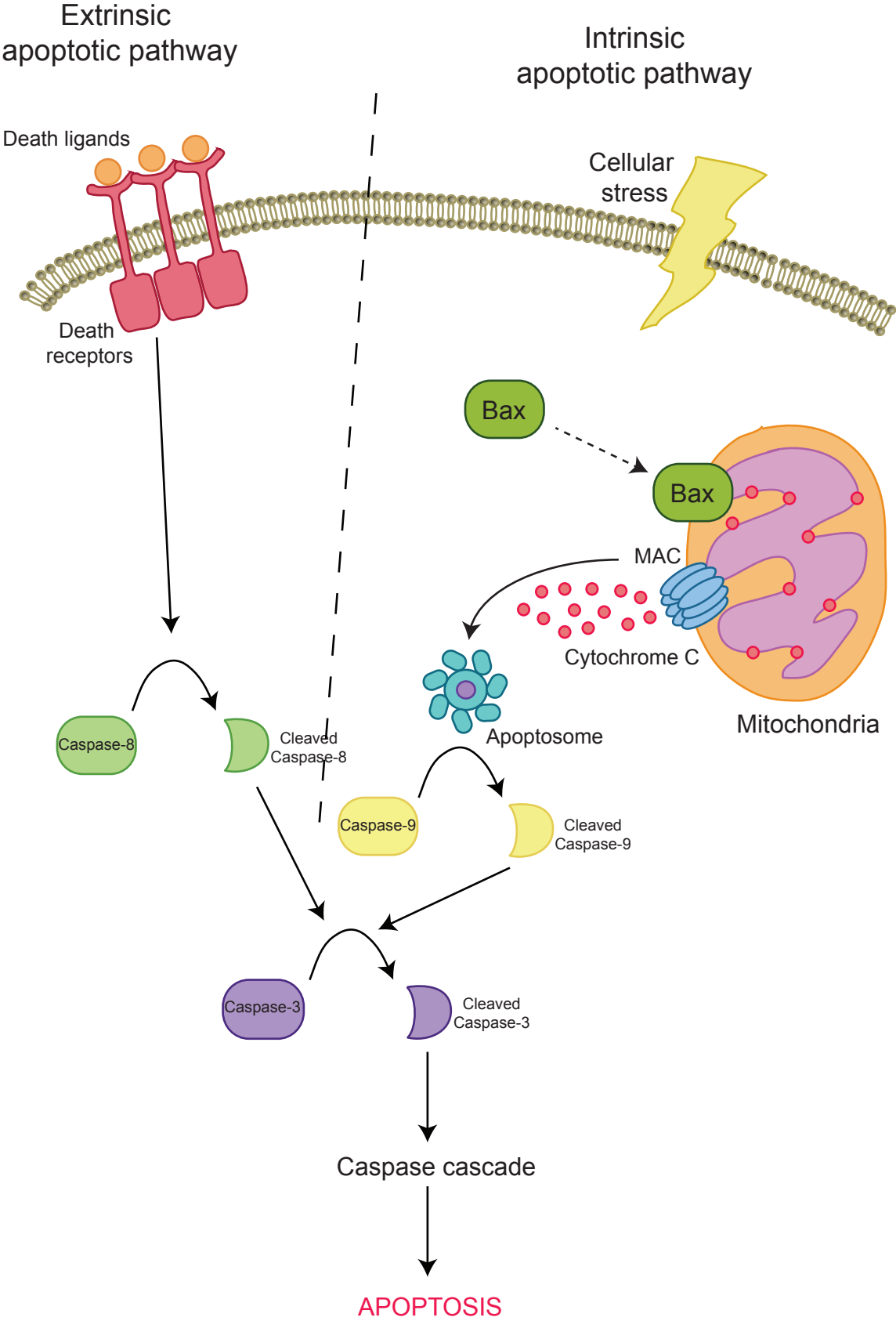
Two main pathways for apoptotic cell death have been identified: the extrinsic and intrinsic pathway.

The extrinsic apoptotic pathway is stimulated by proapoptotic, extracellular ligands that bind to their respective death receptors (reviewed in Ashkenazi, 2008; Figure 1.2). Proapoptotic receptors are members of the tumour necrosis factor (TNF) family (reviewed in Fulda and Debatin, 2006). The TNF superfamily consists of over 20 proteins



**Figure 1.2. The extrinsic and intrinsic apoptosis pathway.**

The extrinsic apoptosis program is mediated by the binding of death ligands to their death receptors, which stimulates the cascade caspase via caspase-8 activation. The intrinsic apoptotic pathway is stimulated within the cell in response to signals resulting from cellular stress. Such stimuli then activate downstream caspases to induce apoptosis (reviewed in Fulda and Debatin, 2006).



involved in a variety of cellular functions, ranging from regulation of cell survival and cell death to immune responses (Walczak and Krammer, 2000). TNF death receptors are characterized by an 80 amino acid-long, cytoplasmic domain that has been designated the “death domain” (reviewed in Fulda and Debatin, 2006). The death domain plays a critical role in relaying extracellular signals from death ligands on the cell surface, to activate downstream signalling pathways within the cell (reviewed in Fulda and Debatin, 2006; Figure 1.2). Once they have been activated, the death receptors recruit the execution procaspases 8 and 10 as well as the Fas-associated death domain adaptor molecule to their death domains. Together, these molecules form the death-inducing signalling complex (DISC) (reviewed in Ashkenazi, 2008). These DISCs then stimulate the caspase cascade via cleavage and consequent activation of procaspases 8 and 10. Active caspases 8 and 10, in turn, activate downstream effectors, such as caspase-3, 6, and 7, ultimately leading to apoptosis (Leblanc et al., 2002). In cultured keratinocytes, apoptosis triggered through UVB exposure is a result of the activity of pre-synthesized proteins, rather than *de novo* transcriptional processes (reviewed in Raj et al., 2006). Studies conducted on the human HaCaT keratinocyte cell line have demonstrated that caspase-8 becomes activated as a result of UVB-induced multimerization of the Fas death receptors (Takahashi et al., 2001a).

The intrinsic pathway, also known as the mitochondrial pathway, is stimulated from within the cell, often in response to signals resulting from DNA damage, loss of cell survival factors, or cellular stress (reviewed in Fulda and Debatin, 2006; Figure 1.2). In this pathway, the activation of downstream caspases is caused by permeabilization of the outer membrane of mitochondria (Green and Kroemer, 2004). This process relies on the

Bcl-2 protein family, which is responsible for regulating mitochondrial membrane permeability. Bcl-2 proteins determine whether a pro- or anti-apoptotic process will be activated. For example, Bax, Bak, and Bid promote, whereas Bcl-2 and Bcl-xl inhibit apoptosis (Wei et al., 2001). Bax and Bak are predominantly cytosolic. However, they translocate to the mitochondria in response to apoptotic stimuli, such as excessive DNA damage or elevated concentrations of free radical species (Wei et al., 2001). Once localized to the mitochondrial membrane, Bax and Bak form homo- and/or heterodimers to create the mitochondrial apoptosis-induced channel (MAC), which is responsible for the release of apoptogenic factors, such as cytochrome c, into the cytoplasm (reviewed in Fulda and Debatin, 2006). In the cytoplasm, cytochrome c interacts with apoptotic protease activating factor 1 (Apaf-1), to form an apoptosome (reviewed in Raj et al., 2006; Figure 1.2). The apoptosome then recruits and activates the initiator procaspase-9, which stimulates caspase-mediated apoptosis (Zou et al., 2003). The mitochondria can also activate the caspase program through the release of Smac/DIABLO, which interferes with the effects of apoptosis-inhibiting proteins (reviewed in Raj et al, 2006).

The extrinsic and intrinsic apoptosis pathways are interdependently regulated. Although they differ in their modes of activation, there are a number of proteins involved in both processes. Specifically, caspase-3 and caspase-7 are shared targets of these two apoptosis programs (reviewed in Raj et al., 2006). The cleavage and subsequent activation of caspase-3 and caspase-7 are mediated extrinsically by caspase-8, and intrinsically by caspase-9 (reviewed in Raj et al., 2006). The enzymatic properties of these executioner caspases lead to the cleavage of downstream proteins that are involved in DNA repair and the structural stability of the cytoskeleton and nuclear membrane (reviewed in Raj et al.,

2006). Ultimately, the protease activity of these terminal caspases is responsible for the disassembly and degradation of the cell.

Both the intrinsic and extrinsic apoptosis pathways are activated in keratinocytes by a diverse array of stress stimuli, including UV exposure, heat shock, oxidative stress, and exposure to cytotoxic chemicals (reviewed in Raj et al., 2006). The detrimental effects that arise due to UV-induced apoptosis appear to be of a synergistic combination of pathways activated in response to damaged DNA, activation of death receptors, and the formation of reactive oxygen species (ROS) (Kulms et al., 1999; Kulms et al., 2002). UV radiation is the primary cause of most skin cancers, and elicits its effects in the absence of any specific tumour promoter, making it a potent and dangerous carcinogen (reviewed in Assefa et al., 2005). UV-induced skin cancer is characterized by irreversible DNA damage, and the release of harmful photoproducts. Any unrepaired DNA can lead to mutations in both oncogenes and/or tumour suppressor genes, and subsequent tumour development (reviewed in Assefa et al., 2005).

### **1.3 Reactive oxygen species**

Free radical species are molecules that bear one or more unpaired electrons (Halliwell and Gutteridge, 1989). “ROS” is a generalized term used to describe both oxygen radicals, such as peroxy ( $\text{RO}_2\bullet$ ), hydroxyl ( $\text{OH}\bullet$ ), and superoxide ( $\text{O}_2^-\bullet$ ) radicals, as well as some nonradical oxidizing compounds (reviewed in Bayir, 2005). Such oxidizing agents include hydrogen peroxide ( $\text{H}_2\text{O}_2$ ), which can be readily converted into reactive radical



species (reviewed in Bayir, 2005). Although they are typically associated with deleterious effects, ROS are actually generated as a normal biproduct of oxidative metabolism (reviewed in Bayir, 2005). In particular, they are involved in cellular processes such as electron transport in the mitochondria, enzymatic reactions, signal transduction, and immunological responses against microbial threats (reviewed in Bayir, 2005). Growth factors and cytokines can stimulate increases in ROS production, necessary for various cellular processes (reviewed in Simm and Brömme et al., 2005). For example, in vascular smooth muscle cells, the presence of  $H_2O_2$  is essential for functional tyrosine phosphorylation and proper DNA synthesis stimulated by platelet-derived growth factor (PDGF) (Sundaresan et al., 1995). In addition, the ERK and the pro-survival phosphatidylinositol 3-kinase/Akt pathways can be activated through various growth factor receptors in response to oxidizing agents (reviewed in Simm and Brömme et al., 2005). At the level of transcription, ROS are also involved in the activation of the pro-survival, NF- $\kappa$ B pathway, which is involved in the inflammatory response of the skin (reviewed in Bickers and Athar, 2006). In human T-cell and murine fibrosarcoma cell lines, NF- $\kappa$ B can be activated by  $H_2O_2$ , either through the degradation of the NF- $\kappa$ B inhibitor, I $\kappa$ B, or by preventing NF- $\kappa$ B association with DNA via oxidation of its DNA-binding domain (Schreck et al., 1991; Schenk et al., 1993). Finally, in mouse fibroblasts, ROS production by NADPH-oxidases is stimulated as a defense response to microbial infections or to pathogens invading the cells (Taddei et al., 2007). Thus, despite the destructive nature of oxidative radicals, a moderate level of ROS is necessary for proper cellular signalling and function.

### 1.3.1 Sources of ROS

In mammalian cells, ROS are produced as a result of both enzymatic and nonenzymatic processes (reviewed in Bayir, 2005). In particular, the catalytic activity of certain enzymes, including nicotinamide adenine dinucleotide phosphate (NADPH) oxidase, contributes to the formation of free radical species (reviewed in Bayir 2005). NADPH oxidase is a membrane-bound enzymatic complex that uses NADPH-supplied electrons to produce  $O_2^{\cdot-}$  from oxygen (reviewed in Bayir, 2005). NADPH oxidase is activated in leukocytes in response to inflammatory stimuli (reviewed in Bayir, 2005), leading to a vast production of  $O_2^{\cdot-}$ , which provides leukocytes with the ability to eliminate microorganisms (Vignais, 2002). In addition to endogenous sources, ROS can also be generated through exogenous oxidizing agents, such as chemicals, environmental pollutants, cigarette smoke, xenobiotics, and UV radiation (reviewed in Vallyathan and Shi, 1997). Ultimately, excessive endogenous and/or exogenous ROS can have damaging effects on the cell.

### 1.3.2 ROS in keratinocytes

Epidermal keratinocytes must be able to cope with external ROS-generating stressors, such as UV radiation and oxygen (reviewed in Bito and Nishigori, 2012). On one hand, ROS can be beneficial through their role in signalling processes. Findings by Huang et al. (2001) demonstrated that in epidermal cells, the phosphorylation and activation of protein kinase B (Akt) could be induced by  $H_2O_2$  in a dose-dependent fashion. Similarly through *in vivo* studies, Bito et al. (2010) showed that ROS play a direct role in the signal transduction of keratinocytes. On the other hand, UVB photons from the sun are

particularly detrimental to keratinocytes, causing damage to DNA through the generation of reactive (6-4) photoproducts, pyrimidine dimers (Mitchell et al., 1992), and hydroxy-2'-deoxyguanosine (Hattori et al., 1996). The formation of these oxidative radicals accounts for approximately 50% of the damage produced by UV radiation (reviewed in Bito and Nishigori, 2012).

Under normal circumstances, the epidermis is able to withstand oxidative stress because keratinocytes produce sufficient antioxidants to protect and buffer the harmful effects of radical species (reviewed in Bito and Nishigori, 2012). Keratinocytes contain a physiological threshold of antioxidants, such as  $\alpha$ -tocopherol (VE), ascorbic acid (VC), and glutathione (GSH), which act to scavenge oxidative radicals. Other contributions to ROS scavenging are superoxide dismutase, which converts  $O_2^{\cdot-}$  to  $H_2O_2$  and  $O_2$ , as well as catalase and glutathione peroxidase, which reduce  $H_2O_2$  to  $H_2O$  and  $O_2$  in peroxisomes and mitochondria, respectively (Matés, 2000). However, when the amount of oxidative stress exceeds the cell's capacity to quench ROS, substantial DNA damage can occur (reviewed in Assefa et al., 2005). If the cell damage is not too extensive, a variety of repair programs are activated, namely the base excision repair (BER) and nucleotide excision repair pathways (reviewed in Lu et al., 2001). BER involves DNA glycosylases, which eliminate improper base incorporations into DNA (reviewed in Lu et al., 2001). In the epidermis, the overproduction of cellular ROS acts to reduce endogenous levels of antioxidants, including the aforementioned VE, VC, and GSH (Hanada et al., 1997). By disrupting the intracellular redox balance, the repair ability and reducing properties of the cell become compromised. Thus, cells become even more susceptible to the detrimental effects of oxidative stress. Therefore, the redox potential of keratinocytes is critical for

reducing intracellular ROS levels, and to prevent excessive damage and cell death (reviewed in Bito and Nishigori, 2012).

### **1.3.3 Stress-induced apoptosis**

Depending on the nature and extent of stressors received by a cell, the extrinsic and/or intrinsic apoptosis pathway can be activated. The mitogen-activated protein kinases (MAPKs) are a group of enzymes frequently involved in stress-induced apoptosis through extrinsic and intrinsic programs (reviewed in Bito and Nishigori, 2012; Kyriakis et al., 1994). In particular, UVB-induced apoptosis in keratinocytes is associated with increased phosphorylation and activation of c-Jun N-terminal kinase (JNK) and p38 (Shimizu et al., 1999; Van Laethem et al., 2006). The activation by ROS of JNK and p38 are well established in many cell types (Shiah et al., 1999; Benhar et al., 2001; El-Najjar et al., 2010). Interestingly, the response of another MAPK protein, extracellular signal-regulated kinase (ERK) appears to have contrasting effects with respect to ROS, depending on the cell type (Xia et al., 1995; Tan and Chiu, 2013). However, in keratinocytes, ERK is activated by H<sub>2</sub>O<sub>2</sub> through transforming growth factor- $\beta$ 1 (TGF- $\beta$ 1) (Kim et al., 2006). Studies have demonstrated that ROS stimulates TGF- $\beta$ 1 signalling pathways that lead to the activation of ERK. ERK stimulation then induces the apoptotic programs associated with the terminal differentiation processes of keratinocytes (Kim et al., 2006; Iglesias et al., 2000). Significantly, the activation of these MAPKs stimulates Bax translocation to the outer mitochondrial membrane, activating apoptosis programs (Van Laethem et al., 2004).

In keratinocytes, stress-induced signals are often mediated by different transmembrane protein receptors to induce cell growth, adhesion or apoptosis (reviewed in Taddei et al., 2007). Integrins, in particular, are a family of transmembrane proteins that participate in transducing extracellular signals into the cell (Zeller et al., 2013). Recently, it has been proposed that ROS production, commonly associated with microbial infection or apoptosis execution, can also stimulate the same enzymatic reactions linked to the redox-dependent processes during integrin signal transduction (Taddei et al., 2007; Zeller et al., 2013). Specifically, mitochondrial ROS generation has been associated with the early stages of cell-ECM adhesion through integrins (Taddei et al., 2007). Thus, cells likely require a threshold level of ROS for cell attachment and spreading, in addition to programmed cell death.

## 1.4 Integrins

Integrins are heterodimeric, transmembrane proteins that link the actin cytoskeleton with the extracellular matrix (reviewed in Hynes, 2002). In mammals, the integrin family is composed of 18  $\alpha$ - and 8  $\beta$ -subunits that make up 24 heterodimeric members (reviewed in van der Flier and Sonnenberg, 2001). Targeted inactivation of genes encoding integrins leads to a wide array of defects, ranging from subtle phenotypic abnormalities to lethality (van der Flier and Sonnenberg, 2001).

In the epidermis, integrins have been categorized into  $\beta$ 1-containing,  $\alpha$ v-containing, and  $\alpha$ 6 $\beta$ 4 integrins (reviewed in Margadant et al., 2010). These three types of integrins are

constitutively expressed, whereas other classes are induced during wound healing (reviewed in Margadant et al., 2010). The  $\alpha 2\beta 1$  and  $\alpha 3\beta 1$  integrins modulate the actin cytoskeleton through focal adhesion proteins, such as talin and vinculin (reviewed in Watt, 2002; reviewed in Margadant et al., 2010). Integrins containing the  $\alpha 5$  subunit, such as  $\alpha v\beta 5$  and  $\alpha v\beta 8$ , predominantly bind to vitronectin and are expressed at low levels in intact adult epidermis (reviewed in Margadant et al., 2010). Finally,  $\alpha 6\beta 4$  integrins bind to laminin and are critical for basal keratinocytes adhesion to the basement membrane at the dermal-epidermal junction (reviewed in Margadant et al., 2010).

Apart from their role in cell-ECM adhesion, integrins act as signalling modulators in the epidermis. Specifically, they interact with focal adhesion kinase (FAK), kindlins, and integrin-linked kinase (ILK) (reviewed in Margadant et al., 2010). A primary function of FAK is to stimulate signalling events at focal adhesions (Ilić et al., 1995). FAK-deficient mice display defects in the hair cycle, but no abnormalities in the integrity of the epidermis, suggesting that FAK may be involved in the integrin-related pathways downstream or independent of cellular adhesion (Essayem et al., 2006). Similarly, the kindlin family of adaptor proteins is involved in the activation of integrins (Meves et al., 2009). Finally, integrins associate with another adaptor scaffold protein termed ILK. Previous findings have established a role for the direct integrin-ILK interaction in reinforcing the cytoskeletal support of the cell through indirect association with actin via particularly interesting new cysteine-histidine-rich protein (PINCH) and parvin (Legate et al., 2006).

### **1.4.1 Integrins and epidermal homeostasis**

In the epidermis, integrins are involved in maintaining homeostasis through their roles in keratinocyte adhesion, proliferation, differentiation, and survival (reviewed in Margadant et al., 2010).  $\alpha 6\beta 4$  integrin mediates the adhesion of basal keratinocytes to the basement membrane, although their role in keratinocyte proliferation and survival remains unresolved (reviewed in Margadant et al., 2010). Integrin-mediated signals are necessary to inhibit apoptosis by promoting the pro-survival PI3-kinase/Akt pathway and stimulating cell cycle progression through the ERK pathway (Hynes, 2002). Further, a reduction in the fraction of proliferating cells in the epidermis of mice expressing a mutant  $\beta 4$  integrins has been reported (reviewed in Margadant et al., 2010). Mice lacking expression of integrin  $\alpha 3$  and/or integrin  $\alpha 6$  display a severe blistering phenotype, likely as a result of impaired epidermal integrity due to keratinocyte detachment (reviewed in Margadant et al., 2010). Mice with conditional inactivation of the gene encoding integrin  $\beta 1$  exhibit a plethora of phenotypic defects, including blistering, reduced proliferative capacity, abnormalities of the basement membrane, epidermal inflammation, and hair loss (reviewed in Margadant et al., 2010).

## **1.5 Integrin-linked kinase**

ILK is a ubiquitous adaptor protein that binds to integrins (Hannigan et al., 1996). ILK functions as a scaffold between the cytoplasmic domain of  $\beta 1$  or  $\beta 3$  integrins and the actin cytoskeleton (Hannigan et al., 1996).

ILK is composed of three main domains (Chiswell et al., 2008; Figure 1.3). It has five N-terminal ankyrin repeats, which mediate binding to PINCH. ILK-PINCH complexes are critical for the localization of ILK to focal adhesions (Wu, 1999; Figure 1.4). ILK also has a pleckstrin-homology-like domain that indirectly associates with phosphoinositides, which are involved in cell growth, cell survival, and protein trafficking (reviewed in Hannigan et al., 2005). Finally, its C-terminal kinase-like domain is responsible for the interaction of ILK with many proteins, including paxillin and parvins (reviewed in Qin & Wu, 2012). The association of ILK with the parvin family is responsible for its involvement in focal adhesions at the cell surface (Tu et al., 2001; Yamaji et al., 2001).

### **1.5.1 ILK as a pseudokinase**

The kinase properties of ILK have long been debated. A key source of the conflicting notion that ILK possesses kinase activity stems from the high degree of homology between the amino acid sequence of ILK to that of *bona fide* serine-threonine kinases (Maydan et al., 2010). However, although sequencing of the kinase-like, C-terminus of ILK shares homology with other kinases, the lack of catalytic activity can be attributed to the divergence in 3D structural configuration (reviewed in Dagnino, 2011). Whereas ILK shares an APE moiety and ATP-binding lysine residue with other serine-threonine kinases, it lacks DFG and HRD motifs conserved in most kinases (Maydan et al., 2010). Thus, despite its ability to bind ATP, ILK lacks essential kinase function, as its kinase-like domain does not directly catalyze ATP hydrolysis (Fukuda et al., 2009).

*In vitro* studies to determine the kinase properties of ILK have also generated contrasting results. A GST-ILK fusion protein purified from bacteria was previously shown to





**Figure 1.3. ILK protein domains.**

ILK is composed of three distinct domains: an N-terminus consisting of 5 ankyrin repeats, a pleckstrin homology-like (PH) domain, and a C-terminus kinase-like domain (Chiswell et al., 2008).

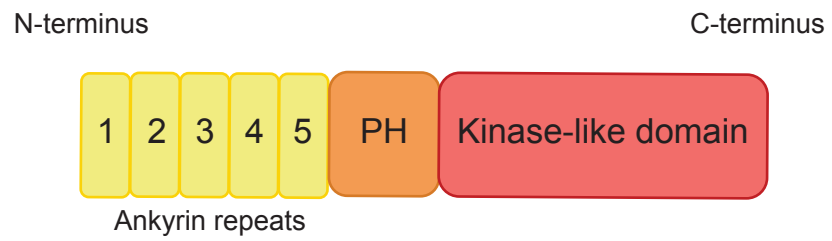
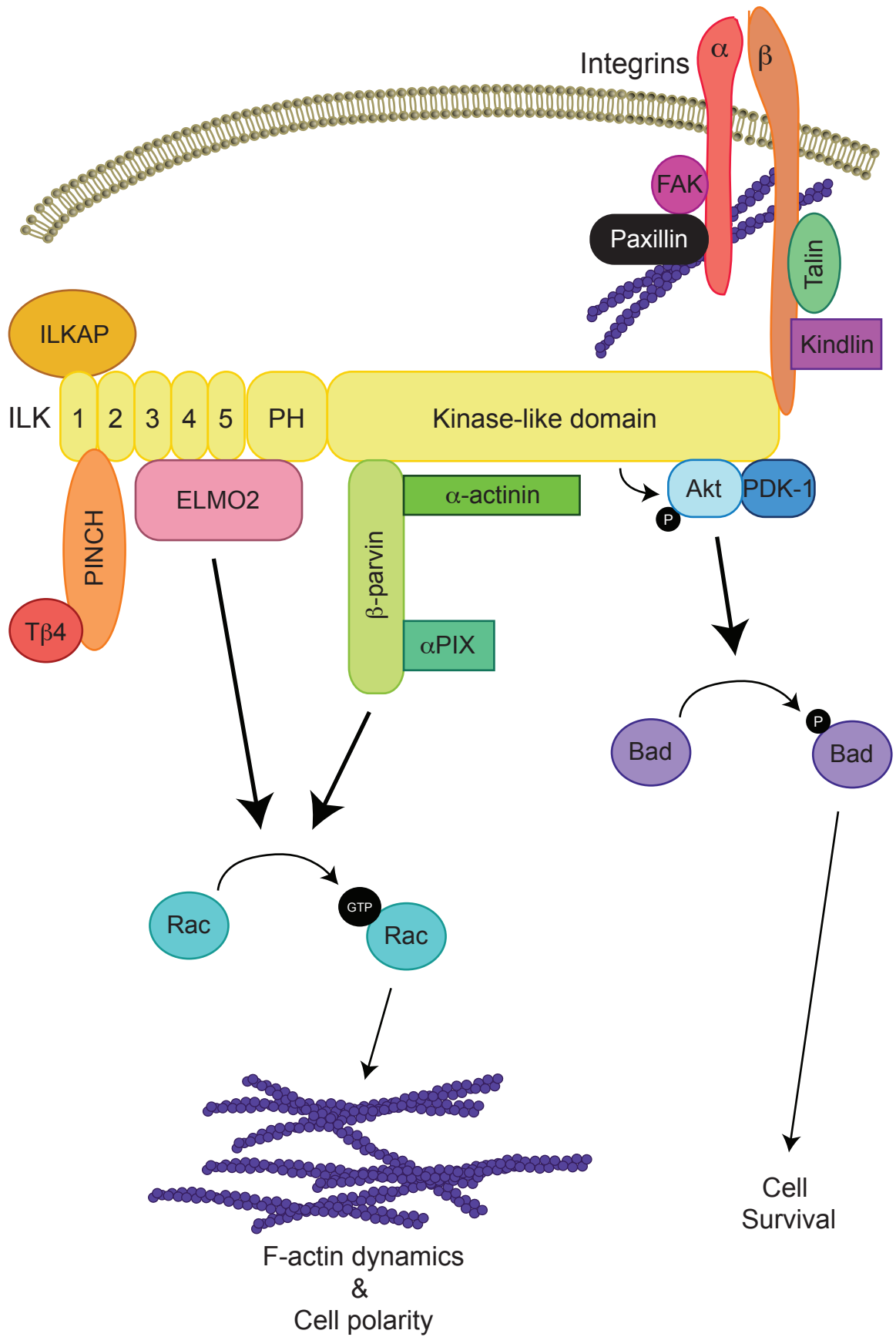




**Figure 1.4. ILK signalling pathway.**

ILK is involved in a number of cellular processes including cell-ECM adhesion via integrins, F-actin dynamics and cell polarity via Rac1, parvins, and ELMO2, and cell survival via Akt activation.



phosphorylate certain substrates, including myelin basic protein (Hannigan et al., 1996). In spite of this, Fukuda et al. (2009) demonstrated that neither a bacterially produced nor a commercial, recombinant form of ILK elicited any kinase activity. Further, the expression of ILK mutant ILK E359K (which possesses no “kinase” properties) does not alter the phosphorylation of its reported substrates, Akt and glycogen synthase kinase-3 $\beta$  (GSK-3 $\beta$ ), in immortalized kidney fibroblasts and chondrocytes (Sakai et al., 2003; Grashoff et al., 2003). However, conflicting findings of ILK in its modulation of Akt phosphorylation in HEK 293 human embryonic kidney cells and Schwann cells have suggested a cell type-specific response (Delcommenne et al., 1998; Pereira et al., 2009).

Experiments conducted *in vivo* have also supported the notion of a dispensable “kinase” domain of ILK. Zervas et al. (2001) showed that embryonic lethality consequent to the absence of ILK in *Drosophila melanogaster* embryos could be rescued through the introduction of the ILK E359K mutant. Embryos expressing E359K or wild-type ILK were phenotypically indistinguishable. Similarly in *Caenorhabditis elegans* deficient in ILK, Mackinnon et al. (2002) demonstrated that ILK E359K expression could restore the associated defects in muscle assembly.

A study conducted by Lange et al. (2009) involved the generation of point mutations of the *Ilk* gene that were predicted to impair any kinase activity ILK may elicit. However, mice expressing these mutants in the absence of wild type ILK exhibited no phenotypic defects (Lange et al., 2009). Additionally, epidermal keratinocytes isolated from mice expressing these ILK mutant proteins displayed normal adhesion, spreading, and actin cytoskeleton (Lange et al., 2009). Thus, the findings from this study suggest that ILK functions as a pseudokinase in epidermal keratinocytes.

### **1.5.2 ILK in different cell types**

ILK has some distinct functions in different cell types. Deng et al. (2001) demonstrated that ILK is involved in mediating smooth muscle contraction through myosin phosphorylation. Chondrocyte-specific inactivation of the *Ilk* gene leads to perinatal death in mice due to respiratory defects (Grashoff et al., 2003). These mice also develop chondrodysplasia that leads to irregularities in chondrocyte morphology and reduced proliferation (Grashoff et al., 2003). ILK-deficient embryos fail to implant as a result of impaired polarization of the epiblast, leading to lethality at the peri-implantation stage (Sakai et al., 2003). Specifically in the dermal layer of the skin, ILK-deficient fibroblasts also experience defects in their ability to spread and a delayed formation of focal adhesions (Sakai et al., 2003). Recent work conducted in our laboratory has also demonstrated a critical role for ILK in transducing signals necessary for proper dermal fibroblasts to myoblast transition – a process essential for proper skin repair after injury (Vi et al., 2011).

### **1.5.3 ILK in the epidermis**

Studies conducted in our laboratory have shown that ILK modulates polarity in keratinocytes through its interaction with Engulfment and Cell Motility 2 (ELMO2) (Ho et al., 2009). This ILK-ELMO2 complex has been shown to direct keratinocyte migration and lamellapodia formation through RhoG activity (Ho and Dagnino, 2011; Figure 1.4). Additionally, ILK has been found to play a critical role in the phagocytic capacity of keratinocytes (Sayedyahosseini et al., 2012). ILK-deficient cells exhibit defects in their capacity for engulfment that can likely be attributed to an impaired activation of Rac1



(Sayedyahosseini et al., 2012). We have also shown that in the absence of ILK, wound healing is impaired due to abnormal transformation growth factor- $\beta$  signalling in dermal fibroblasts (Vi et al., 2011). Recent work in our laboratory has focused on the role of ILK in maintaining epidermal function. Nakrieko et al. (2008) demonstrated that *Ilk* gene inactivation in the epidermis of mice is associated with impaired hair follicle morphogenesis and polarized keratinocyte motility. Histologically, these ILK-deficient mice display many phenotypic defects, including reduced adhesion to the basement membrane, compromised epidermal integrity, perinatal death, and failure to thrive (Nakrieko et al., 2008). In addition, *Ilk* gene inactivation in the stem cell population of hair follicle bulges results in defective wound healing as well as a reduced contribution of stem cell progeny to the regenerating epidermis after injury (Nakrieko et al., 2011). Thus, ILK is involved in many aspects of skin function.

#### **1.5.4 The role of ILK in cell survival**

ILK promotes survival of various cell types (Bock-Marquette et al., 2004; Delcomenne et al., 1998). In primary neonatal cardiomyocytes, thymosin  $\beta$ 4, an actin sequestering protein, forms a complex with ILK and PINCH to initiate a pro-survival pathway through Akt activation (Bock-Marquette et al., 2004). Similarly in IEC-18 intestinal epithelial cells, ILK promotes cell survival and inhibits apoptosis through the phosphoinositide-3-OH kinase-dependent activation of GSK-3 $\beta$  and Akt (Delcomenne et al., 1998). Additionally, the loss of ILK in mouse hepatocytes leads to abnormal levels of apoptosis, as well as hepatitis (Gkretsi et al., 2007). Finally in SCP2 mouse mammary epithelial cells and breast cancer cell lines, ILK suppresses anoikis and promotes cell survival

through Akt activation (Attwell et al., 2000; Troussard et al., 2006). However, despite the established role of ILK in cell survival in the above-mentioned cell types, its role in keratinocyte survival remains unknown.

## 1.6 Rationale and hypothesis

Previous findings in our laboratory have demonstrated an essential role of ILK in maintaining epidermal integrity and function (Nakrieko et al., 2008). Mice with *Ilk* epidermis-restricted gene inactivation display severe phenotypic defects including impaired hair follicle morphogenesis, reduced adhesion to the basement membrane, failure to thrive, and perinatal death (Nakrieko et al., 2008). Apart from its adaptor scaffolding function, ILK has recently been found to play a substantial role in suppressing anoikis and apoptosis in various epithelial cell types (Benoit et al., 2007; Attwell et al., 2000). However, specific aspects of how ILK-insufficiency leads to impaired epidermal integrity are poorly understood. Based on observations of our ILK-deficient mice, ILK appears to play a critical modulatory role in maintaining normal keratinocyte survival and retaining proper epidermal function. In addition to histological defects detected in the epidermis, we have consistently observed phenotypic abnormalities that resemble cells undergoing apoptosis in keratinocytes with *Ilk* gene inactivation. Thus, the aforementioned findings led me to hypothesize that ILK is required to maintain keratinocyte viability. To test my hypothesis, my specific aims were as follows:

1. To determine the role of ILK in keratinocyte viability.

2. To identify the mechanisms whereby ILK contributes to keratinocyte survival.

## Chapter 2 – Materials and Methods

### 2.1 Reagents

Reagents and their sources are shown in Table 1.

**Table 1: Reagents**

Reagent	Source	Catalogue No.
Amersham ECL Prime Western blotting detection reagent	GE Healthcare, Mississauga, ON	RPN2232
Aprotinin	Bioshop, Burlington, ON	APR200
Bradford protein quantification solution	Bio-Rad, Mississauga, ON	500-0006
Ca <sup>2+</sup> -free Eagle's minimum essential medium (EMEM)	Lonza, Walkersville, MD	06-174G
Chelex 100 resin	Bio-Rad, Mississauga, ON	142-2842
Cholera toxin	List Biological Laboratories Inc, Burlington, ON	100
2'-7'-Dichlorofluorescein diacetate (DCFDA)	Calbiochem (EMD Millipore), Billerica, MA	4091-99-0
Epidermal growth factor (EGF)	Sigma, St. Louis, MO	E4127
FBS for keratinocytes	Lonza, Walkersville, MD	14-561F
Fetal bovine serum (FBS)	Gibco, Burlington, ON	12483
Hoeschst 33342	Life Technologies, Burlington, ON	H1399

<b>Reagent</b>	<b>Source</b>	<b>Catalogue No.</b>
Hydrocortisone	Sigma, St. Louis, MO	H4001
Immu-mount mounting medium	Thermo Scientific, Pittsburgh, PA	9990402
Insulin	Sigma, St. Louis, MO	I6634
Leupeptin	Bioshop, Burlington, ON	LEU001
<i>N</i> -Acetyl-L-cysteine	Sigma, St. Louis, MO	A9165
NaF	Sigma, St. Louis, MO	S7920
Na <sub>3</sub> VO <sub>4</sub>	Bioshop, Burlington, ON	SOV664
Paraformaldehyde (PFA)	Fisher Scientific, Whitby, ON	AC416780030
Penicillin (10,000 U/ml) and streptomycin (10 mg/ml) solution	Gibco, Burlington, ON	15140
Pepstatin	Bioshop, Burlington, ON	PEP605
Phenylmethylsulfonylfluoride (PMSF)	Bioshop, Burlington, ON	PMS123
Phospho Safe extraction reagent	Novagen, San Diego, CA	71296-3
Proteinase K	Life Technologies, Burlington, ON	AM2542
Rat tail collagen I	BD Biosciences, Bedford, MA	354236
Triiodothyronine (T3)	Sigma, St. Louis, MO	T6397
Triton X-100	EMD, Darmstadt, Germany	CATX 1568
2.5% trypsin	Gibco, Burlington, ON	15090-046
0.25% trypsin/0.9 mM ethylenediaminetetraacetic acid (EDTA)	Gibco, Burlington, ON	25200-056

## 2.2 Antibodies

Antibodies, their sources, and working dilutions are shown in Table 2.

**Table 2: Antibodies**

Antibody	Source	Catalogue No.	Dilution <sup>a</sup>
Bax (N-20)	Santa Cruz Biotechnology, Santa Cruz, CA	sc-493	1:150 (IF)
5-bromo-2'-deoxyuridine (BrdU)	Developmental Studies Hybridoma Bank, Iowa City, IA	N/A	1:1000 (IF)
Cleaved Caspase-3	Cell Signalling, Pickering, ON	9661	1:1000 (IB)
Cleaved PARP (Poly ADP Ribose Polymerase)	Cell Signalling, Pickering, ON	9544	1:1000 (IB)
Glyceraldehyde 3-phosphate dehydrogenase (GAPDH)	Assay Designs, Ann Arbor, MI	CSA-335	1:5000 (IB)
MTCO1 [1D6E1A8]	Abcam, Cambridge, MA	ab14705	1:50 (IF)
Phospho-Akt (Thr308)	Cell Signalling, Pickering, ON	9275	1:1000 (IB)
Akt	Cell Signalling, Pickering, ON	9272	1:1000 (IB)
Phospho-histone H2A.X (Ser139) ( $\gamma$ H2A.X)	Cell Signalling, Pickering, ON	9718	1:1000 (IB) 1:200 (IF)
Phospho-p44/42 MAPK (Thr202/Tyr204) (D13.14.4E)	Cell Signalling, Pickering, ON	4370	1:1000 (IB)

Antibody	Source	Catalogue No.	Dilution <sup>a</sup>
p44/42 MAPK (Erk1/2)	Cell Signalling, Pickering, ON	9102	1:1000 (IB)
Phospho-SAPK/JNK (Thr183/Tyr185) (81E11)	Cell Signalling, Pickering, ON	4668	1:1000 (IB)
SAPK/JNK	Cell Signalling, Pickering, ON	9252	1:1000 (IB)
ILK	BD Transduction Laboratories, Lexington, KY	611802	1:5000 (IB)
$\gamma$ -tubulin	Sigma, St. Louis, MO	T6557	1:150 (IB)
HRP-conjugated goat anti-mouse IgG	Jackson ImmunoResearch, West Grove, PA	115-038-003	1:500 (IB)
HRP-conjugated goat anti-rabbit IgG	Cell Signalling, Pickering, ON	7074	1:500 (IB)
AlexaFluor <sup>TM</sup> 488 - conjugated goat anti-mouse IgG	Molecular Probes/Invitrogen, Eugene, OR	A11001	1:5000 (IF)
AlexaFluor <sup>TM</sup> 488 - conjugated goat anti-rabbit IgG	Molecular Probes/Invitrogen, Eugene, OR	A11008	1:5000 (IF)
AlexaFluor <sup>TM</sup> 594 - conjugated goat anti-mouse IgG	Molecular Probes/Invitrogen, Eugene, OR	A11005	1:5000 (IF)
AlexaFluor <sup>TM</sup> 594 - conjugated goat anti-rabbit IgG	Molecular Probes/Invitrogen, Eugene, OR	A11012	1:5000 (IF)

a IF = Immunofluorescence  
IB = Immunoblot

## 2.3 Mouse strains and genotyping

Mice with epidermis-restricted inactivation of the *Ilk* gene have been generated in our laboratory, and previously described (Nakrieko et al., 2008). These mice are generated by

breeding *Ilk<sup>tm1Star</sup>* mice, in which exons 4 and 12 of the *Ilk* allele are flanked by lox P sites (hereafter termed *Ilk<sup>ff</sup>*; ref. 17) and *Tg(KRT14-cre)1Amc/J* mice (hereafter termed *K14Cre*; stock no. 004782; Jackson Laboratory; ref. 18). In this manner, we have mice that express *Ilk* in the epidermis (*K14Cre<sup>+/-</sup>;Ilk<sup>ff/+</sup>*), and ILK-deficient littermates (*K14Cre<sup>+/-</sup>;Ilk<sup>ff/ff</sup>*).

To determine the genotypes of mice in each litter, genomic DNA was isolated from tail clippings (1-2 mm in length), obtained at the time of skin harvesting (please see Section 2.4). The tails were placed in microcentrifuge tubes, and digested with 100  $\mu$ l of P-K buffer (20 mM Tris Cl pH 8.3, 50 mM KCl, 2.5 mM MgCl<sub>2</sub>, 0.5% Tween-20) containing 6  $\mu$ l of Proteinase K stock (20 mg/ml). The samples were incubated in a thermomixer at 58°C with shaking at 3,000 rpm for 3-16 hours. The digested tissue solution was mixed by vortexing, and then heated to 95°C in a thermomixer with shaking (3,000 rpm) for 15 minutes. Digested tissue samples were diluted 1:10 with HPLC-grade water (Fischer, Catalogue No. W5-1), and used as templates for polymerase chain reaction (PCR) amplification. PCR amplification was conducted for 34 cycles (94°C for 45 seconds; 55°C for 30 seconds, 72°C for 45 seconds), using *Taq* DNA Polymerase kits (Qiagen, Catalogue No. 201205) and the appropriate primers. *Cre* transgene amplicons were obtained using a multiplex assay, with primer sets specific for *Cre* mixed with primers specific for the *Cpxm1* gene (Institut Clinique de la Souris; [http://www.ics-mci.fr/mousecre/pdf/standard\\_cre\\_genotyping.pdf](http://www.ics-mci.fr/mousecre/pdf/standard_cre_genotyping.pdf)). The primer sequences are: *Ilk*, forward: 5'-CTGTTGCAATACAAGGCTGAC-3', reverse: 5'-CTCGGAGAAGCTCTCTAAGGGG-3'; *Cre*, forward: 5'-CCATCTGCCACCAGCCAG-3', reverse: 5'TCGCCATCTTCCAGCAGG-3'; *Cpxm1*,



forward: 5'-ACTGGGATCTTCGAACTCTTTGGAC-3', reverse: 5'-GATGTTGGGGCACTGCTCATTACC-3'. Amplicons were resolved on 3% agarose gels, and gel images were obtained with an AlphaImager 1220 Version 5.5 (ProteinSimple). Amplicon sizes were 360 bp for the wild type *Ilk* allele, 380 bp for the floxed *Ilk* allele, 281 bp for *Cre*, and 420 bp for *Cpxm1*.

## 2.4 Isolation and culture of primary mouse epidermal keratinocytes

Three-day-old *K14Cre<sup>+/+</sup>;Ilk<sup>fl/fl</sup>* and *K14Cre<sup>+/+</sup>;Ilk<sup>fl/fl</sup>* littermates were euthanized by CO<sub>2</sub> inhalation, and skins were harvested as described (Dagnino et al., 2010; Ho et al., 2009). Following euthanasia, mice were immersed for 15 minutes in 70% isopropanol at room temperature. The skins were harvested and each skin was placed dermis-side down in a well of a 6-well plate containing 2 ml of freshly diluted 0.25% trypsin. The skins were incubated at 4°C for 16 hours. Concurrently, tail clippings for genotyping were isolated. After determining the genotype of each skin, the trypsin was removed by aspiration, and replaced with fresh 0.25% trypsin. The skins were then incubated at 37°C for 20 minutes. The epidermis was mechanically separated from the dermis using forceps, placed into 50-ml Falcon™ conical tubes (BD, Catalogue No. 352098) containing keratinocyte growth medium (Ca<sup>2+</sup>-free EMEM supplemented with 8% Chelex resin-treated fetal bovine serum (FBS), 100 U/ml penicillin, 100 µg/ml streptomycin, 74 ng/ml hydrocortisone, 5 µg/ml insulin, 9.5 ng/ml cholera toxin, 5 ng/ml epidermal growth factor (EGF), and 6.7

ng/ml triiodothyronine (T3)), and minced with scissors. The epidermis fragments were gently rocked in a tissue culture incubator at 37°C for 20 minutes to obtain a cell suspension. The latter was filtered through 70- $\mu$ m pore size Falcon™ cell strainers (BD, Catalogue No. 352350) to remove cornified envelope fragments. Trypan blue-excluding, viable cells were counted on a haemocytometer. The cells were plated onto 60- or 100-mm Primaria™ culture dishes (Corning, Catalogue No. 734-0071; 734-0072, respectively) at a density of  $3 \times 10^6$  cells/21 cm<sup>2</sup> or  $7.5 \times 10^6$  cells/58 cm<sup>2</sup> for *K14Cre<sup>+/-</sup>;Ilk<sup>fl/+</sup>* keratinocytes, or  $3.5 \times 10^6$  cells/21 cm<sup>2</sup> or  $9 \times 10^6$  cells/58 cm<sup>2</sup> for *K14Cre<sup>+/-</sup>;Ilk<sup>fl/fl</sup>* keratinocytes. After 24 hours, the growth medium was replaced, and medium changes were subsequently conducted every 48 hours. Keratinocytes were cultured at 37°C in a humidified atmosphere containing 5% CO<sub>2</sub>. All experiments were conducted on keratinocytes that had been cultured for 48-72 hours, and that had reached 70-80% confluence.

Where indicated, cells were cultured in Ca<sup>2+</sup>-free EMEM supplemented only with fetal bovine serum (FBS), without FBS but with hydrocortisone, insulin, cholera toxin, EGF, and T3 (HICE T3), or supplemented only with 25  $\mu$ M bovine serum albumin (BSA).

For experiments containing H<sub>2</sub>O<sub>2</sub> treatments, a stock of 50 mM H<sub>2</sub>O<sub>2</sub> was originally diluted from commercially available 30% H<sub>2</sub>O<sub>2</sub> diluted in phosphate buffered saline (PBS), and sterilized by filtration through 0.2- $\mu$ m pore size filters prior to use. Working H<sub>2</sub>O<sub>2</sub> dilutions were then prepared using culture medium, immediately before use.

For experiments involving treatment with *N*-Acetyl-L-cysteine (NAC), this chemical was diluted in sterile PBS to a final concentration of 125 mM, and 1 M NaOH was used to

adjust the pH to 7.4. The NAC solution was sterilized by filtration through a 0.2- $\mu\text{m}$  pore size filter prior to addition to cell cultures.

## 2.5 Measurement of cell proliferation

Keratinocytes isolated from *Ilk<sup>fl/fl</sup>*, *K14Cre<sup>+/-</sup>;Ilk<sup>fl/+</sup>*, or *K14Cre<sup>+/-</sup>;Ilk<sup>fl/fl</sup>* epidermis were plated at  $2 \times 10^5$  cells/2 cm<sup>2</sup>. At timed intervals after plating, cells were washed once with PBS and incubated with 200  $\mu\text{l}$  of 0.25% trypsin-EDTA for 5-10 minutes at 37°C. The detached cells were collected and an equal volume of 0.5% trypan blue dye was added to each sample. Trypan-blue excluding cells were counted on a haemocytometer.

## 2.6 Measurement of DNA synthesis

Primary mouse keratinocytes were plated in 24-well culture dishes at  $2.5 \times 10^5$  cells/2 cm<sup>2</sup>. At timed intervals after plating, cells were incubated in growth medium containing 10  $\mu\text{M}$  bromodeoxyuridine (BrdU) for 2 hours at 37°C. The cells were fixed, permeabilized, and washed as described in Section 2.11. Nuclear DNA was denatured by incubating with 2 M HCl for 20 minutes at 22°C. The samples were thoroughly washed five times with PBS, for 10 minutes each wash, and incubated with anti-BrdU antibody, with gentle rocking for 2 hours at 22°C, or for 16 hours at 4°C. Incubation with primary antibody was followed by washes and incubation with AlexaFluor<sup>TM</sup>-conjugated goat anti-mouse antibodies. The samples were washed and mounted as described Section 2.11.

## 2.7 Apoptosis measurements

Apoptosis was measured using Cell Death Detection ELISA kits (Roche, Catalogue No. 11544675001), following the manufacturer's instructions. *K14Cre<sup>+/-</sup>;Ilk<sup>fl/+</sup>* and *K14Cre<sup>+/-</sup>;Ilk<sup>fl/fl</sup>* keratinocytes were plated at a density of  $1 \times 10^5$  cells/2 cm<sup>2</sup> on a 24-well plate. Twenty-four hours after plating, the cells were washed once with sterile PBS and the growth medium was replaced with treatment media (Complete, FBS, HICET3, or BSA). Cells were cultured for 16 hours at 37°C. The cells were washed with sterile PBS and then lysed using a modified RIPA buffer (50 mM Tris-HCl pH 7.4, 150 mM NaCl, 1% NP-40, 0.5% sodium deoxycholate, 1 mM PMSF, 10 mM Na<sub>3</sub>VO<sub>4</sub>, 1 µg/ml NaF, 1 µg/ml aprotinin, 1 µg/ml pepstatin, 1 µg/ml leupeptin) for 40 minutes on ice. Triplicate, 20-µl samples of each lysate were added to the 96-well streptavidin-coated microplate provided in the kit. Next, 80 µl of a solution containing anti-DNA-peroxidase and anti-histone-biotin was transferred to each well and incubated for 90 minutes at 22°C. Cells were washed once with sterile PBS, 100 µl of 2,2'-azino-bis(3-ethylbenzothiazoline-6-sulphonic acid) substrate were added to each well and incubation proceeded for 15 minutes at 22°C. The absorbance of these solutions was measured at 490 nm (reference wavelength), and 405 nm with respect to a substrate solution blank containing no lysate. In separate, untreated wells, cells were trypsinized using 0.25% trypsin-EDTA and trypan-blue excluding cells were counted on a haemocytometer. The absorbance values obtained in each sample were then normalized for cell number.

## 2.8 Preparation of cell lysates for protein analysis

To prepare keratinocyte lysates, cells were gently scraped from culture dishes using a Teflon cell scraper, and collected in the culture medium. This cell suspension was transferred to a 15-ml conical tube and centrifuged at 200 x g for 10 minutes at 22°C. After centrifugation, the supernatants were removed by aspiration, and the cell pellets were either processed immediately to prepare lysates, or frozen in liquid nitrogen for storage at -80°C until used.

For immunoblotting experiments, keratinocyte pellets were resuspended in approximately four pellet volumes of a modified radioimmunoprecipitation assay (RIPA) buffer (50 mM Tris-HCl pH 7.4, 150 mM NaCl, 1% NP-40, 0.5% sodium deoxycholate, 1 mM PMSF, 10 mM Na<sub>3</sub>VO<sub>4</sub>, 1 µg/ml NaF, 1 µg/ml aprotinin, 1 µg/ml pepstatin, 1 µg/ml leupeptin) and incubated on ice for 30 minutes. Lysates were then centrifuged at 18,000 x g for 10 minutes at 4°C, and the supernatants were transferred to a new microcentrifuge tube. The protein concentration in each lysate sample was determined using Bradford assays.

In experiments involving analysis of phosphorylated proteins, cell pellets were resuspended as above, but the buffer used was PhosphoSafe extraction reagent supplemented with 1 mM PMSF. Unless otherwise indicated, 50 µg of protein per sample were used for immunoblot analyses.

## **2.9 Denaturing polyacrylamide gel electrophoresis and immunoblotting**

Cell lysates were heated to 99°C for 7 minutes, and then resolved by denaturing polyacrylamide gel electrophoresis (SDS-PAGE), (5% stacking and 10% or 15% resolving polyacrylamide). Proteins in the gel were transferred to Immobilon-P Polyvinylidene fluoride (PVDF) membranes (Millipore, Catalogue No. IPVH00010) using a semi-dry transfer apparatus. After transfer, the membranes were blocked in 5% skim milk diluted in Tris-buffered saline supplemented with 0.05% Tween-20 (TBST, 100 mM Tris-HCl pH 7.5, 0.9% NaCl) with gentle rocking for 1 hour at 22°C. The membranes were probed with primary antibodies indicated in individual experiments, diluted in TBST. For incubations with primary antibodies, the membranes were placed in 50-ml Falcon™ tubes containing 5 ml of the appropriate antibody dilutions, and the tubes were secured to a rotating platform. The tubes were rotated at 8 rpm for 2 hours at 22°C, or overnight at 4°C. Following incubation with primary antibodies, the membranes were washed three times with TBST for 5 minutes per wash. They were then incubated with the appropriate HRP-conjugated secondary antibody (1:5000 v/v in 5% skim milk diluted in TBST) for 1 hour at 22°C. Membranes were washed thoroughly three times with TBST for 15 minutes per wash. Amersham ECL Prime Western Blotting Detection Reagent was added to the membranes and proteins were visualized using UltraCruz autoradiography film (Santa Cruz, Catalogue No. SC-201697). All results presented are a representative of 3-5 biological replicates.

When necessary, the PVDF membranes were stripped using a guanidine hydrochloride-based stripping solution (20 mM Tris-HCl pH 7.5, 6 M guanidine hydrochloride, 0.02% NP-40, 0.8% 2-mercaptoethanol) (Yeung and Stanley, 2009). To this end, membranes were incubated with gentle rocking in stripping solution for 10 minutes at 22°C. The solution was replaced with fresh stripping solution and incubation proceeded for 10 additional minutes. The membranes were then washed thrice with 15 ml of TBST (10 minutes per wash), before probing with another primary antibody.

To quantify protein levels in immunoblots, densitometry analysis was conducted using ImageJ (Fiji) (Schindelin et al., 2012). Rectangles of equal size were drawn around the bands of interest on scanned images of immunoblots. A profile plot of each band as well as the background area was obtained, which represented the pixel density in a given rectangle. Background values were subtracted, and the densitometric value of each lane was obtained.

## **2.10 Preparation of glass coverslips**

Glass coverslips were incubated for 4 to 16 hours in 1 M HCl at 50-60°C. Once cooled, the glass coverslips were rinsed thoroughly with 18 M $\Omega$  water, washed with ethanol, and allowed to dry. The coverslips were then coated with poly-L-lysine (PLL) (1 mg/ml) by rocking for 1 hour at 22°C. PLL-coated coverslips were washed thoroughly with 18 M $\Omega$  water and allowed to dry. The glass coverslips were then sterilized by immersion 70% ethanol for 10 minutes at 22°C, and washed three times with sterile PBS. Sterile

coverslips were further coated overnight at 37°C with a solution containing 50 µg/ml rat tail collagen type I dissolved in 0.02 N acetic acid, followed by three washes with sterile PBS.

## **2.11 Confocal and immunofluorescence microscopy**

For experiments involving immunofluorescence or confocal microscopy, primary keratinocytes isolated from ILK-expressing and ILK-deficient epidermis were seeded on glass coverslips at a density of  $3 \times 10^5$  cells/2 cm<sup>2</sup> and  $8 \times 10^5$  cells/2 cm<sup>2</sup>, respectively. When cells reached 80% confluence, they were fixed with freshly diluted 4% PFA for 40 minutes on ice, and washed thoroughly with PBS three times. Cells were permeabilized with 0.1% Triton X-100 solution in PBS for 20 minutes at 22°C and then washed with PBS three times. The samples were blocked in 3% skim milk containing 5% goat serum for 1 hour at 22°C with gentle rocking. After three washes with PBS, primary antibody solution was added and incubation proceeded at 22°C for 2 hours, or 4°C overnight with gentle rocking, as indicated in individual experiments. Primary antibodies were diluted in PBS containing 5% goat serum. Cells were then washed three times with PBS at 22°C with gentle rocking (5 minutes per wash) and incubated with the appropriate AlexaFluor<sup>TM</sup>-conjugated secondary antibody (1:500 v/v in PBS with 3% skim milk and 1% goat serum) for 1 hour at 22°C, protected from light. Cells were washed three times with PBS (10 minutes per wash) and then incubated with Hoechst 33342 to visualize nuclear DNA (1:10,000 v/v, 1 µg/ml, final) for 15 minutes at 22°C with gentle rocking. Following three 5-minute washes with PBS, the glass coverslips were mounted onto



microscope slides, using Immu-mount mounting medium. Samples were allowed to dry overnight at 22°C in the dark before analysis. Immunofluorescence micrographs were obtained with a Leica DMIRBE fluorescence microscope (Leica Microsystems, Wetzlar, Germany) equipped with an Orca-ER digital camera (Hamamatsu Photonics, Hamamatsu, Japan), using Volocity 4.3.2 software. Confocal images were obtained using ZEN 2009 software (Zeiss, Germany) and a Zeiss LSM5 DUO scanner laser confocal microscope (Jena, Germany), equipped with a 63X/1.4 NA oil immersion lens.

For analysis of Bax localization to the mitochondrial marker Tom20, colocalization analysis was conducted on a pixel-by-pixel basis using the ZEN2009 software. For each biological replicate, the regions of interest (ROI) of 27 to 33 cells were selected. The pixel distributions of each ROI were displayed and colocalization values were calculated. The green (Bax) and red (Tom20) colocalization coefficients were calculated by summing the number of colocalized pixels of each ROI and dividing by the total sum of either green or red pixels, respectively. Colocalization values were adjusted for pixel intensity of the individual channels, giving rise to the weighted colocalization coefficients.

## **2.12 Quantification of reactive oxygen species (ROS)**

*K14Cre<sup>+/-</sup>;Ilk<sup>fl/+</sup>* and *K14Cre<sup>+/-</sup>;Ilk<sup>fl/fl</sup>* keratinocytes were plated at a density of  $1 \times 10^5$  cells/0.32 cm<sup>2</sup> on a 96-well plate coated with a 50 µg/ml collagen solution. Two days after plating, the cells were washed once with sterile PBS and incubated with 100 µl of

10  $\mu\text{M}$  2',7'-dichlorofluorescein diacetate (DCFDA) dye dissolved in sterile PBS for 45 minutes at 37°C in the dark. The DCFDA solution was removed by aspiration, and cells were washed once with sterile PBS. Solutions containing  $\text{H}_2\text{O}_2$  (50, 100, 200, 400, and 500  $\mu\text{M}$ ) were prepared using sterile PBS from a 50 mM  $\text{H}_2\text{O}_2$  stock (as described in Section 2.4). In duplicate, 100  $\mu\text{l}$  of each  $\text{H}_2\text{O}_2$  dilution was then added to each well. Fluorescence was read on a microplate reader at timed intervals after  $\text{H}_2\text{O}_2$  addition (5, 10, 15, 20, 35, 50 minutes), with an excitation wavelength of 490 nm and an emission wavelength of 535 nm using Softmax Pro Version 5 software. In separate, untreated wells, cells were trypsinized using 50  $\mu\text{l}$  of 0.25% trypsin-EDTA and trypan-blue excluding cells were counted on a haemocytometer. Fluorescence values were normalized for cell number.

In experiments using N-acetylcysteine, cells were washed once with sterile PBS and incubated with 100  $\mu\text{l}$  of 2 or 5 mM NAC diluted in culture medium for 40 minutes at 37°C prior to the addition of DCFDA. The cells were then processed as described above.

## **2.13 Statistical analysis**

Statistical analyses were conducted using one-way analysis of variance (ANOVA) with Bonferroni post-hoc test using GraphPad Prism version 5. Significance was set to  $P \leq 0.05$ .

All experiments were conducted 3-5 times.

## Chapter 3 – Results

All experiments were completed by Michelle Im except for the following: (i) measurement of apoptosis was performed by T.S. Irvine.

### 3.1 Proliferation of ILK-deficient keratinocytes

Integrins and their downstream effectors play a key role in cell-ECM attachment and signal transduction (reviewed in Hinz, 2010). Specifically, in epidermal keratinocytes, integrins are essential for keratinocyte spreading, adhesion, and proliferation (Choma et al., 2006; Raghavan et al., 2000). ILK is a  $\beta 1$  integrin effector, but its contribution to keratinocyte proliferation and viability remain unknown. To begin to address this issue, I first determined the role of ILK in keratinocyte proliferation by comparing changes in cell numbers as a function of time in ILK-expressing and ILK-deficient cultures. Keratinocytes isolated from ILK-expressing *K14Cre;Ilk<sup>fl/fl</sup>* and ILK-deficient *K14Cre;Ilk<sup>fl/fl</sup>* mice were seeded on 24-well plates at a density of 200,000 cells per well. Twenty-four hours after plating, the number of trypan blue-excluding, viable cells averaged 114,000 and 95,000 cells per well in the ILK-expressing and ILK-deficient cultures, respectively (Figure 3.1). This indicates a plating efficiency of 50-55% for cells of both genotypes. The number of *K14Cre;Ilk<sup>fl/fl</sup>* keratinocytes remained constant until 72 hours after plating, and increased thereafter, so that by 120 hours in culture, the number of cells averaged 200,000 per well (Figure 3.1). In contrast, the number of ILK-deficient *K14Cre;Ilk<sup>fl/fl</sup>* cells progressively decreased, reaching approximately 30,000 cells per well 120 hours after plating. This decrease in cell number suggests that ILK-deficient keratinocytes may



**Figure 3.1. Proliferation of ILK-deficient keratinocytes.**

Keratinocytes isolated from *Ilk<sup>fl/fl</sup>*, *K14Cre;Ilk<sup>fl/+</sup>*, and *K14Cre;Ilk<sup>fl/fl</sup>* mice were plated at  $2 \times 10^5$  cells/2 cm<sup>2</sup>. At the indicated times after plating, the number of cells was determined. The results are expressed as the mean  $\pm$ SD (n=3). \* indicate  $p < 0.05$ , relative to cell numbers at the corresponding times in *Ilk<sup>fl/fl</sup>* keratinocytes (ANOVA).

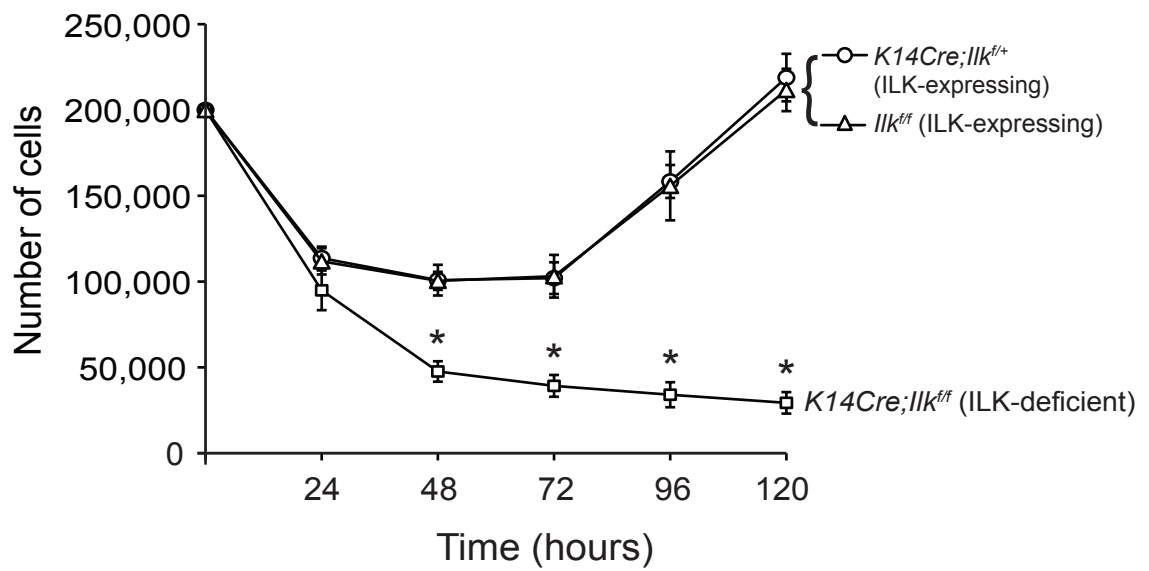


exhibit survival and proliferation defects. Similar experiments were conducted with *Ilk<sup>fl/fl</sup>* cells, which contain two functional *Ilk* alleles. The changes in cell number over time in these cells were indistinguishable from those observed in *K14Cre;Ilk<sup>fl/fl</sup>* cells (Figure 3.1), suggesting that gene dosage effects on proliferation are negligible, if any.

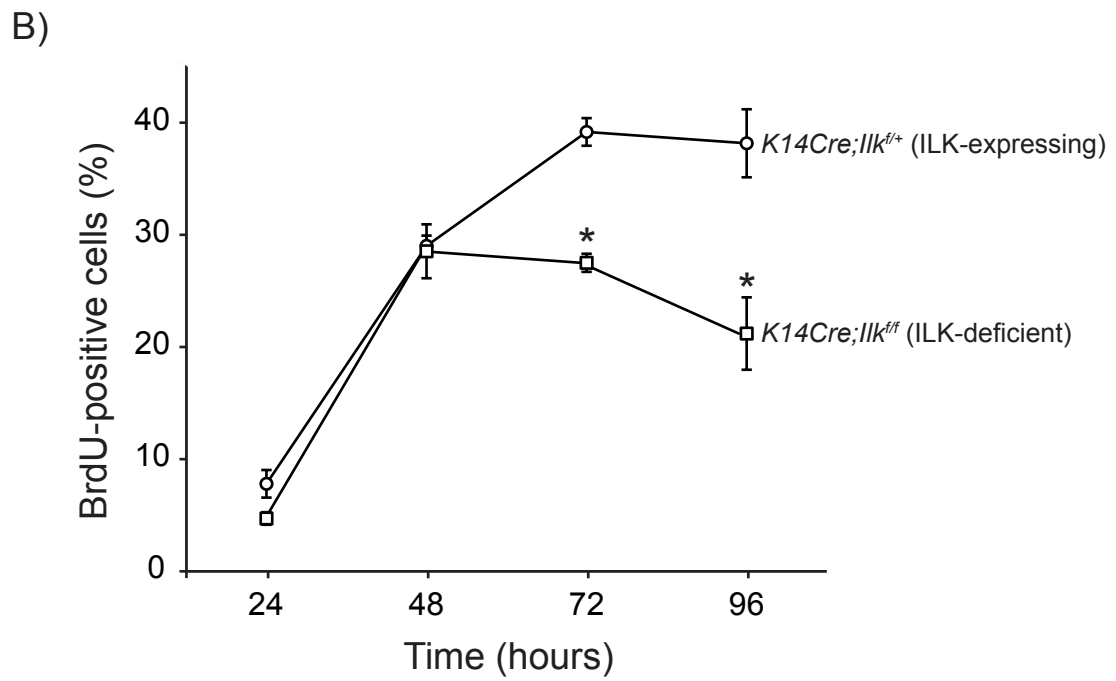
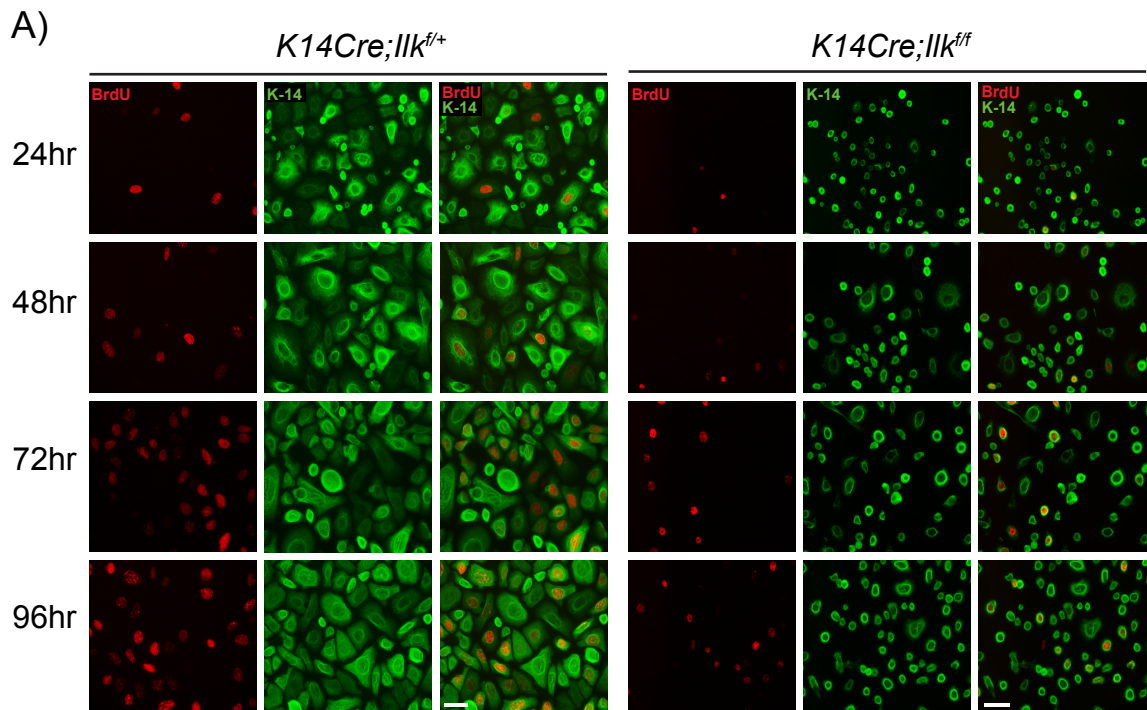
In a complementary approach, I measured the fraction of cells synthesizing DNA in these cultures. To this end, I determined the fraction of cells capable of incorporating bromodeoxyuridine (BrdU) into their DNA. BrdU is a synthetic thymidine analog used to quantify proliferating cells, as it is incorporated into DNA during the S phase of the cell cycle (Pierce et al., 1994). To quantify the percentage of keratinocytes in S-phase, *K14Cre;Ilk<sup>fl/fl</sup>* and *K14Cre;Ilk<sup>fl/fl</sup>* cells were incubated with BrdU for 2 hours, and the fraction of BrdU-positive was then determined by immunofluorescence microscopy (Figure 3.2A). Twenty-four hours after plating, the percentage of BrdU-positive keratinocytes was 8% and 5%, in cells isolated from ILK-expressing and ILK-deficient epidermis, respectively (Figure 3.2B). By 48 hours, the proportion of BrdU-positive keratinocytes significantly increased to approximately 30% in both cell types. However, 72 hours after plating, there was a significant decrease in BrdU-positive ILK-deficient cells and after 96 hours in culture, the percentage of BrdU-positive keratinocytes had reached approximately 40% in ILK-expressing cells, whereas it was only 20% in ILK-deficient cells. Together, these findings indicate that ILK-deficient keratinocytes have a reduced proliferative capacity compared to ILK-expressing cells.





**Figure 3.2. Proportion of BrdU-positive cells in ILK-deficient epidermis.**

Keratinocytes isolated from *K14Cre;Ilk<sup>fl/+</sup>* and *K14Cre;Ilk<sup>fl/fl</sup>* mice were plated at  $2 \times 10^5$  cells/2 cm<sup>2</sup>. Epidermal keratinocytes were incubated with 10 μM bromodeoxyuridine (BrdU) for 2 hours at 37°C. A) The presence of BrdU was assessed by immunofluorescence microscopy. At the indicated times after plating, the number of BrdU-positive cells was determined. Bar, 32 μm. B) The results are expressed as the mean ±SE of 100 cells per genotype (n=3). \* indicate p<0.05, relative to percentages of BrdU-positive cells at corresponding times in ILK-expressing *K14Cre;Ilk<sup>fl/+</sup>* keratinocytes (ANOVA).



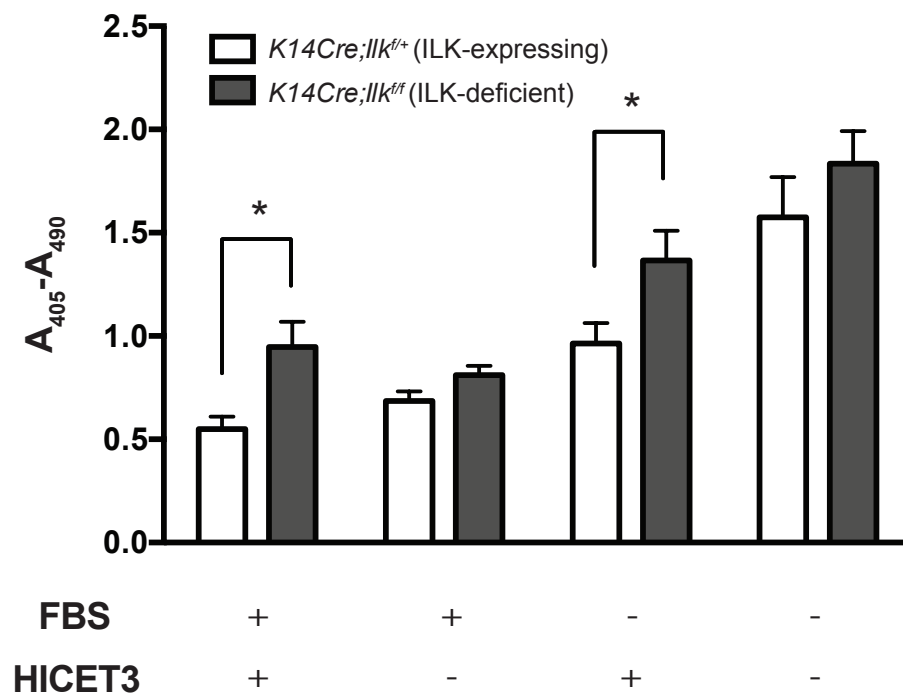
## 3.2 Apoptosis in cultured ILK-deficient keratinocytes

The reduction in the number of ILK-deficient cells observed in the experiments of Figure 3.1 may arise from decreases in cell viability, in addition to an impaired ability to traverse the cell cycle. Cell death can occur through various mechanisms, including apoptosis. Apoptosis is a highly regulated programme of cell death, characterized at its latest stages by the activation of endogenous nucleases, which cleave DNA at accessible internucleosomal sites (Yoshida et al., 2006). Thus, I next examined if there are differences in the levels of mono- and oligonucleosomes in cytosolic fractions of cell lysates, indicative of apoptotic cells in these cultures. Under optimal culture conditions (i.e. in the presence of serum and growth factors necessary to maintain keratinocytes), ILK-deficient keratinocytes exhibited a higher content of mono- and oligonucleosomes than ILK-expressing cells (Figure 3.3), indicating a larger proportion of apoptotic cells in these cultures. Culture of mammalian cells requires growth and survival factors. In keratinocyte cultures, these factors are provided by the fetal bovine serum and HICET3 supplements (hydrocortisone, insulin, cholera toxin, EGF, and triiodothyronine) present in the growth medium. To investigate if ILK-deficient keratinocytes are more sensitive than normal cells to growth factor deprivation, I measured apoptosis in cells cultured in the absence of HICET3, FBS, or both. In medium with FBS but lacking HICET3, there were no significant differences in the proportion of apoptotic cells between ILK-expressing and ILK-deficient cultures (Figure 3.3). In contrast, ILK-deficient keratinocytes cultured with HICET3, but without FBS, demonstrated significantly greater apoptosis than ILK-expressing cells (Figure 3.3). Finally, both cell types displayed



**Figure 3.3. Effect of *Ilk* gene inactivation on apoptosis.**

Keratinocytes isolated from *K14Cre;Ilk<sup>f/+</sup>* and *K14Cre;Ilk<sup>ff</sup>* mice were plated at  $1 \times 10^5$  cells/  $2 \text{ cm}^2$ . Cells were cultured in the indicated treatment conditions for 16 hours. Cell death was photometrically quantified as a function of mono- and oligonucleosome concentration in the cytoplasmic fraction of cell lysates in indicated conditioned medium. The results are expressed as the mean +SEM (n=6) and \* indicate  $p < 0.05$ , relative to absorbance in ILK-expressing *K14Cre;Ilk<sup>f/+</sup>* keratinocytes (ANOVA). Absorbance was measured at 490 nm as the reference wavelength, and 405 nm with respect to a substrate solution blank.



similar levels of apoptosis in the absence of all growth factors (when medium was only supplemented with BSA) (Figure 3.3). These findings indicate that, in addition to a diminished ability to proliferate, ILK-deficient cells have increased sensitivity to growth factor deprivation and enhanced susceptibility to apoptosis, even in “optimal” culture conditions.

### **3.2.1 Role of the Akt pathway in increased apoptosis in ILK-deficient keratinocytes**

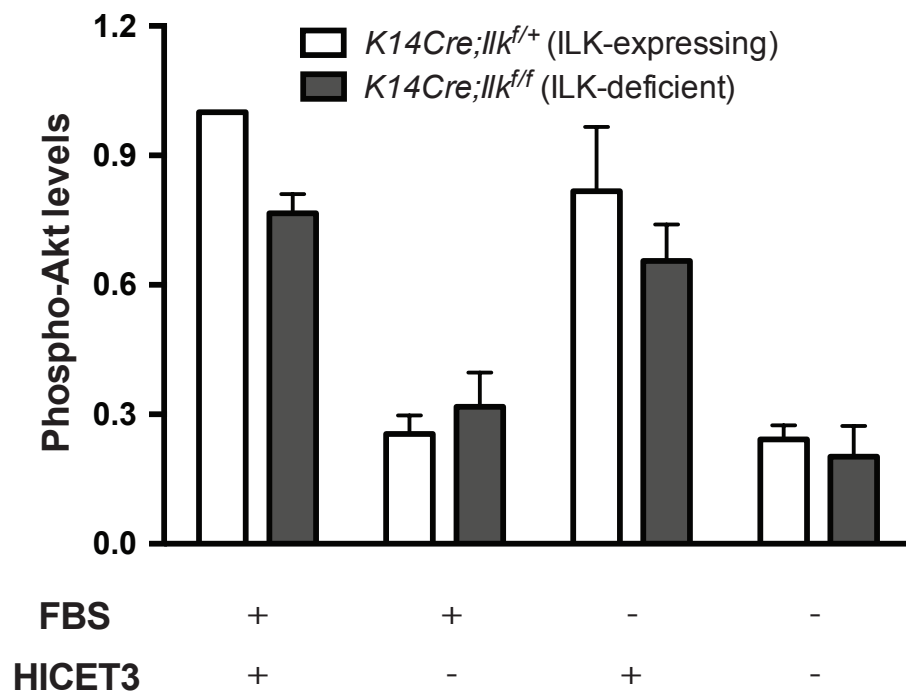
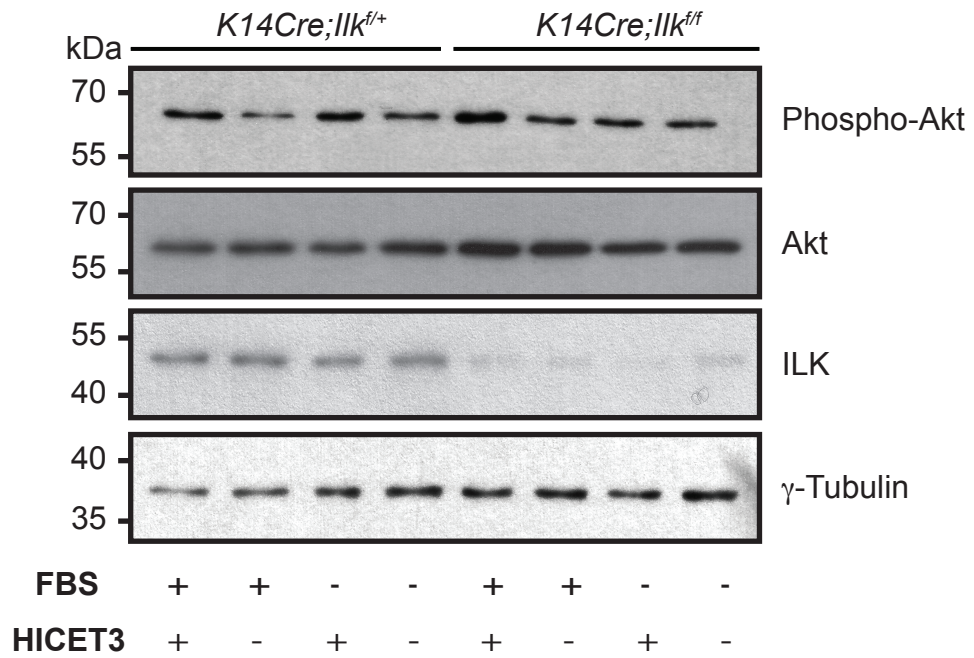
To begin to elucidate the signalling pathway involved in the ILK-mediated survival of keratinocytes, I investigated changes in levels of proteins that specifically participate in cell survival. Protein kinase B (Akt), having an established role in promoting survival in a number of cell types (Song, et al., 2005; Zhao et al., 2006), has often been linked to ILK and even suggested to be one of its direct, downstream substrates (McDonald et al., 2008). Cells from *K14Cre;Ilk<sup>f/+</sup>* and *K14Cre;Ilk<sup>f/f</sup>* mice were cultured under optimal growth conditions, or in medium containing only FBS, HICET3, or BSA, for 16 hours, and levels of phosphorylated, active Akt (phospho-Akt) were determined. Under all treatment conditions, there were no significant differences in phosphorylated levels of Akt between ILK-expressing and ILK-deficient keratinocytes (Figure 3.4). Thus, my findings suggest that *Ilk* inactivation does not lead to altered activation of Akt and the increased apoptosis observed in ILK-deficient keratinocytes seems to be independent of the Akt pathway.





**Figure 3.4. Effect of *Ilk* gene inactivation on Akt phosphorylation.**

Keratinocytes isolated from *K14Cre;Ilk<sup>f/+</sup>* and *K14Cre;Ilk<sup>f/f</sup>* epidermis were cultured in the indicated treatment conditions for 16 hours. Protein lysates were prepared and resolved by denaturing gel electrophoresis, followed by immunoblot analysis using indicated antibodies (top panel). Densitometry analyses are expressed as the mean +SEM (n=3) relative to corresponding expression levels in ILK-expressing *K14Cre;Ilk<sup>f/+</sup>* keratinocytes in Complete medium (set to 1).



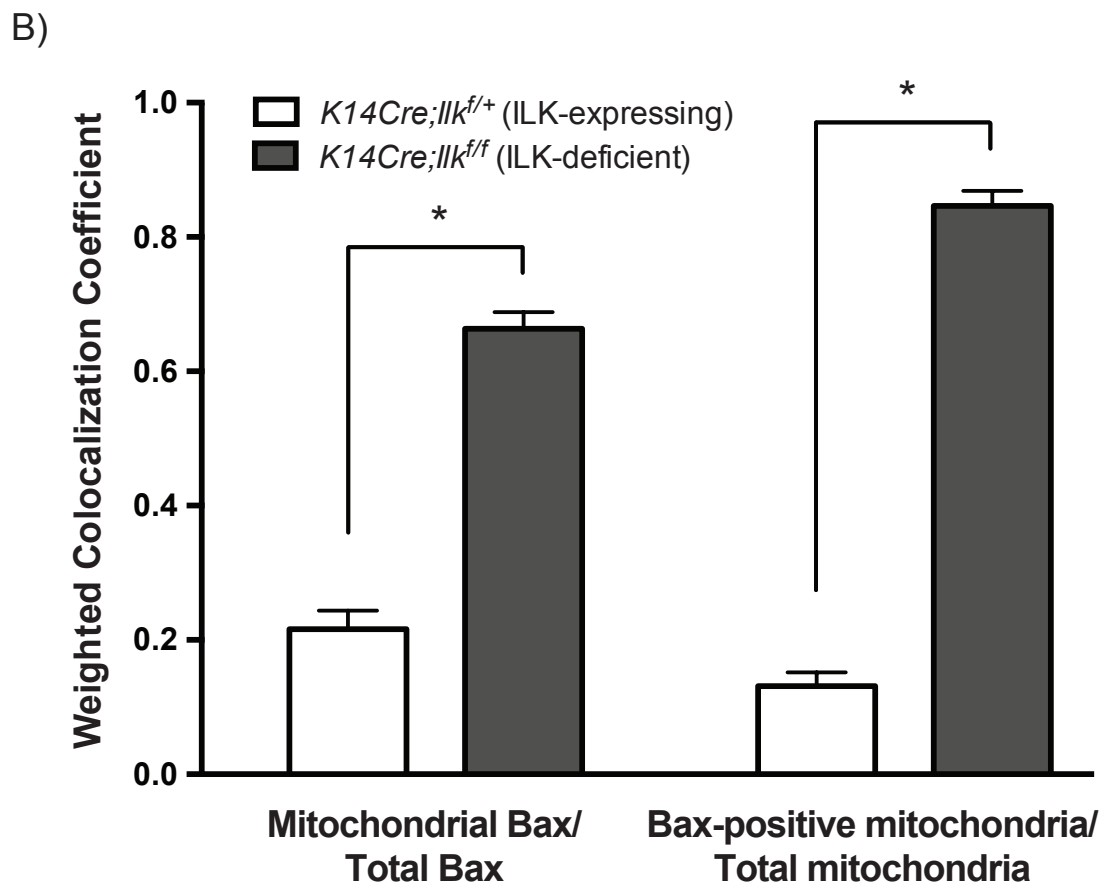
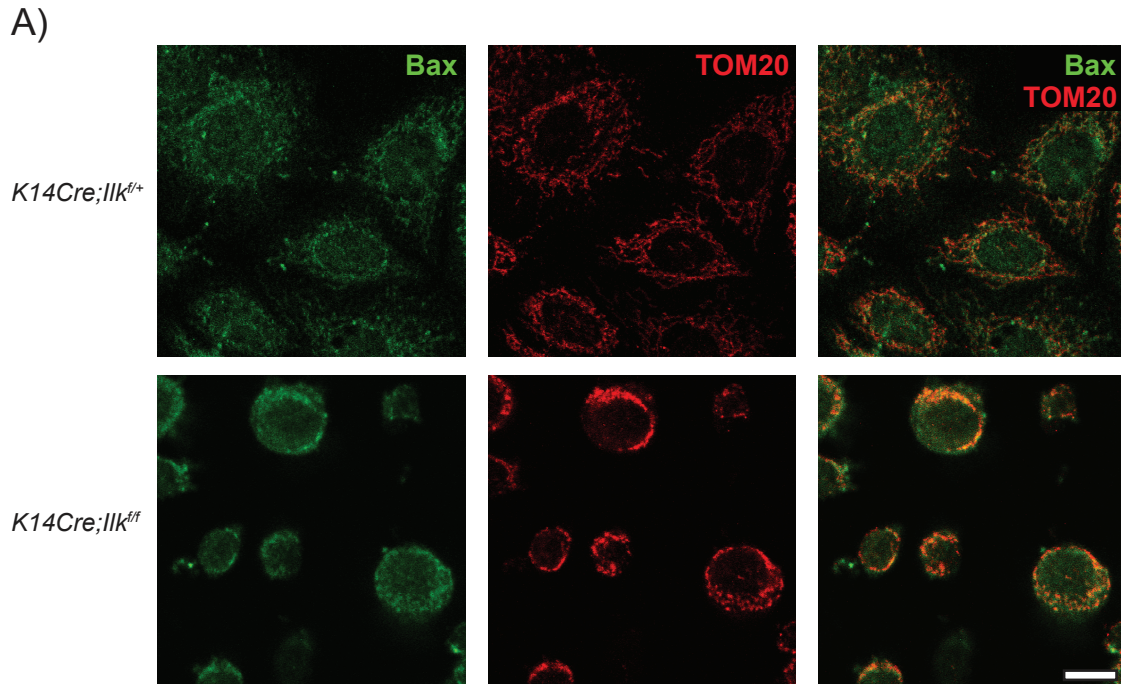
### **3.3 Role of the mitochondrial localization of Bax in apoptosis of ILK-deficient keratinocytes**

Bax is a pro-apoptotic protein that localizes to the cytoplasm in viable cells, but translocates to the outer membrane of the mitochondria to mediate the release of additional pro-apoptotic proteins into the cytoplasm, eventually resulting in cell death (Stankiewicz et al., 2005). Mitochondrial translocation of Bax is involved in the activation of the caspase-dependent intrinsic apoptotic pathway (Laethem et al., 2004). To investigate if changes in Bax distribution accompany the increased apoptosis observed in ILK-deficient keratinocytes, I examined its subcellular localization by confocal microscopy. *K14Cre;Ilk<sup>+/+</sup>*, and *K14Cre;Ilk<sup>ff</sup>* cells were plated, fixed, and stained with Bax and Tom20 antibodies. Colocalization analysis on 27 to 33 individual cells per genotype was conducted based on pixel distribution. Colocalization coefficients were calculated for each cell and adjusted for pixel intensity of the individually, coloured channels. Whereas Bax was predominantly localized to the cytoplasm in ILK-expressing cells, a higher proportion of Bax was found to co-localize to the mitochondria in ILK-deficient keratinocytes (Figure 3.5A). In ILK-expressing keratinocytes, approximately 20% of the total cellular Bax was localized in the mitochondria. However, almost 65% of the total Bax were found to localize to the mitochondria in ILK-deficient cells (Figure 3.5B). Similarly, whereas ILK-expressing cells exhibited roughly 15% of Bax-positive mitochondria, almost 85% of the mitochondria in ILK-deficient keratinocytes co-localized with Bax (Figure 3.5B). My observations are consistent with the notion that this



**Figure 3.5. Bax mitochondrial localization in ILK-deficient cells.**

Keratinocytes isolated from *K14Cre;Ilk<sup>fl/+</sup>* and *K14Cre;Ilk<sup>fl/fl</sup>* mice were plated  $3 \times 10^5$  cells/2 cm<sup>2</sup> and  $8 \times 10^5$  cells/2 cm<sup>2</sup>, respectively. Epidermal keratinocytes were then fixed with 4% paraformaldehyde and stained for Bax and Tom20. A) Stained cells were visualized by confocal microscopy. Bar, 15 μm. B) Weighted colocalization coefficients were calculated using ZEN2009 software. The results are expressed as the mean ±SE of 27 to 33 cells per genotype (n=3). \* indicate p<0.05 (student's t-test).



increased Bax mitochondrial translocation may be involved in activating the downstream caspase-mediated apoptosis pathway in the absence of ILK. Thus, increased apoptosis in ILK-deficient keratinocytes is associated with Bax localization to the mitochondria, which may be involved in stimulating downstream caspases.

### **3.3.1 Activation of the MAPK pathway in ILK-deficient keratinocytes**

Bax translocation to the mitochondria is triggered by both intracellular and extracellular stress stimuli. The activation of the mitogen-activated protein kinase (MAPK) pathway is highly involved in cellular stress response and mediates the mitochondrial localization of Bax, ultimately leading to stress-induced apoptosis (Katiyar et al., 2001). Specifically, I sought to determine the effect of *Ilk* inactivation on the activation by phosphorylation of c-Jun N-terminal kinase (JNK) and extracellular signal-regulated kinase (ERK). ILK-deficient keratinocytes displayed higher levels of phospho-JNK (Figure 3.6) and phospho-ERK (Figure 3.7) compared to those in ILK-expressing cells, irrespective of whether the cells were cultured under optimal growth conditions or in growth factor-deficient medium. Thus, my findings suggest a possible involvement of the MAPK pathway in mediating apoptotic levels of keratinocytes, specifically through its modulatory role in the activation of the pro-apoptotic function of Bax.

### **3.3.2 Activation of Bax-caspase pathway in apoptosis in ILK-deficient keratinocytes**

The above observations prompted me to investigate if the increased apoptosis in ILK-deficient cells was accompanied by the formation of active caspases. During apoptosis,





**Figure 3.6. ILK-deficiency is associated with JNK phosphorylation.**

Keratinocytes isolated from *K14Cre;Ilk<sup>f/+</sup>* and *K14Cre;Ilk<sup>fl/fl</sup>* epidermis were cultured in the indicated treatment conditions for 16 hours. Protein lysates were prepared and resolved by denaturing gel electrophoresis, followed by immunoblot analysis using indicated antibodies (top panel). Levels of phospho-JNK are expressed as the mean +SEM (n=3) relative levels in ILK-expressing *K14Cre;Ilk<sup>f/+</sup>* keratinocytes in Complete medium (set to 1). \* indicate p<0.05, relative to expression levels in ILK-expressing *K14Cre;Ilk<sup>f/+</sup>* keratinocytes in corresponding conditioned medium (ANOVA, bottom panel).

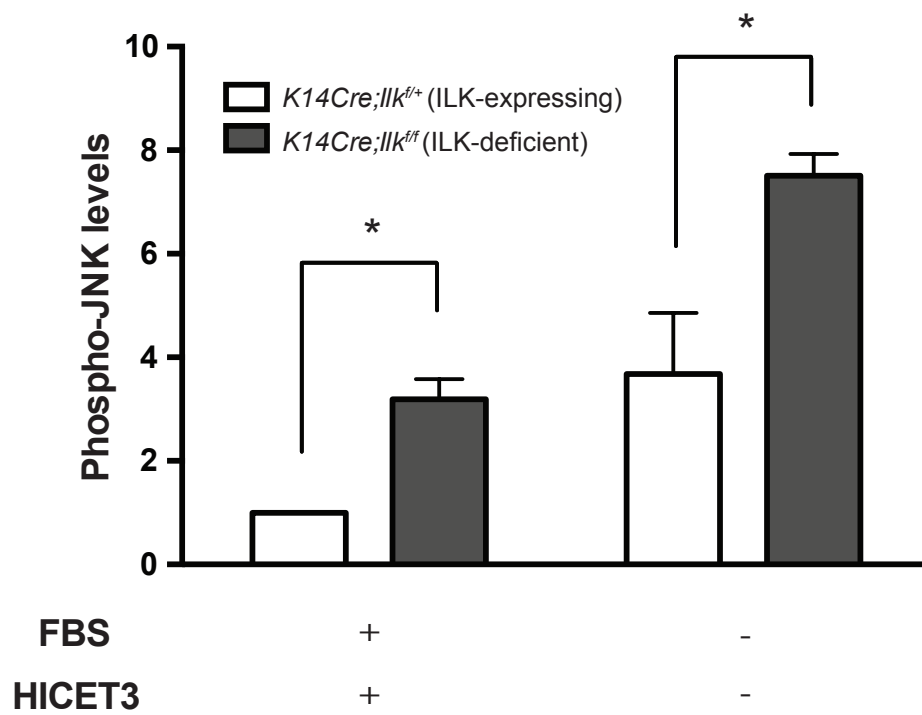
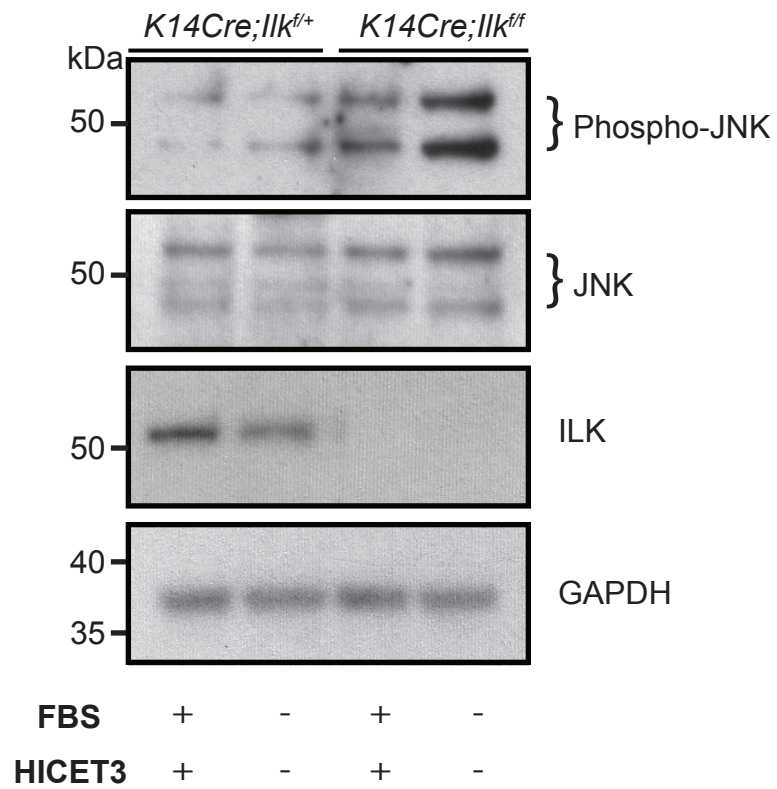
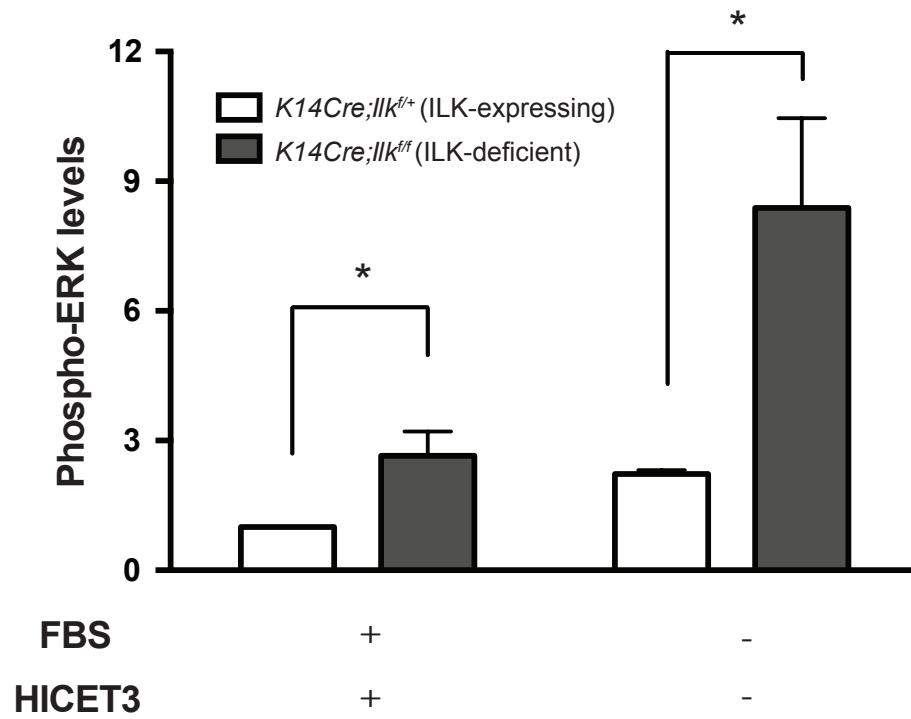
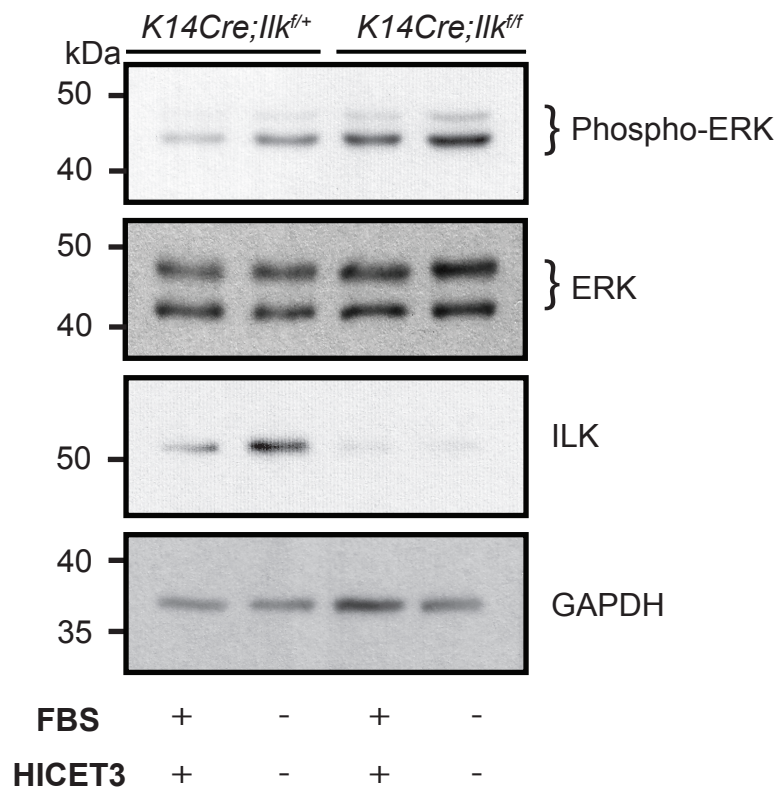




**Figure 3.7 ILK-deficiency is associated with ERK phosphorylation.**

Keratinocytes isolated from *K14Cre;Ilk<sup>f/+</sup>* and *K14Cre;Ilk<sup>fl/fl</sup>* epidermis were cultured in the indicated treatment conditions for 16 hours. Protein lysates were prepared and resolved by denaturing gel electrophoresis, followed by immunoblot analysis using indicated antibodies (top panel). Levels of phospho-ERK are expressed as the mean +SEM (n=3) relative levels in ILK-expressing *K14Cre;Ilk<sup>f/+</sup>* keratinocytes in Complete medium (set to 1). \* indicate p<0.05, relative to expression levels in ILK-expressing *K14Cre;Ilk<sup>f/+</sup>* keratinocytes in corresponding conditioned medium (ANOVA, bottom panel).



cytochrome c released from the mitochondria into the cytosol binds to the apoptotic protease-activating factor 1 to form apoptosomes (Du et al., 2000). This oligomerized complex then induces the autoactivation of procaspase-9, which in turn cleaves and activates downstream caspases, including caspase-3 (Du et al., 2000). Therefore, I examined the levels of active, cleaved caspase-3 in keratinocyte lysates cultured under normal or growth-factor deprivation conditions, as described in Section 3.2. Under optimal growth conditions, cleaved caspase-3 levels were significantly higher in ILK-deficient cells, relative to ILK-expressing keratinocytes (Figure 3.8). In medium containing only FBS, there were no significant differences in cleaved caspase-3 levels between cells isolated from ILK-expressing and ILK-deficient epidermis. Similarly, cleaved caspase-3 levels in ILK-deficient keratinocytes cultured in medium lacking FBS but containing HICET3, were indistinguishable from those displayed by ILK-expressing cells (Figure 3.8). However, ILK-deficient keratinocytes cultured in serum- and growth factor-free medium only supplemented with BSA displayed significantly increased levels of cleaved caspase-3 compared to ILK-expressing cells, even though cleaved caspase-3 abundance in BSA-containing medium was substantially higher in both ILK-expressing and ILK-deficient cells (Figure 3.8).

To complement these experiments, I also measured levels of cleaved Poly-ADP Ribose Polymerase (PARP). PARP is normally involved in repairing DNA damage; however, during apoptosis, caspase-3 cleaves and inactivates PARP (Boulares et al., 1999). Thus, the presence of cleaved PARP is indicative of the activation of caspase-3. Under optimal growth conditions, ILK-deficient keratinocytes displayed significantly greater levels of cleaved PARP relative to ILK-expressing cells (Figure 3.9). Similarly in medium with



**Figure 3.8. Effect of *Ilk* gene inactivation on cleavage of caspase-3.**

Keratinocytes isolated from *K14Cre;Ilk<sup>f/+</sup>* and *K14Cre;Ilk<sup>ff</sup>* epidermis were cultured in the indicated treatment conditions for 16 hours. Protein lysates were prepared and resolved by denaturing gel electrophoresis, followed by immunoblot analysis using indicated antibodies (top panel). Levels of cleaved Caspase-3 are expressed as the mean +SEM (n=3) relative levels in ILK-expressing *K14Cre;Ilk<sup>f/+</sup>* keratinocytes in Complete medium (set to 1). \* indicate p<0.05, relative to expression levels in ILK-expressing *K14Cre;Ilk<sup>f/+</sup>* keratinocytes in corresponding conditioned medium (ANOVA, bottom panel).



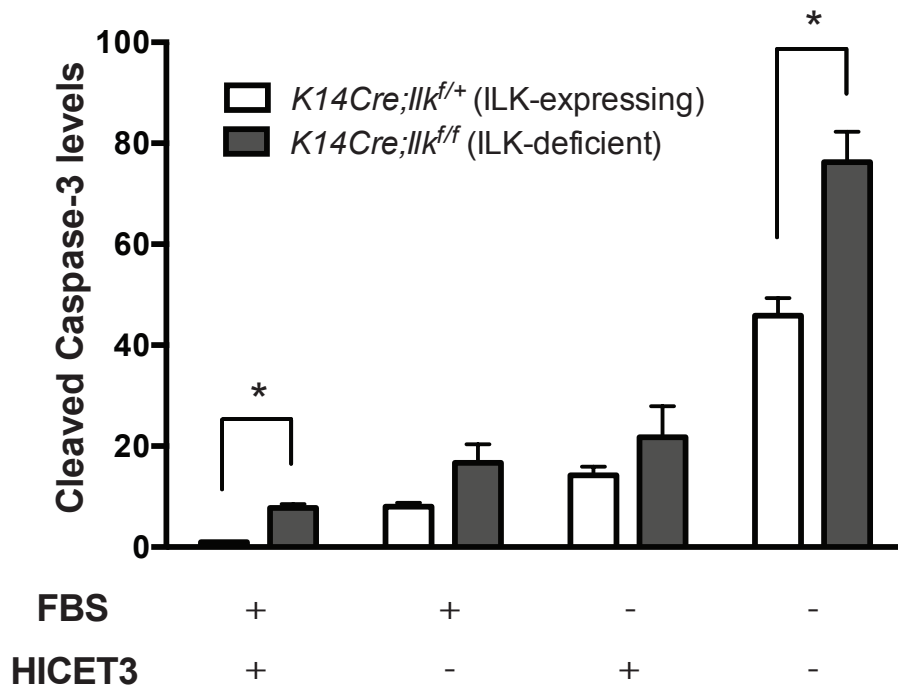
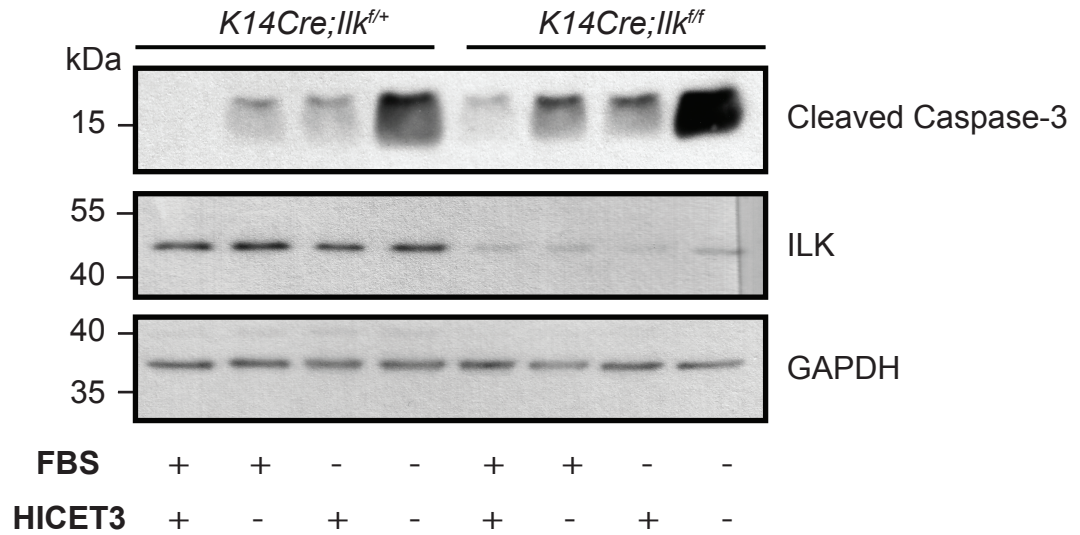
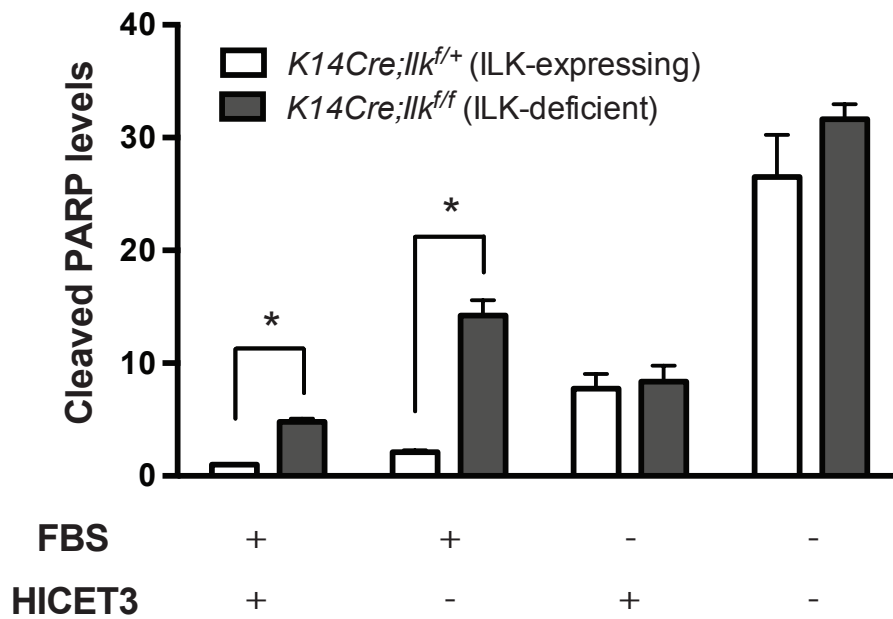
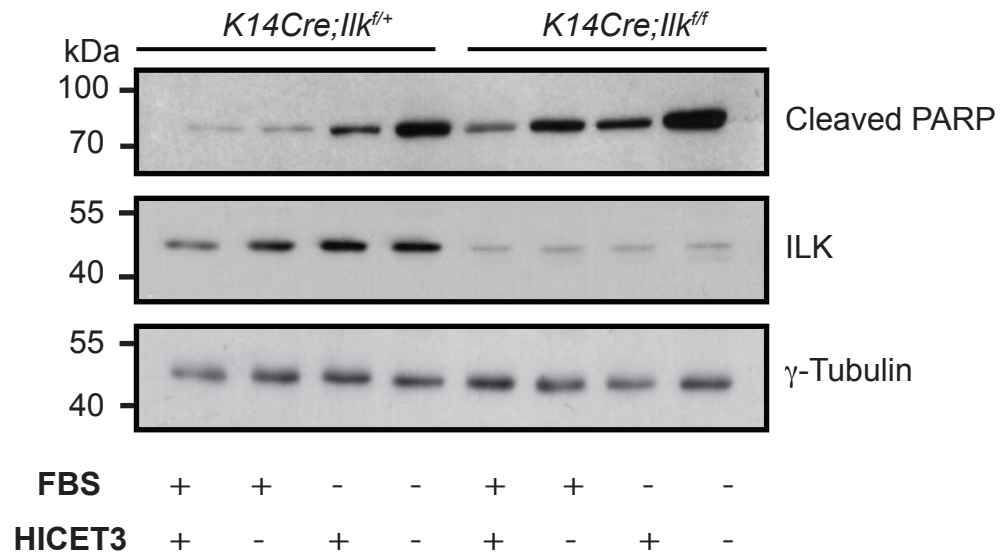




**Figure 3.9. ILK-deficiency is associated with PARP activation.**

Keratinocytes isolated from *K14Cre;Ilk<sup>f/+</sup>* and *K14Cre;Ilk<sup>fl/fl</sup>* epidermis were cultured in the indicated treatment conditions for 16 hours. Protein lysates were prepared and resolved by denaturing gel electrophoresis, followed by immunoblot analysis using indicated antibodies (top panel). Levels of cleaved PARP are expressed as the mean +SEM (n=3) relative levels in ILK-expressing *K14Cre;Ilk<sup>f/+</sup>* keratinocytes in Complete medium (set to 1). \* indicate p<0.05, relative to expression levels in ILK-expressing *K14Cre;Ilk<sup>f/+</sup>* keratinocytes in corresponding conditioned medium (ANOVA, bottom panel).



only FBS, cleaved PARP levels were significantly higher (approximately 5-fold) in ILK-deficient cells, relative to ILK-expressing control keratinocytes. In cultures maintained in medium with HICET3 or BSA only, levels of cleaved PARP were indistinguishable between keratinocytes isolated from ILK-expressing and ILK-deficient epidermis, and cellular levels of cleaved PARP were highest in growth factor-deprived cultures (Figure 3.9). These findings are consistent with the notion that the increases in apoptosis observed in ILK-deficient cells occur through pathways that involve caspase activation, both under normal conditions and under growth factor deprivation.

### **3.4 Reactive oxygen species in ILK-deficient cells**

Caspase-dependent apoptosis can be triggered by a variety of stimuli, including elevated levels of reactive oxygen species (ROS) (Denning et al., 2002). Thus, I examined if the increased apoptosis observed in ILK-deficient keratinocytes was associated with altered cellular ROS. To quantify hydroxyl radicals, peroxy radicals, and superoxide anions, cells were incubated with the fluorogenic dye, 2',7'-dichlorofluorescein-diacetate (DCFDA). DCFDA passively diffuses through the plasma membrane into the cytoplasm, where it is deacetylated by endogenous esterases to yield a non-fluorescent, membrane-impermeable conjugate (Wang and Joseph, 1999). The resulting compound is subsequently oxidized to a fluorescent species upon reaction with intracellular ROS (Wang and Joseph, 1999). For these studies, I incubated *K14Cre;Ilk<sup>f/f+</sup>* and *K14Cre;Ilk<sup>f/f</sup>* keratinocytes in medium with 10  $\mu$ M DCFDA for 45 minutes at 37°C. The DCFDA-loaded cells were then challenged with various concentrations of hydrogen peroxide (0,

50, 100, 200, 400, and 500  $\mu\text{M}$   $\text{H}_2\text{O}_2$ ), an established source of free radicals. ROS levels were then determined as a function of time. In the absence of  $\text{H}_2\text{O}_2$ , keratinocytes lacking *Ilk* gene expression exhibited significantly higher ROS levels compared to ILK-expressing control cells at all incubation times (Figure 3.10; Figure 3.11A). Increase in ROS levels in ILK-deficient cells was further enhanced when cells were challenged with 500  $\mu\text{M}$   $\text{H}_2\text{O}_2$  (Figure 3.11B). ROS levels for both cell types increased gradually over the 45-minute incubation period, both in the presence and absence of  $\text{H}_2\text{O}_2$ . These experiments indicate that ILK-deficient cells have an altered redox state, and suggest that increased ROS may be a potential source of stress triggering the activation of the apoptosis pathway in ILK-deficient keratinocytes.

Keratinocytes with *Ilk* gene inactivation display increased levels of intracellular ROS compared to ILK-expressing keratinocytes (Figure 3.10), which may be caused by an increase in overall ROS production and/or a diminished ability to quench free radical species. Thus, I aimed at investigating the latter by treating cells with *N*-Acetyl-L-cysteine (NAC), a synthetic derivative of intracellular cysteine that serves as a precursor in the biosynthesis of glutathione, an antioxidant (Aruoma et al., 1989). *K14Cre;Ilk<sup>f/+</sup>* and *K14Cre;Ilk<sup>f</sup>* keratinocytes were cultured on a 96-well plate and supplemented with 2 or 5 mM NAC in normal culture medium for 40 minutes at 37°C. Cells were then incubated with 10  $\mu\text{M}$  DCFDA for 45 minutes at 37°C, and subsequently challenged with 500  $\mu\text{M}$   $\text{H}_2\text{O}_2$ . ROS-associated fluorescence was quantified on a microplate reader immediately (Figure 3.12A) and 45 minutes after (Figure 3.12B) the addition of  $\text{H}_2\text{O}_2$ , and normalized for cell number. In the presence of 500  $\mu\text{M}$   $\text{H}_2\text{O}_2$ , ROS levels in both ILK-expressing and ILK-deficient cells increased significantly. However, when ILK-deficient cells were



**Figure 3.10. Effect of *Ilk* gene inactivation on cellular ROS levels.**

Keratinocytes isolated from *K14Cre;Ilk<sup>f/+</sup>* and *K14Cre;Ilk<sup>ff</sup>* mice were plated at  $1 \times 10^5$  cells/0.32 cm<sup>2</sup>. Epidermal keratinocytes were incubated with 10  $\mu$ M 2',7'-dichlorofluorescein diacetate (DCFDA) dye for 45 minutes at 37°C in the dark. Fluorescence was read in arbitrary units on a plate reader, with an excitation wavelength of 490 nm and an emission wavelength of 535 nm and normalized for cell number. The results are expressed as the mean  $\pm$ SE (n=3). \* indicate  $p < 0.05$ , relative to fluorescence of corresponding ILK-expressing *K14Cre;Ilk<sup>f/+</sup>* keratinocytes (t-test).



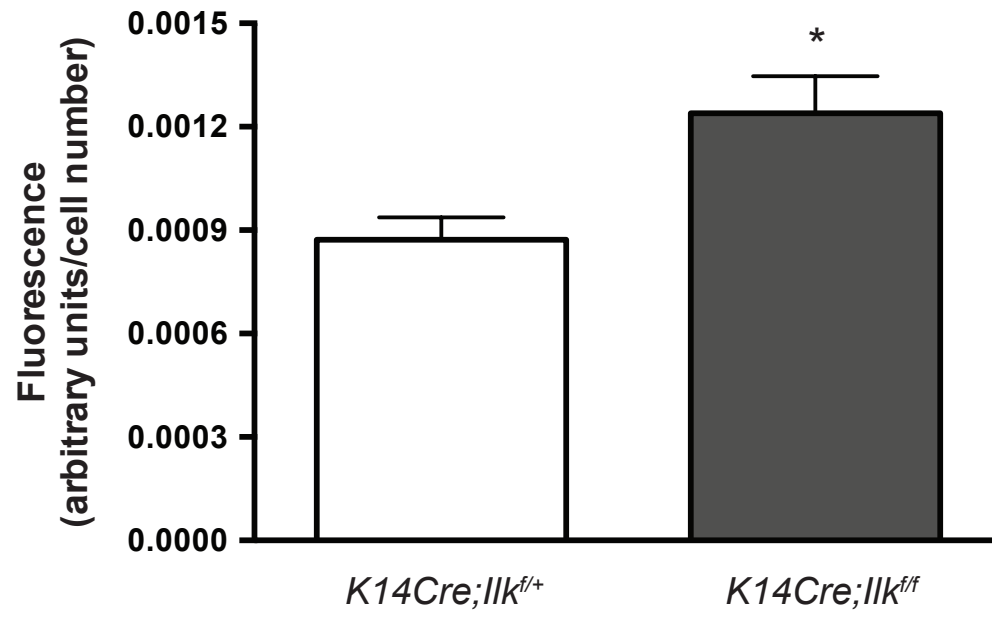
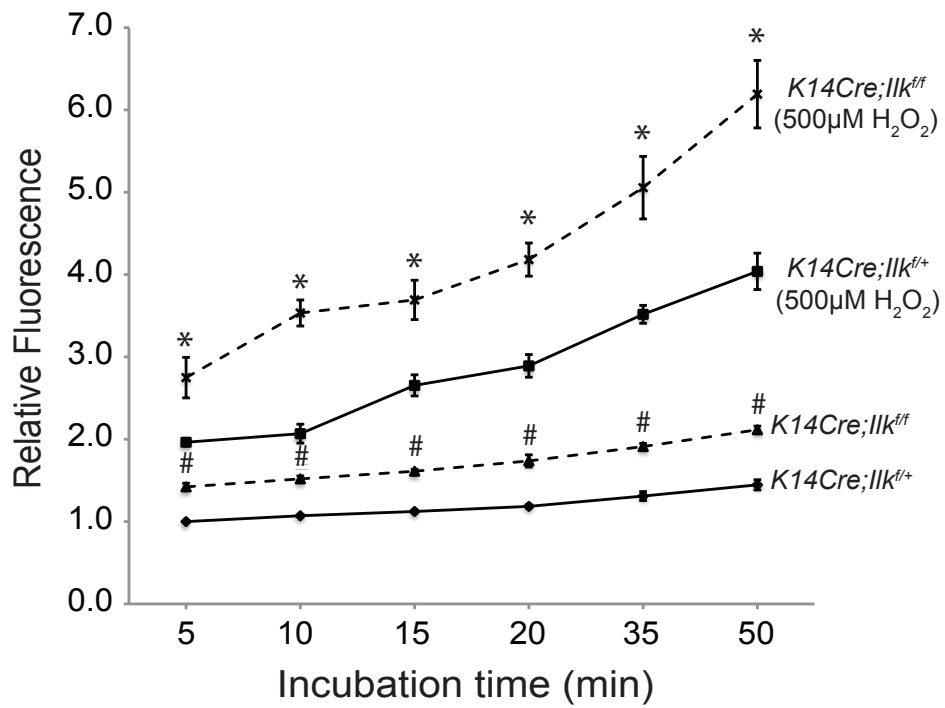




### Figure 3.11. ROS in ILK-deficient keratinocytes.

Keratinocytes isolated from *K14Cre;Ilk<sup>f/+</sup>* and *K14Cre;Ilk<sup>f/f</sup>* mice were plated at  $1 \times 10^5$  cells/0.32 cm<sup>2</sup>. Epidermal keratinocytes were incubated with 10  $\mu$ M 2',7'-dichlorofluorescein diacetate (DCFDA) dye for 45 minutes at 37°C in the dark. Keratinocytes were treated with increasing A) incubation time and B) concentration of hydrogen peroxide (H<sub>2</sub>O<sub>2</sub>). Fluorescence was read on a plate reader, with an excitation wavelength of 490 nm and an emission wavelength of 535 nm and normalized for cell number. The results are expressed as the mean  $\pm$ SE (n=3), relative to corresponding fluorescence in ILK-expressing *K14Cre;Ilk<sup>f/+</sup>* epidermis with no H<sub>2</sub>O<sub>2</sub> (set to 1). \* and # indicate p<0.05, relative to fluorescence of corresponding H<sub>2</sub>O<sub>2</sub> treated and untreated ILK-expressing *K14Cre;Ilk<sup>f/+</sup>* keratinocytes, respectively (ANOVA).

A)



B)

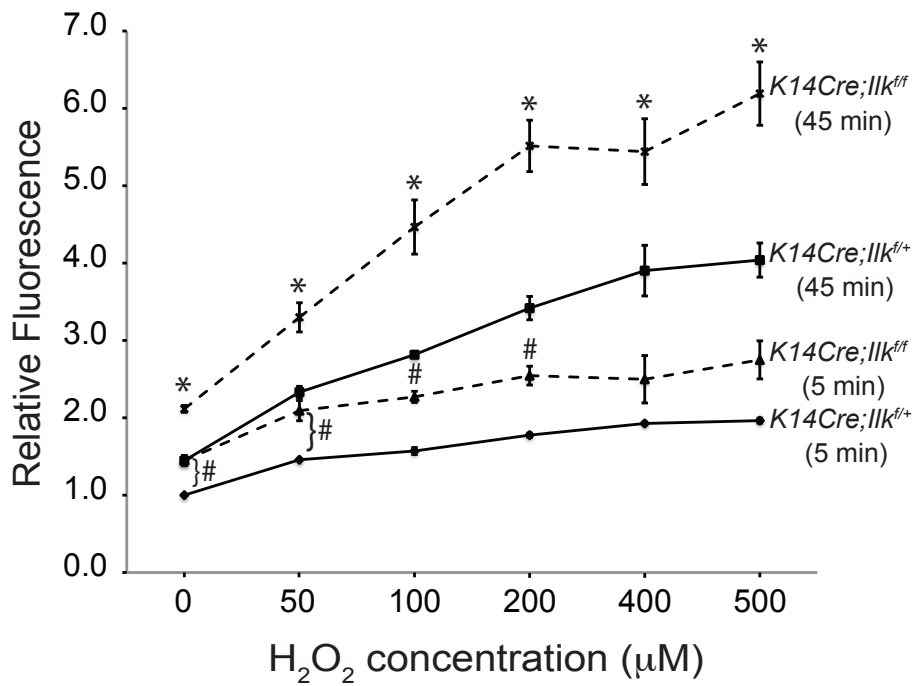
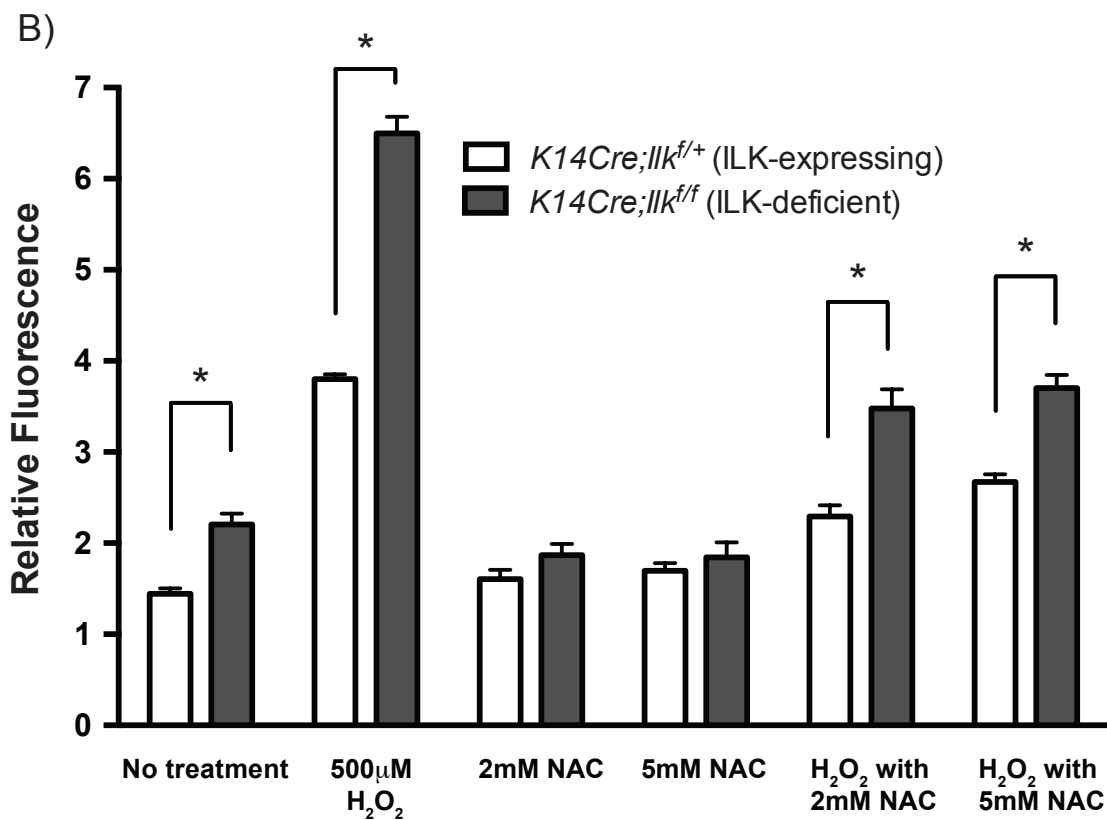
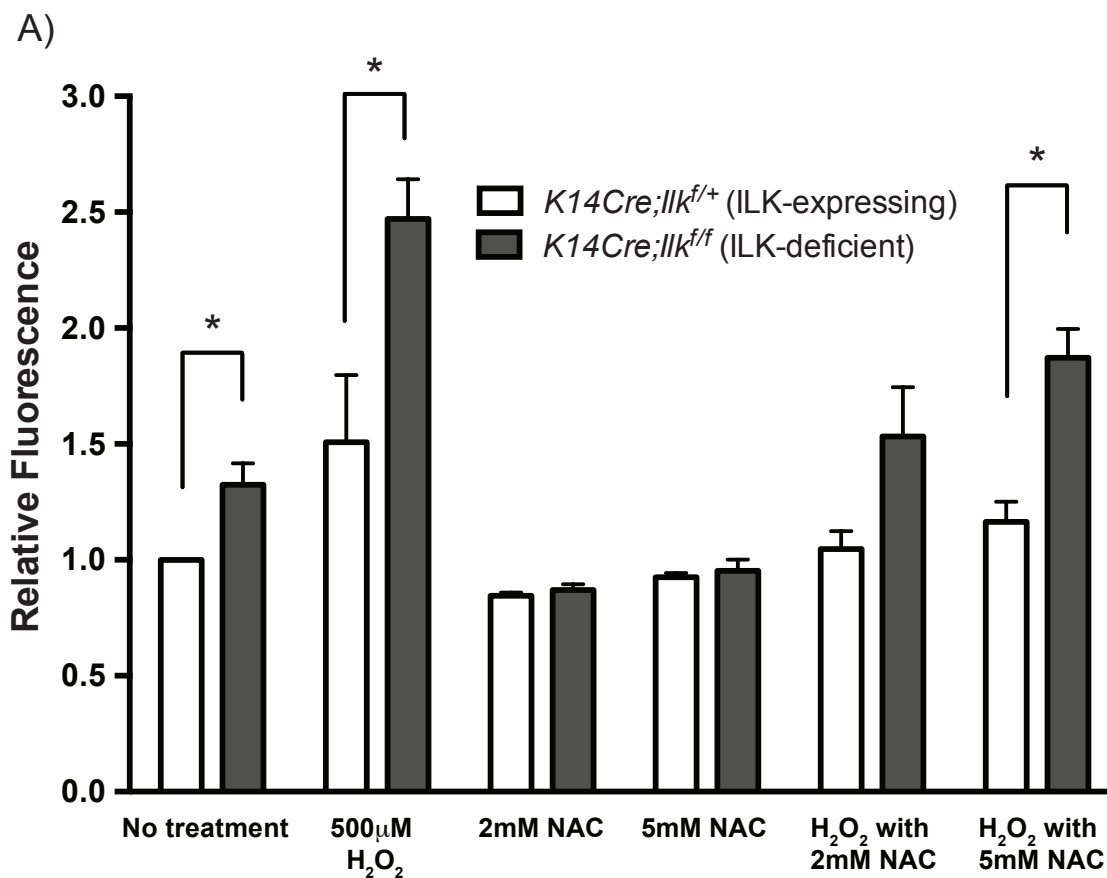




**Figure 3.12. Effect of NAC on ROS in ILK-deficient keratinocytes.**

Keratinocytes isolated from *K14Cre;Ilk<sup>f/+</sup>* and *K14Cre;Ilk<sup>ff</sup>* mice were plated at  $1 \times 10^5$  cells/0.32 cm<sup>2</sup>. Epidermal keratinocytes were incubated with 2 or 5 mM NAC for 40 minutes at 37°C and replaced with 10 μM 2',7'-dichlorofluorescein diacetate (DCFDA) dye for 45 minutes at 37°C in the dark. Fluorescence was read on a plate reader A) immediately and B) 45 minutes after addition of H<sub>2</sub>O<sub>2</sub>, with an excitation wavelength of 490 nm and an emission wavelength of 535 nm and normalized for cell number.



incubated with 2 or 5 mM NAC, ROS abundance diminished to levels indistinguishable from those in ILK-expressing keratinocytes (Figure 3.12). Additionally, when NAC-treated cells were challenged with H<sub>2</sub>O<sub>2</sub>, ROS levels were significantly reduced, compared to the amount ROS in vehicle-treated cells. However, even in the presence of NAC, ROS levels were higher in ILK-deficient cells, compared with ILK-expressing keratinocytes. Our findings suggest that apart from the possibility that cells lacking ILK may be generating excessive ROS, they may also have a reduced ability to quench and eliminate intracellular free radicals.

### **3.5 DNA damage markers in ILK-deficient keratinocytes**

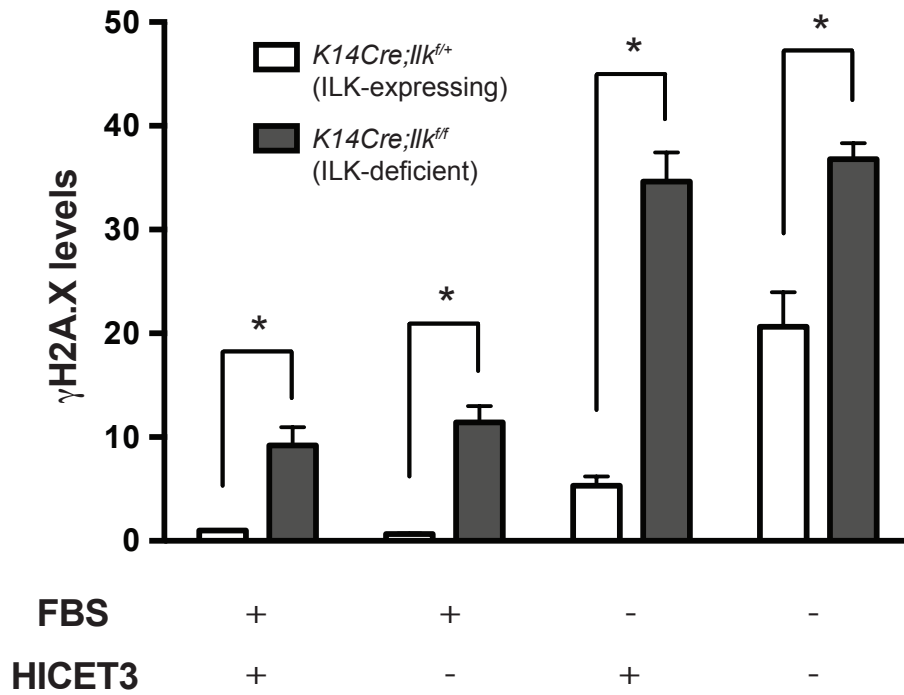
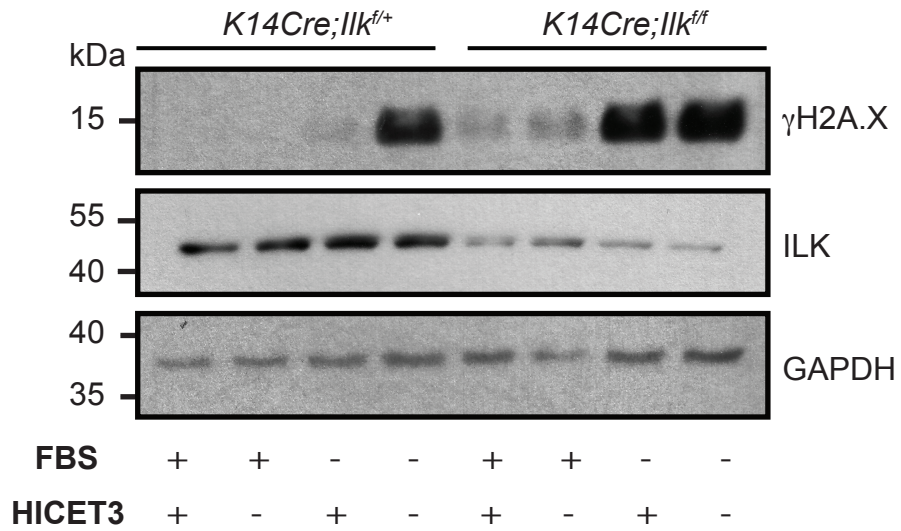
Increased cellular ROS levels may cause oxidative damage to DNA (Shi et al., 2004). To investigate if the loss of *Ilk* gene expression is accompanied by DNA damage, I measured levels of  $\gamma$ H2A.X in keratinocytes cultured in normal growth medium, or subjected to growth factor deprivation. The levels of  $\gamma$ H2A.X, a well-established marker for the activation of DNA damage response, such as DNA double-stranded breaks (DSB), were then analyzed. Under optimal culture conditions, I found significantly higher  $\gamma$ H2A.X levels in ILK-deficient keratinocytes relative to ILK-expressing cells (Figure 3.13). Similarly, in keratinocytes cultured in medium containing only FBS, only HICET3, or only BSA,  $\gamma$ H2A.X were significantly higher in ILK-deficient cells than ILK-expressing cells (Figure 3.13). Together, with the data from Section 3.4, these findings suggest that, in the absence of ILK, an increase in free radicals may contribute to elevated levels of  $\gamma$ H2A.X as a consequent of DNA damage.





**Figure 3.13. Effect of *Ilk* gene inactivation on  $\gamma$ H2A.X levels.**

Keratinocytes isolated from *K14Cre;Ilk<sup>f/+</sup>* and *K14Cre;Ilk<sup>f/f</sup>* epidermis were cultured in the indicated treatment conditions for 16 hours. Protein lysates were prepared and resolved by denaturing gel electrophoresis, followed by immunoblot analysis using indicated antibodies (top panel). Levels of  $\gamma$ H2A.X are expressed as the mean  $\pm$ SEM (n=3) relative levels in ILK-expressing *K14Cre;Ilk<sup>f/+</sup>* keratinocytes in Complete medium (set to 1). \* indicate  $p < 0.05$ , relative to expression levels in ILK-expressing *K14Cre;Ilk<sup>f/+</sup>* keratinocytes in corresponding conditioned medium (ANOVA, bottom panel).



## **Chapter 4 - Discussion**

### **4.1 Summary and general discussion**

When the *Ilk* gene is inactivated in mouse epidermal keratinocytes, the epidermal integrity becomes compromised and the viability of keratinocytes diminishes. Thus, the skin is unable to fulfill its defensive functions and becomes susceptible to oxidative stress and damage (Omari et al., 2008). ILK plays a role in suppressing anoikis and apoptosis in various epithelial cell types (Benoit et al., 2007; Attwell et al., 2000); however, its role in maintaining keratinocyte viability remains poorly understood. My work now shows that ILK is necessary for keratinocyte viability, both under normal conditions and during growth factor deprivation. Further, I have begun to elucidate the mechanism whereby ILK limits stress-induced apoptosis in keratinocytes.

#### **4.1.1 Modulatory role of ILK on keratinocyte viability**

Basal keratinocytes, which are the predominant cell type in the basal layer of the epidermis, have a high proliferative capacity and are responsible for the self-renewal properties of the skin (Régnier et al., 1986). However, in the absence of ILK, keratinocytes lose their normal ability to divide and display a lower proportion of cells in S-phase, indicative of a reduced proliferative capacity. The diminished cell viability consequent to *Ilk* gene inactivation is associated with elevated levels of cell death through apoptosis, specifically involving the caspase pathway. My observations have shown that under optimal growth culture conditions, ILK-deficient keratinocytes display

significantly higher levels of cleaved caspase-3 and cleaved PARP compared to ILK-expressing control cells, both indicative of the activation of the pro-apoptosis enzymatic caspase cascade. Notably, despite being the direct downstream substrate of caspase-3, cleaved PARP levels in ILK-expressing and ILK-deficient cells varied in expression pattern from cleaved caspase-3 levels under different culture conditions (and vice versa). Cleaved PARP was increased significantly in ILK-deficient keratinocytes in conditions of HICET3 growth supplement deprivation, whereas cleaved caspase-3 levels were elevated in ILK-deficient keratinocytes in the BSA serum-starved treatment. Such discrepancies observed in the different growth deprivation treatments could likely be attributed to either a potential role of ILK in promoting growth factor-mediated cell survival or parallel pathways facilitating the cleavage of either caspase-3 or PARP under specific culture conditions. Clearly, this hypothesis needs to be further investigated.

The increased activation of the caspase pathway appears to also involve an increase in Bax localization to the mitochondria, a phenomenon necessary for the formation of the mitochondrial apoptosis-induced channel (MAC). MAC is a complex upstream of the intrinsic caspase pathway, which mediates the release of cytochrome c and ultimately, the activation of caspase-mediated apoptosis (Dejean et al., 2005). Although the role of ILK in the intrinsic apoptosis pathway has never been investigated in keratinocytes, previous findings conducted on SCP2 mouse mammary epithelial cells have shown that ILK overexpression interferes with the activation of caspase-3 and caspase-8, suppressing anoikis (Attwell et al., 2000). As caspase-8 is another key activator of caspase-3 via the extrinsic apoptotic pathway, these findings are consistent with the notion that ILK may play a role in modulating the intrinsic activation of apoptosis as well. However, in

addition to an increase in apoptosis, the diminished capacity of ILK-deficient keratinocytes to effectively proliferate could also be associated with increased senescence. Thus, it would be interesting to investigate differences in senescence between ILK-expressing and ILK-deficient keratinocytes.

It is interesting to note that in epidermal keratinocytes, loss of ILK expression did not affect levels of active, pro-survival phosphorylated Akt. Under all culture treatment conditions used in my experiments, the levels of the activated form of Akt in ILK-deficient keratinocytes remained indistinguishable from those observed in ILK-expressing cells, indicating that the increased apoptosis in ILK-deficient keratinocytes is likely independent of Akt. Similarly, Akt is not altered in ILK-deficient fibroblasts and chondrocytes (Sakai et al., 2003; Grashoff et al., 2003; Boudeau et al., 2006). It would be interesting to investigate if ILK-deficiency has an effect on any of the downstream substrates of Akt, including Bcl-associated death promoter, or BAD. Measuring levels of phosphorylated BAD in the presence and absence of ILK could yield information regarding whether a different pathway may be activated in parallel to the intrinsic caspase-mediated apoptosis pathway. However, my experiments thus far suggest that ILK promotes cell survival in a manner independent of Akt in primary keratinocytes.

#### **4.1.2 Modulatory role of ILK on ROS-induced apoptosis**

One possible explanation for the significant increase in apoptosis observed in ILK-deficient cells is elevated levels of cellular stress (Paz et al., 2007), and one of the most common sources of intracellular stress is reactive oxygen species (ROS) (Kovacs et al., 2009). My findings show significantly increased ROS levels in ILK-deficient

keratinocytes. These novel observations suggest excessive production of oxidative radicals. Elevated cellular ROS were also observed in ILK-deficient keratinocytes challenged with H<sub>2</sub>O<sub>2</sub>, a known producer of ROS. Thus, my experiments suggest a novel role for ILK in the cellular redox state of keratinocytes. Though the mechanism whereby ILK modulates oxidative stress has yet to be explored, the abnormal ROS levels in ILK-deficient keratinocytes may contribute to elevated apoptosis observed in these cells. Interestingly, over-production and accumulation of ROS within the endoplasmic reticulum (ER) have been shown to perturb ER function (Chaudhari et al., 2014). Such ER stress leads to the misfolding of proteins, and in cases of excessive stimulation by ROS, even apoptosis (Puthalakath et al., 2007). Thus, based on its role in modulating ROS levels in keratinocytes, ILK may also be involved in mediating ROS-induced apoptosis through the ER, as well as the mitochondria.

Such marked differences in ROS levels in ILK-deficient keratinocytes may arise from increased production and/or an impaired ability to quench free radicals. Notably, ROS abundance was reduced to levels indistinguishable from those in ILK-expressing control cells in the presence of the reducing agent NAC. As a synthetic precursor of glutathione, a known endogenous antioxidant produced in cells, exogenous NAC indirectly acts as a ROS scavenger (Sun, 2010). My observations suggest that keratinocytes with *Ilk* gene inactivation may produce insufficient amounts of reducing compounds, thus resulting in elevated free radical species. More experiments will need to be conducted to support this hypothesis.

Elevated levels of ROS can contribute to DNA damage, such as strand breaks (Shi et al., 2004). Intracellular ROS induce damaged lesions to DNA, specifically through the

targeted conversion of guanine bases to reactive, oxidized 8-hydroxyguanine (Wiseman and Halliwell, 1996). Such base or sugar damage can ultimately lead to intra- and/or inter-strand breaks in DNA, triggering apoptosis (Flores et al., 2002). My experiments have shown that, in addition to abnormal levels of ROS, ILK-deficient keratinocytes display higher levels of  $\gamma$ H2A.X, a marker for the activation of DNA damage responses, which is activated to repair DNA double-strand breaks. ILK-deficient keratinocytes may also have defects in their ability to effectively repair DNA, even under normal levels of oxidative stress. Whether increased DNA damage is associated with increased apoptosis observed in ILK-deficient keratinocytes has yet to be determined. When DNA is damaged, the cell can either attempt to repair it or initiate programmed cell death (Bouchard et al., 2003). If DNA damage is not excessive, Poly ADP ribose polymerase (PARP) is activated, binding to DNA strand breaks to facilitate the recruitment of proteins involved in DNA repair (Herceg and Wang, 2000). However, if DNA damage is too extensive, excessive PARP stimulation leads to  $\text{NAD}^+$  depletion through the overproduction of signalling PAR chains (Bouchard et al., 2003). Without  $\text{NAD}^+$ , ATP cannot be synthesized and apoptosis is subsequently induced, as the cell exhausts all its energy sources (Bouchard et al., 2003). According to the PARP suicide hypothesis, this pathway then triggers the cleavage and inactivation of PARP by upstream caspases (Bouchard et al., 2003). Together with the observed increase in  $\gamma$ H2A.X levels, my findings suggest that the increased levels of inactive, cleaved PARP observed in ILK-deficient keratinocytes may be associated with irreparable ROS-induced DNA damage. Together, my observations suggest that ILK may participate in the suppression of oxidative stress-induced DNA damage and subsequent activation of the caspase-



dependent apoptotic pathway. Clearly, this hypothesis remains to be tested experimentally.

As mentioned earlier, the mitochondrial localization of Bax indicates the activation of intrinsic apoptosis pathways, normally in response to various stimuli including elevated ROS (Simon et al., 2000). The activation of the Bax-mitochondrial pathway may result from the phosphorylation and activation of mitogen-activated protein kinases (MAPK) (Wong et al., 2010). Specifically, I observed an increase in the levels of active, phosphorylated c-Jun N-terminal kinase (JNK) and extracellular signal-regulated kinase (ERK) in ILK-deficient keratinocytes compared to ILK-expressing cells. When cells are exposed to abnormal ROS levels or other stressors, JNK is phosphorylated and activated as part of the intrinsic apoptotic triggers. Once activated, apoptotic stimuli can then either stimulate Bax mitochondrial translocation and/or activate the caspase cascade (Tournier et al., 2000). Previous experiments conducted on embryonic fibroblasts and erythroleukemia cells support my findings of increased levels of phosphorylated JNK in response to cells experiencing elevated levels of oxidative stress (Tournier et al., 2000; Nagata and Todokoro, 1999). However, there are a number of contrasting studies with respect to ROS-induced ERK phosphorylation that implicate a cell-type specific response (Xia et al., 1995). For example, similar to my observations in ILK-deficient keratinocytes, Xu et al. (2010) showed that triptolide, a potent epoxide, stimulates the generation of ROS in colorectal cancer cells. This increase in ROS levels lead to an increase in ERK activation and apoptosis (Tan and Chiu, 2013). However, in a study conducted by Xia et al. (1995), phospho-ERK levels decreased in response to apoptosis triggered by nerve growth factor withdrawal in cortical neurons, whereas phospho-JNK

levels increased. It appears that at least in cultured ILK-deficient keratinocytes, ERK phosphorylation is increased, potentially in response to elevated levels of ROS observed in these cells. Recent findings have also suggested that ERK may elicit either cell proliferation or apoptosis, depending on the degree of oxidative stress (Tan and Chiu, 2013).

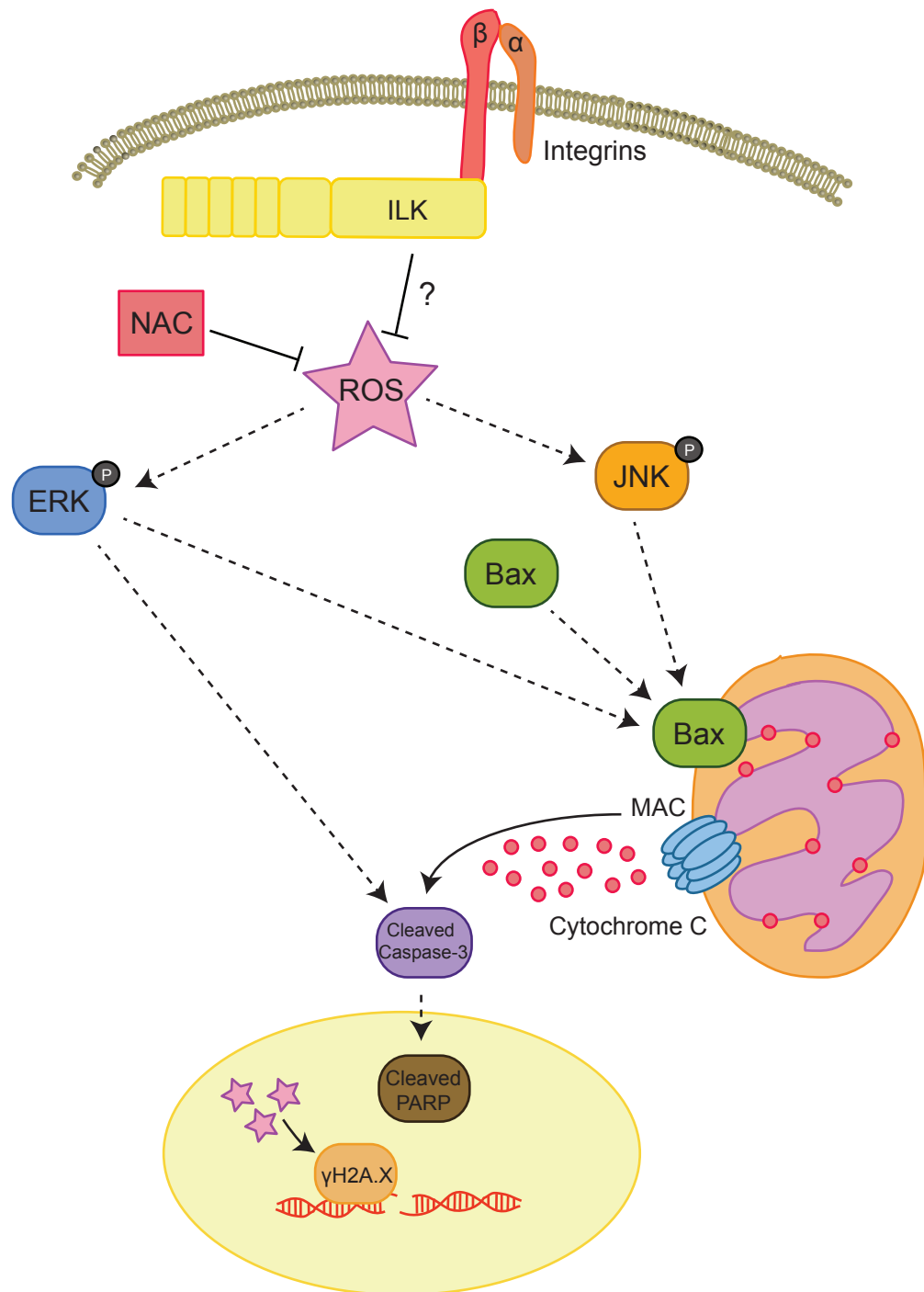
Specifically, the JNK signalling pathway has been implicated in the activation of BH3-only proteins, including Bim, Hrk, and Puma (Harris and Johnson, 2001). In cortical neurons, Bim and Hrk are stimulated by phosphorylated JNK upstream of the Bax mitochondrial complex to induce apoptosis (Harris and Johnson, 2001). Similarly, JNK has been shown to elicit its antiapoptotic function in hematopoietic pro-B cells through the phosphorylation and subsequent inactivation of proapoptotic Bcl-2 family protein, BAD (Yu et al., 2004). In human gingival fibroblasts, JNK activation by nitric oxide is associated with Bcl-2 family modulation and caspase activation via the mitochondrial pathway (Baek et al., 2014). Some studies have even suggested that stress-activated JNK and p38 kinases are directly involved in the phosphorylation and consequent mitochondrial translocation of Bax (Kim et al., 2006; Lei et al., 2002).

These findings are consistent with a model I am proposing, based on my experimental observations (Figure 4.1). In this model ILK, which binds to  $\beta 1$  integrins, regulates ROS intracellular levels. This tight modulation of oxidative stress helps to suppress the hyperactivation of caspase-mediated apoptosis. However, in the absence of ILK, elevated ROS levels induce Bax to translocate to the mitochondria and stimulate the enzymatic caspase cascade, ultimately leading to apoptosis.



**Figure 4.1. Proposed model of stress-induced apoptosis modulation by ILK.**

ILK-deficient keratinocytes display increased levels of apoptosis and intracellular ROS, suggesting that ILK may play a role in modulating stress-induced activation of the Caspase-3 pathway.



## 4.2 Significance

Survival of keratinocytes is necessary for proper function of the skin (Chung et al., 2003). As a scaffold protein, ILK is involved in cell-cell and cell-ECM adhesion through its interaction with integrins (Teo et al., 2014). In the absence of ILK, epidermal integrity becomes compromised and the skin cannot maintain its protective function (Nakrieko et al., 2008; Eckes et al., 2014). My experiments demonstrate a novel role for ILK in modulating ROS levels in cultured keratinocytes. I have shown that ILK may play a role in maintaining keratinocyte survival, and that ILK loss is associated with ROS production and apoptosis. These findings could help elucidate the mechanisms by which the epidermis becomes susceptible to damage when the *Ilk* gene has been inactivated. For example, the kindlin family of adaptor proteins interacts with  $\beta$ -integrins to regulate integrin activation, similar to ILK (Böttcher et al., 2009). Kindler Syndrome is a rare, recessive disease of the skin that is caused by mutations in the *kindlin-1* gene (Böttcher et al., 2009). Kindler Syndrome patients suffer severe blistering and abnormal pigmentation (Duperret and Ridkey, 2014), closely resembling the phenotypic defects observed in mice with epidermis-restricted inactivation of the *Ilk* gene (Nakrieko et al., 2008). Based on the functional similarities of ILK and kindlin in their integrin-related scaffolding functions, delineating the downstream factors involved in ILK-mediated keratinocyte survival could lead us to better understand the causes of various diseases, like Kindler Syndrome, that arise due to compromised integrity and function.

My findings suggest a novel involvement of ILK in regulating apoptosis in keratinocytes. Apoptosis is a normal cellular process, necessary for proper maintenance and regulation

of cellular populations (Zuckerman et al., 2009). On one hand, insufficient levels of apoptosis are often correlated with tumorigenesis (Elmore, 2007; Nicholson, 2000). ILK has been proposed to be potential therapeutic target in various cancers (Hannigan et al., 2005). ILK expression is elevated in prostate, gastric, and ovarian cancers, as well as in malignant melanomas (Hannigan et al., 2005). These findings may generate therapeutic solutions for maintaining epidermal health and even derive cancer therapies for oncogenic diseases affecting the epidermis. On the other hand, uncontrolled levels of apoptosis may have pathological consequences (Nicholson, 2000). In the skin, Stevens-Johnson syndrome (SJS) is a specific subtype of erythema multiforme that is characterized by elevated levels of cell death (Inachi et al., 1997). This abnormal level of apoptosis often leads to separation of the epidermis from the dermis, causing severe blistering and shedding of the skin that closely resembles symptoms found in Kindler Syndrome patients (Abe et al., 2003) and in mice with ILK-deficient epidermis (Nakrieko et al., 2008). Consequently, patients suffering from this syndrome are left susceptible to infection due to the diminished protective capacity of the skin (Abe et al., 2003). Mice with epidermis-restricted inactivation of the *Ilk* gene exhibit a number of phenotypic defects, including reduced adhesion to the basement membrane and disrupted epidermal integrity (Nakrieko et al., 2008; Lorenz et al., 2007). As the external layer of protection, the skin is often exposed to external stressors such as UV radiation, a known generator of genomic instability and free radical species (Phillipson et al., 2001). Normally, keratinocytes are adequately self-protected against oxidative stress, through the production of endogenous antioxidants (Bito and Nishigori, 2012). However, if the epidermis becomes overloaded with UV-induced ROS, physiological antioxidant levels

are reduced and impair the cellular redox balance (Bito and Nishigori, 2012). Consequently, the cells undergo apoptosis. Thus, elucidating the involvement of ILK in suppressing intracellular ROS levels has important implications with respect to skin biology. In addition, UV irradiation is a common source of DNA damage, and based on my observations, ILK may be involved in regulating proper DNA repair. Additional experiments would need to be conducted to validate this hypothesis.

### **4.3 Future Directions**

Recent work has shown a potential link between ILK and apoptosis; however, the definitive cause for how ILK-deficiency leads to increased levels of ROS and subsequently, apoptosis has yet to be determined. It would be worthwhile to investigate any alterations in the signalling pathways involved in regulating oxygen-derived radicals and to determine if they are directly downstream of ILK. For example, Rac1, a small GTPase, is regulated by ILK (Ho et al., 2012; Sayedyahosseini et al., 2013). In addition to its role in controlling actin cytoskeletal reorganization (Filipenko et al., 2005), Rac1 has also been shown to mediate intracellular ROS production through its control over NADPH oxidase activation (Rygiel et al., 2008; Bokoch and Diebold, 2002). Specifically in cultured keratinocytes, we have demonstrated that *Ilk* gene inactivation leads to reduced activation of Rac1, resulting in impaired development of front-rear cell polarity (Ho et al., 2010; 2012). Thus, it would be interesting to investigate a possible correlation between levels of active Rac1 and NADPH oxidase activity.



I also showed that the increased levels of apoptosis in ILK-deficient keratinocytes may be caspase-mediated, based on the abnormal localization of Bax to the mitochondria and increased levels of cleaved caspase-3 and PARP in these cells. However, it has yet to be confirmed whether apoptosis can be prevented through the addition of a caspase inhibitor. Thus, Z-VAD-FMK, a cell-permeable, general caspase inhibitor, could be introduced to ILK-deficient cells in culture to determine if the cleaved caspase-3 levels could be reduced to those observed in control cells and apoptotic levels could be rescued. Also, as the majority of my experiments were focused on how apoptosis may be activated intracellularly, the study of the effect of *Ilk* inactivation on the extrinsic apoptotic pathway could help elucidate the mechanisms by which ILK-deficiency leads to increased apoptosis. The extrinsic apoptotic pathway involves the activation of transmembrane death receptors through the binding of apoptosis-inducing ligands (Ashkenazi, 2008). Cellular FLICE-inhibitory protein (c-FLIP) is a catalytically inactive homologue of caspase-8/10 that directly impedes with the formation of the Death Inducing Signalling Complex at the level of the death receptors (Peter, 2004). As both the intrinsic and extrinsic pathways activate executioner caspases, it would be interesting to see if cleaved caspase-3 and/or cleaved PARP levels can be diminished in ILK-deficient keratinocytes with the overexpression of c-FLIP (Kreuz et al., 2001).

In addition to an increase in ROS levels,  $\gamma$ H2A.X, an established marker of double-strand breaks, was also increased in ILK-deficient cells. However, despite using an indirect marker of DNA damage, the actual amount of damaged DNA was not quantitatively measured for comparison between the two cell types. I also demonstrated that under optimal culture conditions, the increase in  $\gamma$ H2A.X levels correlates to elevated ROS in

ILK-deficient keratinocytes. However, elevated levels of  $\gamma$ H2A.X could also be attributed to an impaired repair capacity of these cells. Repair of ROS-induced damage could be assessed through the measurement of anti-pyrimidine (6-4) pyrimidone photoproducts (6-4PP) and cyclobutane pyrimidine dimers (CPD), two predominant forms of DNA damage. The quantification of 6-4PP and CPD products that remain in the genomic DNA of ILK-expressing and ILK-deficient epidermis can then provide an indication as to the extent of ROS-induced DNA damage that remains in each cell type over time (Biswas et al., 2014). Additionally, levels of proteins specifically involved in DNA single-strand or double-strand break repair, such as XRCC1 and Ku, respectively, could be quantified to assess any discrepancies in the repairing mechanisms of ILK-deficient keratinocytes.

Finally, I demonstrated that ROS levels in ILK-deficient keratinocytes could be reduced with the addition of NAC. However, I did not measure and/or compare the scavenging capacity of cells lacking ILK to ILK-expressing cells. Thus, to determine if ILK-deficiency is associated with an impaired capacity to quench oxidative radicals, the measurement of catalase activity would be informative. Similarly to peroxidases, catalase is the enzyme mainly responsible for the conversion of highly reactive  $H_2O_2$  to water and oxygen (DeJong et al., 2007). The increase in ROS levels under optimal culture conditions in ILK-deficient keratinocytes may be attributed to a reduced detoxification of ROS by catalase. More experiments are necessary to confirm if catalase activity would be affected by ILK-deficiency.

In summary, my studies demonstrate a novel role for ILK in maintaining keratinocyte viability. The epidermis serves to defend the body from harmful, external insults, including UV radiation and oxidative radicals. I have shown a newfound involvement of

ILK in modulating cellular ROS levels, as well as regulating stress-induced apoptosis, likely via the intrinsic, caspase cascade. Though the direct link between ILK and ROS has yet to be explored, I have delineated one of the possible mechanisms by which ILK modulates ROS-induced apoptosis in cultured keratinocytes. By achieving a better understanding of the function of ILK in promoting keratinocyte survival, we could identify the epidermal characteristics associated with the presence of ILK that are necessary to maintain normal development and sustainability of the skin.

## References

- Abe R, Shimizu T, Shibaki A, Nakamura H, Watanabe H & Shimizu H (2003). Toxic Epidermal Necrolysis and Stevens-Johnson Syndrome are induced by soluble Fas ligand. *Am J Pathol* **162**, 1515-1520.
- Adams JC & Watt FM (1989). Fibronectin inhibits the terminal differentiation of human keratinocytes. *Nature* **340**, 307-309.
- Aruoma OI, Halliwell B, Hoey BM & Butler J (1989). The antioxidant action of *N*-acetylcysteine – its reaction with hydrogen-peroxide, hydroxyl radical, superoxide, and hypochlorous acid. *Free Radic Biol Med* **6**, 593-597.
- Ashkenazi A (2008). Targeting the extrinsic apoptosis pathway in cancer. *Cytokine Growth F R* **19**, 325-331
- Assefa Z, Laethem AV, Garmyn J & Agostinis P (2005). Ultraviolet radiation-induced apoptosis in keratinocytes: on the role of cytosolic factors. *Biochim Biophys Acta* **1755**, 90-106.
- Attwell S, Roskelley C & Dedhar S (2000). The integrin-linked kinase (ILK) suppresses anoikis. *Oncogene* **19**, 3811-3815.
- Baek M-W, Seong K-J, Jeong Y-J, Kim G-M, Park H-J, Kim S-H, Chung H-J, Kim W-J & Jung J-Y (2014). Nitric oxide induces apoptosis in human gingival fibroblast through mitochondria-dependent pathway and JNK activation. *Int Endod J*.
- Bayir H (2005). Reactive oxygen species. *Crit Care Med* **33**, 498-501.
- Benhar M, Dalyot I, Engelberg D & Levitzki A (2001). Enhanced ROS production in oncogenically transformed cells potentiates c-Jun N-terminal kinase and p38 mitogen-activated protein kinase activation and sensitization to genotoxic stress. *Mol Cell Biol* **21**, 6913-6926.

Benoit DS, Tripodi MC, Blanchette JO, Langer SJ, Leinwant LA & Anseth KS (2007). Integrin-linked kinase production prevents anoikis in human mesenchymal stem cells. *J Biomed Mater Res* **81**, 259-268.

Bickers DR & Athar M (2006). Oxidative stress in the pathogenesis of skin disease. *J Invest Dermatol* **126**, 2565-2575.

Biswas AK, Mitchell DL & Johnson DG (2014). E2F1 responds to ultraviolet radiation by directly stimulating DNA repair and suppressing carcinogenesis. *Cancer Res* **74**, 3369-3377.

Bito T & Nishigori C (2012). Impact of reactive oxygen species on keratinocyte signaling pathways. *J Dermatol Sci* **68**, 3-8.

Bito T, Izu K & Tokura Y (2010). Evaluation of toxicity and Stat3 activation induced by hydrogen peroxide exposure to the skin in healthy individuals. *J Dermatol Sci* **58**, 157-19.

Bock-Marquette I, Saxena A, White MD, DiMaio JM & Srivastava D (2004). Thymosin  $\beta$ 4 activates integrin-linked kinase and promotes cardiac cell migration, survival and cardiac repair. *Nature* **432**, 466-472.

Bokoch GM & Diebold BA (2002). Current molecular models for NADPH oxidase regulation by Rac GTPase. *Blood* **100**, 2692-2695.

Böttcher RT, Lange A & Fässler R (2009) How ILK and kindlins cooperate to orchestrate integrin signaling. *Curr Opin Cell Biol* **21**, 670-675.

Bouchard VJ, Rouleau M & Poirier GG (2003). PARP-1, a determinant of cell survival in response to DNA damage. *Exp Hematol* **31**, 446-454.

Boudeau J, Miranda-Saavedra D, Barton GJ & Alessi DR (2006). Emerging roles of pseudokinases. *Trends Cell Biol* **16**, 443-452.

Boulares AH, Yakovlev AG, Ivanova V, Stoica BA, Wang G, Iyer S & Smulson M (1999). Role of Poly(ADP-ribose) Polymerase (PARP) cleavage in apoptosis: caspase-3 resistant PARP mutant increases rates of apoptosis in transfected cells. *J Biol Chem* **274**, 22932-22940.

Candi E, Schmidt R & Melino G (2005). The cornified envelope: a model of cell death in the skin. *Nat Rev Mol Cell Bio* **6**, 328-340.

Chaudhari N, Talwar P, Parimisetty A, d'Hellencourt CL & Ravanan P (2014). A molecular web: endoplasmic reticulum stress, inflammation, and oxidative stress. *Front Cell Neurosci*.

Chiswell BP, Zhang R, Murphy JW, Boggon TJ & Calderwood DA (2008). The structural basis of integrin-linked kinase-PINCH interactions. *Proc Natl Acad Sci USA* **105**, 20677-20682.

Choma DP, Milano V, Pumiglia K & DiPersto CM (2006). Integrin  $\alpha 3\beta 1$ -dependent activation of FAK/Src regulates Rac1-mediated keratinocyte polarization of laminin-5. *J Invest Dermatol* **127**, 31-40.

Chung JH, Han JH, Hwang EJ, Seo JY, Cho KH, Kim KH, Young JI & Eun HC (2003). Dual mechanisms of green tea extract (EGCG)-induced cell survival in human epidermal keratinocytes. *FASEB J* **17**, 1913-1915.

Dagnino, L (2011). Integrin-linked kinase: a scaffold protein unique among its ilk. *J Cell Commun Signal* **5**, 81-83.

Dagnino L, Ho E & Chang WY (2010). Expression and analysis of exogenous proteins in epidermal cells. *Methods Mol Biol* **585**, 93-105.

Dejean LM, Martinez-Caballera S, Guo L, Hughes C, Teijido O, Ducret T, Ichas F, Korsmeyer ST, Antonsson B, Jonas EA & Kinnally KW (2005). Oligomeric Bax is a component of the putative cytochrome c release channel MAC, mitochondrial apoptosis-induced channel. *Mol Biol Cell* **16**, 2424-2432.

Dejong RJ, Miller LM, Molina-Cruz A, Gupta L, Kumar S & Barillas-Mury C. (2007). Reactive oxygen species detoxification by catalase is a major determinant of fecundity in the mosquito *Anopheles gambiae*. *Proc Natl Acad Sci* **104**, 2121-2126.

Delcommenne M, Tan C, Gray V, Rue L, Woodgett J & Dedhar S (1998). Phosphoinositide-3-OH kinase-dependent regulation of glycogen synthase kinase 3 and protein kinase B/AKT by the integrin-linked kinase. *Proc Natl Acad Sci USA* **95**, 11211-11216.

Deng JT, Van Lierop JE, Sutherland C, & Walsh MP (2001). Ca<sup>2+</sup>-independent smooth muscle contraction: a novel function for integrin-linked kinase. *J Biol Chem* **276**, 16365-16373.

Denning TL, Takaishi H, Crowe SE, Boldogh I, Jevnikar A & Ernst PB (2002). Oxidative stress induces the expression of Fas and Fas ligand and apoptosis in murine intestinal epithelial cells. *Free Radic Biol Med* **33**, 1641-1650.

Du C, Fang M, Li Y, Li L & Wang X (2000). Smac, a mitochondrial protein that promotes cytochrome c-dependent caspase activation by eliminating IAP inhibition. *Cell* **102**, 33-42.

Duperret EK & Ridky TW (2014). Kindler syndrome in mice and men. *Cancer Biol Ther* **15**, 1-4.

Eckes B, Krieg T & Wickström (2014). Role of integrin signalling through integrin-linked kinase (ILK) in skin physiology and pathology. *Exp Dermatol*.

El-Najjar N, Chatila M, Moukadem H, Vuorela H, Ocker M, Gandesiri M, Schneider-Stock R & Gali-Muhtasib H (2010) Reactive oxygen species mediate thymoquinone-induced apoptosis and activate ERK and JNK signaling. *Apoptosis* **15**, 183-195.

Elias PM (2007). The skin barrier as an innate immune element. *Sein Immunopathol* **29**, 3-14.

Elmore S (2007). Apoptosis: a review of programmed cell death. *Toxicol Pathol* **35**, 495-516.

Essayem S, Kovacic-Milivojevic B, Baumbusch C, McDonagh S, Dolganov G, Howerton K, Larocque N, Mauro T, Ramirez A, Ramos DM, Fisher SJ, Jorcano JL, Beggs HE, Reichardt LF & Ilić D (2006). Hair cycle and wound healing in mice with a keratinocyte-restricted deletion of FAK. *Oncogene* **25**, 1081-1089.

Filipenko NR, Attwell S, Roskelley C & Dedhar S (2005). Integrin-linked kinase activity regulates Rac- and Cdc42-mediated actin cytoskeleton reorganization via  $\alpha$ -PIX. *Oncogene* **24**, 5837-5849.

Flores ER, Tsai KY, Crowley D, Sengupta S, Yang A, McKeon F & Jacks T (2002). p63 and p73 are required for p53-dependent apoptosis in response to DNA damage. *Nature* **416**, 560-564.

Fukuda K, Gupta S, Chen K, Wu, C & Qin J (2009). The pseudoactive site of ILK is essential for its binding to alpha-Parvin and localization to focal adhesions. *Mol Cell* **36**, 819-830.

Fulda S & Debatin K-M (2006). Extrinsic versus intrinsic apoptosis pathways in anticancer chemotherapy. *Oncogene* **25**, 4798-4811.

Gkretsi V, Mars WM, Bowen WC, Barua L, Yang Y, Guo L, St-Arnaud R, Dedhar S, Wu C & Michalopoulos GK (2007). Loss of integrin linked kinase from mouse hepatocytes in vitro and vivo results in apoptosis in hepatitis. *Hepatology* **45**, 1025-1034.

Grashoff C, Aszodi A, Sakai T, Hunziker EB & Fässler R (2003). Integrin-linked kinase regulates chondrocyte shape and proliferation. *EMBO* **4**, 432-438.

Green DR & Kroemer G (2004). The pathophysiology of mitochondrial cell death. *Science* **305**, 626-629.

Grinnell F (1992). Wound repair, keratinocyte activation and integrin modulation. *J Cell Sci* **101**, 1-5.



Haake A, Scott GA & Holbrook KA (2001). Structure and function of the skin: overview of the epidermis and dermis. *Biol Skin* **2001**, 19-45.

Halliwell B (1989). Free radicals, reactive oxygen species and human disease: a critical evaluation with special reference to atherosclerosis. *Br J Exp Pathol* **70**, 737-757.

Hanada K, Sawamura D, Tamai K, Hashimoto I & Kobayashi S (1997). Photoprotective effect of esterified glutathione against ultraviolet B-induced sunburn cell formation in the hairless mice. *J Invest Dermatol* **108**, 727-730.

Hannigan GE, Leung-Hagasteijin C, Fitz-Gibbon L, Coppolino MG, Radeva G, Filmus J, Bell JC & Dedhar S (1996). Regulation of cell adhesion and anchorage-dependent cell growth by a new beta 1-integrin-linked protein kinase. *Nature* **379**, 91-96.

Hannigan GE, Troussard AA & Dedhar S (2005). Integrin-linked kinases: a cancer therapeutic target unique among its ILK. *Nat Rev Cancer* **5**, 51-63.

Harris CA & Johnson EM (2001). BH3-only Bcl-2 family members are coordinately regulated by the JNK pathway and require Bax to induce apoptosis in neurons. *J Biol Chem* **276**, 37754-37760.

Hattori Y, Nishigori C, Tanaka T, Uchida K, Nikaido O, Osawa T, Hiai H, Imamura S & Toyokuni S (1996). 8-Hydroxy-2'-deoxyguanosine is increased in epidermal cells of hairless mice after chronic ultraviolet B exposure. *J Invest Dermatol* **107**, 733-737.

Herceg Z & Wang Z-Q (2003). Functions of poly(ADP-ribose) polymerase (PARP) in DNA repair, genomic integrity and cell death. *Mutat Res* **447**, 97-110.

Hinz B (2010). The myofibroblast: paradigm for a mechanically active cell. *J Biomech* **43**, 146-155.

Ho E and Dagnino L (2011). Epidermal growth factor induction of front-rear polarity and migration in keratinocytes is mediated by integrin-linked kinase and ELMO2. *Mol Biol Cell* **23**, 492-502

Ho E, Irvine T, Vilk GJA, Lajoie G, Ravichandran KS, D'Souza JA & Dagnino L (2009). Integrin-linked kinase interactions with ELMO2 modulates cell polarity. *Mol Biol Cell* **20**, 3033-3043.

Huang C, Li J, Ding M, Leonard SS, Wang L, Castranova V, Vallyathan V & Shi X (2001). UV induces phosphorylation of protein kinase B (Akt) at Ser-473 and Thr-308 in mouse epidermal Cl 41 cells through hydrogen peroxide. *J Biol Chem* **275**, 40234-40240.

Hynes RO (2002). Integrins: Bidirectional, allosteric signaling machines. *Cell* **110**, 673-787.

Iglesias M, Frontelo P, Gamallo C & Quintanilla M (2000). Blockade of Smad4 in transformed keratinocytes containing a Ras oncogene leads to hyperactivation of the Ras-dependent Erk signalling pathway associated with progression to undifferentiated carcinomas. *Oncogene* **19**, 4134-4145.

Ilić D, Futura Y, Kanazawa S, Takeda N, Sobue K, Nakatsuji N, Nomura S, Fujimoto J, Okada M & Yamamoto T (1995). Reduced cell motility and enhanced focal adhesion contact formation in cells from FAK-deficient mice. *Nature* **377**, 539-544.

Inachi S, Mizutani H & Shimizu M (1997). Epidermal apoptotic cell death in Erythema Multiforme and Stevens-Johnson Syndrome. *Arch Dermatol* **133**, 845-849.

Indra AK & Leid M (2011). Epidermal permeability barrier measurement in mammalian skin. *Method Mol Biol* **763**, 73-81.

Ivanova IA, D'souza SJ & Dagnino L (2005). Signalling in the epidermis: the E2F cell cycle regulatory pathway in epidermal morphogenesis, regeneration and transformation. *Int J Biol Sci* **1**, 87-95.

Jensen JM & Proksch E (2009). The skin's barrier. *G Ital Dermatol Venereol* **144**, 689-700.

Katiyar SK, Afaq F, Azizuddin K & Muktar H (2001). Inhibition of UVB-induced oxidative stress-mediated phosphorylation of mitogen-activated protein kinase signaling

pathways in cultured human epidermal keratinocytes by green tea polyphenol(-)-epigallocatechin-3-gallate. *Toxicol Appl Pharm* **176**, 110-117.

Kim B-J, Ryu S-W & Song B-J (2006). JNK- and p38 kinase mediated phosphorylation of Bax leads to its activation and mitochondrial translocation and to apoptosis of human hepatoma HepG2 cells. *J Biol Chem* **281**, 21256-21265.

Kim YK, Bae GU, Kang JK, Park JW, Lee EK, Lee HY, Choi WS, Lee HW & Han J-W (2006). Cooperation of H<sub>2</sub>O<sub>2</sub>-mediated ERK activation with Smad pathway in TGF-beta1 induction of p21WAF1/CIP1. *Cell Signal* **18**, 236-243.

Kovacs K, Hanto K, Bogнар Z, Tapodi A, Bogнар E, Kiss GN, Szabo A, Rappai G, Kiss T, Sumegi B & Gallyas Jr. F (2009). Prevalent role of Akt and ERK activation in cardioprotective effect of Ca<sup>2+</sup> channel- and beta-adrenergic receptor blockers. *Mol Cell Biochem* **321**, 155-164.

Kreuz S, Siegmund D, Scheurich P & Wajant H (2001). NF-κB inducers upregulate cFLIP, a cycloheximide-sensitive inhibitor of death receptor signalling. *Mol Cell Biol* **21**, 3964-3973.

Kroemer G, Galluzzi L, Vandenabeele P, Abrams J, Alnemri ES, Baehrecke EH, Blagoskionny MV, El-Deiry WS, Golstein P, Green DR, Gengartner M, Knight RA, Kuman S, Lipton SA, Malomi W, Nuñez G, Peter ME, Tschopp J, Yuan J, PLacentini M, Zhivotovsky B & Melino G (2009). Classification of cell death: recommendations of the nomenclature committee on cell death 2009. *Cell Death Differ* **16**, 3-11.

Kulms D, Poppelmann B, Yarosh D, Luger TA, Krutmann J & Schwarz T (1999). Nuclear and cell membrane effects contribute independently to the induction of apoptosis in human cells exposed to UVB radiation. *Proc Natl Acad Sci USA* **96**, 7974-7979.

Kulms D & Schwarz T (2002). Independent contribution of three different pathways to ultraviolet-B-induced apoptosis. *Biochem Pharmacol* **64**, 837-841.

Kulms D, Zeise E, Poppelmann B & Schwarz T (2002). DNA damage, death receptor activation and reactive oxygen species contribute to ultraviolet radiation-induced apoptosis in an essential and independent way. *Oncogene* **21**, 5844-5851.

Kyriakis JM, Banerjee P, Nikolakaki E, Dai T, Rubie EA, Ahmad MF, Avruch J & Woodgett JR (1994). The stress-activated protein kinase subfamily of c-Jun kinases. *Nature* **369**, 156-160.

Lange A, Wickström SA, Jakobson M, Zent R, Saino K & Fässler R (2009). Integrin-linked kinase is an adaptor with essential functions during mouse development. *Nature* **461**, 1002-1006.

LeBlanc H, Lawrence D, Varfolomeev E, Totpal K, Morlan J, Schow P, Fong S, Schwall R, Sinicropi D & Ashkenazi A (2002). Tumor-cell resistance to death receptor-induced apoptosis through mutational inactivation of the proapoptotic Bcl-2 homolog Bax. *Nat Med* **8**, 274-281.

Legate KR, Montanez E, Kudlacek O & Fässler R (2006). ILK, PINCH and parvin: the tIPP of integrin signalling. *Nat Rev Mol Cell Biol* **7**, 20-31.

Lei K, Nimnual A, Zong W-X, Kennedy NJ, Flavell RA, Thompson CB, Bar-Sagi D & Davis RJ (2002). The Bax subfamily of Bcl2-related proteins is essential for apoptotic signal transduction by c-Jun NH(2)-terminal kinase. *Mol Cell Biol* **22**, 4929-4942.

Lorenz Z, Grashoff C, Torka R, Sakai T, Langbein L, Bloch W, Aumalley M & Fässler R (2007). Integrin-linked kinase is required for epidermal and hair follicle morphogenesis. *J Cell Biol* **177**, 501-513.

Lu A-L, Li X, Gu Y, Wright PM & Chang D-Y (2001). Repair of oxidative DNA damage. *Cell Biochem Biophys* **35**, 141-170.

Mackinnon AC, Qadota H, Norman KR, Moerman DG & Williams BD (2002). *C. elegans* Pat-4/ILK functions as an adaptor protein within integrin adhesion. *Curr Biol* **12**, 787-797.

MacNeal RJ (2006). Structure and function of the skin. [http://www.merckmanuals.com/home/skin\\_disorders/biology\\_of\\_the\\_skin/structure\\_and\\_function\\_of\\_the\\_skin.html](http://www.merckmanuals.com/home/skin_disorders/biology_of_the_skin/structure_and_function_of_the_skin.html).

Margadant C, Charafeddine RA & Sonnenberg A (2010). Unique and redundant functions of integrins in the epidermis. *FASEB J* **24**, 4133-4152.

Matés JM (2000). Effects of antioxidant enzymes in the molecular control of reactive oxygen species toxicology. *Toxicology* **153**, 83-104.

Maydan M, McDonald PC, Sanghera J, Yan J, Rallis C, Pinchin S, Hannigan GE, Foster LG, Ish-Horowicz D, Walsh MP & Dedhar S (2010). Integrin-linked kinase is functional  $Mn^{2+}$ -dependent protein kinase that regulates glycogen synthase kinase-3 $\beta$  (GSK-3 $\beta$ ) phosphorylation. *PLoS one* **5**, e12356.

McDonald PC, Oloumi A, Mills J, Dobreva I, Maidan M, Gray V, Wederell ED, Bally MB, Foster LJ & Dedhar S (2008). Rictor and integrin-linked kinase interact and regulate Akt phosphorylation and cancer cell survival. *Cancer Res* **68**, 1618-1624.

Méhul B, Corre C, Capon C, Bernard D & Schmidt R (2003). Carbohydrate expression and modification during keratinocyte differentiation in normal human and reconstructed epidermis. *Exp Dermatol* **12**, 537-545.

Meves A, Stremmel C, Gottschalk K & Fässler R (2009). The Kindlin protein family: new members to the club of focal adhesion proteins. *Trends Cell Biol* **19**, 504-513.

Mitchell DL, Jen J & Cleaver JK (1992). Sequence specificity of cyclobutane pyrimidine dimers in DAN treated with solar (ultraviolet B) radiation. *Nucleic Acids Res* **20**, 225-229.

Nagata Y & Todokoro (1999). Requirement of activation of JNK and p38 for environmental stress-induced erythroid differentiation and apoptosis and of inhibition of ERK for apoptosis. *Blood* **94**, 853-856.

Nakrieko, KA, Rudkouskaya A, Irvine TS, D'Souza SJA & Dagnino L (2011). Targeted inactivation of integrin-linked kinase in hair follicle stem cells reveals an important modulatory role in skin repair after injury. *Mol Biol Cell* **22**, 2532-2540.

Nakrieko KA, Welch I, Dupuis H, Bryce D, Pajak A, St Arnaud R, Dedhar S, D'Souza SJ & Dagnino L (2008a). Impaired hair follicle morphogenesis and polarized keratinocyte movement upon conditional inactivation of integrin-linked kinase in the epidermis. *Mol Biol Cell* **19**, 1462-1473.

Nicholson DW (2000). From bench to clinic with apoptosis-based therapeutic agents. *Nature* **407**, 810-816.

Omori E, Morioka S, Matsumoto K & Ninomiya-Tsuji J (2008). TAK1 regulates reactive oxygen species and cell death in keratinocytes, which is essential for skin integrity. *J Biol Chem* **283**, 26161-26168.

Paz ML, González Maglio DH, Weill FS, Bustamante J & Leoni J (2007). Mitochondrial dysfunction and cellular stress progression after ultraviolet B irradiation in human keratinocytes. *Photodermatol Photo* **24**, 115-122.

Pellettieri J & Sanchez AA (2007). Cell turnover and adult tissue homeostasis: from humans to planarians. *Annu Rev Genet* **41**, 83-105.

Pereira JA, Benninger Y, Baumann R, Goncalves AF, Ozcelik M, Thurnherr T, Tricaud N, Meijer D, Fässler, Suter U & Relvas JB (2009). Integrin-linked kinase is required for radial sorting of axons and Schwann cell remyelination in the peripheral nervous system. *J Cell Biol* **185**, 147-161.

Peter ME (2004). The flip side of FLIP. *Biochem J* **382**, e1-e3.

Phillipson RP, Tobi SE, Morris JA & McMillan TJ (2001). UV-A induces persistent genomic instability in human keratinocytes through an oxidative stress mechanism. *Free Radic Biol Med* **32**, 474-480.

Pierce GF, Yanagihara D, Klopchin K, Danilenko DM, Hsu E, Kenney WC & Morris CF

(1994). Stimulation of epithelial elements during skin regeneration by keratinocyte growth factor. *J Exp Med* **179**, 831-840.

Puthalakath H, O'Reilly LA, Gunn P, Lee L, Kelly PN, Huntington ND, Hughes PD, Michalak EM, McKimm-Breschkin J, Motoyama N, Gotoh T, Akira S, Bouillet P & Strasser A (2007). ER stress triggers apoptosis by activating BH3-only protein Bim. *Cell* **129**, 1337-1349.

Qin J & Wu C (2012). ILK: a pseudokinase in the center stage of cell-matrix & Adhesion and signaling. *Curr Opin Cell Biol* **24**, 607-613.

Raghavan S, Bauer C, Mundschan G, Li Q, Fuchs E (2000). Conditional ablation of beta1 integrin in skin. Severe defects in epidermal proliferation, basement membrane formation, and hair follicle invagination. *J Cell Biol* **150**, 1149-1160.

Raj, D, Brash, DE & Grossman D (2006). Keratinocyte apoptosis in epidermal development and disease. *J Invest Dermatol* **126**, 243-257.

Régnier M, Vaigot P, Darmon M & Pruniéras M (1986). Onset of epidermal differentiation in rapidly proliferating basal keratinocytes. *J Invest Dermatol* **87**, 472-476.

Rygiel TP, Mertens AE, Strumane K, van der Kammen R & Collard JG (2008). The Rac activator Tiam1 prevents keratinocyte apoptosis by controlling ROS-mediated ERK phosphorylation. *J Cell Sci* **21**, 1183-1192.

Sakai T, Li S, Docheva D, Grashoff C, Sakai K, Kostka G, Braun A, Pfeifer A, Yurchenco PD & Fässler R (2003). Integrin-linked kinase (ILK) is required for polarizing the epiblast, cell adhesion, and controlling actin accumulation. *Genes & Dev* **17**, 926-940.

Sayed-yahosseini S, Nini L, Irvine TS & Dagnino L (2012). Essential role of integrin-linked kinase in regulation of phagocytosis in keratinocytes. *FASEB J* **26**, 1-12.

Scatena R (2012). Mitochondria and cancer: a growing role in apoptosis, cancer cell metabolism, and dedifferentiation. *Adv Exp Med Biol* **942**, 287-308.

Schenk H, Klein M, Erdbrugger W, Droge W & Schulze-Osthoff K (1994). Distinct effects of thioredoxin and antioxidants on the activation of transcription factors NF-kappa B and AP-1. *Proc Natl Acad Sci USA* **91**, 1672-1676.

Schindelin J, Arganda-Carreras I, Frise E, Kaynig V, Longair M, Pietzsch T, Preibisch S, Rueden C, Saalfeld S, Schmid B, Tinevez JY, White DJ, Hartenstein V, Eliceiri K, Tomancak P & Cardona A (2012). Fiji: an open-source platform for biological-image analysis. *Nat Methods* **9**, 676-682.

Schreck R, Rieber P & Baeuerle PA (1991). Reactive oxygen intermediates as apparently widely used messengers in the activation of the NF-kappa B transcription factor and HIV-1. *EMBO J* **10**, 2247-2259.

Shi H, Hudson LG, Ding W, Wang S, Cooper KL, Liu S, Chen Y, Shi X & Liu KJ (2004). Arsenite causes DNA damage in keratinocytes via generation of hydroxyl radicals. *Chem Res Toxicol* **17**, 871-878.

Shiah SG, Chuang SE, Chau YP, Shen SC & Kuo ML (1999). Activation of the c-Jun NH<sub>2</sub>-terminal kinase and subsequent CPP32/Yama during topoisomerase inhibitor beta-lapachone-induced apoptosis through an oxidation-dependent pathway. *Cancer Res* **59**, 391-398.

Shimizu H, Banno Y, Sumi N, Naganawa T, Kitajima Y & Nozawa Y (1999). Activation of p38 mitogen-activated protein kinase and caspases in UVB-induced apoptosis of human keratinocyte HaCaT cells. *J Invest Dermatol* **112**, 769-774.

Siegenthaler D (2006). Structure, function and care of human skin. <http://www.myyogaonline.com/healthy-living/natural-beauty/structure-function-and-care-of-human-skin/p2>.

Simm A & Brömme H-J (2006). Reactive oxygen species (ROS) and aging: do we need them – can we measure them – should we block them? *Signal Transduction* **3**, 115-125.

Simon H-U, Jah-Yehia A & Levi-Schaffer F (2000). Role of reactive oxygen species (ROS) in apoptosis induction. *Apoptosis* **5**, 415-418.



Song G, Ouyang G & Bao S (2005). The activation of Akt/PKB signaling pathway and cell survival. *J Cell Mol Med* **9**, 59-71.

Stankiewicz AR, Lachapelle G, Foo CP, Radicioni Sm & Mosser DD (2005). Hsp70 inhibits heat-induced apoptosis upstream of mitochondria by preventing Bax translocation. *J Biol Chem* **280**, 38729-38739.

Sun S-Y (2010). N-acetylcysteine, reactive oxygen species and beyond. *Cancer Biol Ther* **9**, 109-110.

Sundaresan M, Yu ZX, Ferrans VJ, Irani K & Finkel T (1995). Requirement for generation of H<sub>2</sub>O<sub>2</sub> for platelet-derived growth factor signal transduction. *Science* **270**, 296-299.

Taddei ML, Parri M, Mello T, Catalano A, Levine AD, Raugei G, Ramponi G & Chiarugi P (2007). Integrin-mediated cell adhesion and spreading engage different sources of reactive oxygen species. *Antioxid Redox Sign* **9**, 469-481.

Takahashi H, Ishida-Yamamoto A & Iizuka H (2001). Ultraviolet B irradiation induces apoptosis of keratinocytes by direct activation of Fas antigen. *J Invest Dermatol Symp P* **6**, 64-68.

Tan B-J & Chiu GNC (2013). Role of oxidative stress, endoplasmic reticulum stress and ERK activation in triptolide-induced apoptosis. *Int J Oncol* **42**, 1605-1612.

Teo ZL, McQueen-Miscamble L, Turner K, Martinez G, Madakashira B, Dedhar S, Robinson ML & de Longh RU (2014). Integrin-linked kinase (ILK) is required for lens epithelial cell survival, proliferation and differentiation. *Exp Eye Res* **121**, 130-142.

Tournier C, Hess P, Yang DD, Xu J, Turner TK, Nimnual A, Bar-Sagi D, Jones SN, Flavell RA & Ravis RJ (2000). Requirement of JNK for stress-induced activation of the cytochrome c-mediated death pathway. *Science* **228**, 870-874.

Troussard AA, McDonald PC, Wederell ED, Mawji NM, Filipenko NR, Gelmon KA, Kucab JE, Dunn SE, Emerman JT, Bally MC & Dedhar S (2005). Preferential

dependence of breast cancer cells versus normal cells on integrin-linked kinase for protein kinase B/Akt activation and cell survival. *Cancer Res* **66**, 393-403.

Tu Y, Huang Y, Zhang Y, Hua Y & Wu C (2001). A new focal adhesion protein that interacts with integrin-linked kinase and regulates cell adhesion and spreading. *J Cell Biol* **153**, 585-598.

Vallyathan V & Shi X (1997). The role of oxygen free radicals in occupational and environmental lung diseases. *Environ Health Persp* **105**, 165-177.

Van der Flier A and Sonnenberg A (2001). Function and interaction of integrins. *Cell Tissue Res* **301**, 285-298.

Van Laethem A, Nys K, Kelst SV, Claerhout S, Ichijo H, Vandenheede JR, Garmyn M & Agostinis P (2006). Apoptosis signal regulating kinase-1 connects reactive oxygen species to p38 MAPK-induced mitochondrial apoptosis in UVB-irradiated human keratinocytes. *Free Radical Bio Med* **41**, 1361-1371.

Van Laethem A, Van Kelst S, Lippens S, Declercq W, Vandenabeele P, Janssens S, Vandenheede JR, Garmyn M & Agostinis P (2004). Activation of p38 MAPK is required for Bax translocation to mitochondria, cytochrome c release, and apoptosis induced by UVB irradiation in human keratinocytes. *FASEB J* **194**, 1946-1948.

Vi L, de Lasa C, DiGuglielmo GM & Dagnino L (2010). Integrin-linked kinase is required for TGF- $\beta$ 1 induction of dermal myofibroblast differentiation. *J Invest Dermatol* **131**, 586-593.

Vignais PV (2002). The superoxide-generating NADPH oxidase: structural aspects and activation mechanism. *Cell Mol Life Sci* **59**, 1428-1459.

Walczak H & Krammer PH (2000). The CD95 (APO-1/Fas) and the TRAIL (APO-2L) apoptosis systems. *Exp Cell Res* **256**, 58-66.

Walters KS & Roberts MS (2002). The structure and function of skin. *Drugs Pharm Sci* **119**, 1-40.

Wang H & Joseph JA (1999). Quantifying cellular oxidative stress by dichlorofluorescein assay using microplate reader. *Free Radic Biol Med* **27**, 612-616.

Watt FM (2002). Role of integrins in regulating epidermal adhesion, growth and differentiation. *EMBO J* **21**, 3919-3926.

Wei MC Zong WX, Cheng EHY, Lindsten T, Panoutsakopoulou V, Ross AJ, Roth KA, MacGregor GR, Thompson CB & Korsmeyer SJ (2001). Proapoptotic BAX and BAK: a requisite gateway to mitochondrial dysfunction and death. *Science* **292(5517)**, 727-30.

Wiseman H & Halliwell B (1996). Damage to DNA by reactive oxygen and nitrogen species: role in inflammatory disease and progression to cancer. *Biochem J* **313**, 17-29.

Wong CH, Iskandar KB, Yadav SK, Hirpara JL, Lot T & Pervaiz S (2010). Simultaneous induction of non-canonical autophagy and apoptosis in cancer cells by ROS-dependent ERK and JNK activation. *PloS one* **5**, e9996.

Wu C (1999). Integrin-linked kinase and PINCH: partners in regulation of cell-extracellular matrix interaction and signal transduction. *J Cell Sci* **112**, 4485-4489.

Xia Z, Dickens M, Raingeaud J, Davis RJ & Greenberg ME (1995). Opposing effects of ERK and JNK-p38 MAP kinases on apoptosis. *Science* **270**, 1326-1331.

Xu B, Guo X, Mathew S, Armesilla AL, Cassidy J, Darling JL & Wang W (2010). Triptolide simultaneously induces reactive oxygen species, inhibits NF- $\kappa$ B activity and sensitizes 5-fluorouracil in colorectal cancer cell lines. *Cancer Lett* **291**, 200-208.

Yamaji S, Suzuki A, Sugiyama Y, Koide Y, Yoshida M, Kanamori H, Mohri H, Ohno S & Ishigatsubo Y (2001). A novel integrin-linked kinase-binding protein, affixin is involved in the early stage of cell-substrate interaction. *J Cell Biol* **153**, 1251-1264.

Yeung YG & Stanley ER (2009). A solution for stripping antibodies from polyvinylidene fluoride immunoblots for multiple reprobing. *Anal Biochem* **389**, 89-91.

Yoshida A, Pommier Y & Ueda T (2006). Endonuclease activation and chromosomal DNA fragmentation during apoptosis in leukemia cell. *Int J Hematol* **84**, 31-37.

Yu C, Minemoto Y, Zhang J, Liu J, Tang F, Bui TN, Xiang J & Lin A (2004). JNK suppresses apoptosis via phosphorylation of the proapoptotic Bcl-2 protein BAD. *Mol Cell* **13**, 329-340.

Zeller KS, Riaz A, Sarve H, Li J, Tengholm A & Johansson S (2013). The role of mechanical force and ROS in integrin-dependent signals. *PloS one* **8**, 1-13.

Zervas CG, Gregory SL & Brown NH (2001). *Drosophila* integrin-linked kinase is required at sites of integrin adhesion to link the cytoskeleton to the plasma membrane. *J Cell Biol* **152**, 1007-1018.

Zhao H, Sapolsky RM & Steinberg GK (2006). Phosphoinositide-3-kinase/Akt survival signal pathways are implicated in neuronal survival after stroke. *Mol Neurobiol* **34**, 249-269.

Zou H, Yang R, Hao J, Wang J, Sun C, Fesik SW, Wu JC, Tomaselli KJ & Armstrong RC (2003). Regulation of the Apaf-1/Caspase-9 apoptosome by caspase-3 and XIAP. *J Biol Chem* **298**, 8091-8098.

Zuckerman V, Wolyniec K, Sionov RV, Haupt S & Haupt Y (2009). Tumor suppression by p53: the importance of apoptosis and cellular senescence. *J Pathol* **219**, 3-15.

## MICHELLE D. IM

### EDUCATION

---

**University of Western Ontario** | London, ON, Canada

*Master of Science* 2012-Current

- Candidate for Master of Science in Physiology and Pharmacology under supervisor Dr. Lina Dagnino
- Collaborative Graduate Program in Developmental Biology

*Bachelor of Science*

2008-2012

- Graduate of Bachelor of Science with Honours Specialization in Biology

### HONOURS, SCHOLARSHIPS AND AWARDS

---

**University of Western Ontario** | London, ON, Canada

2013-2014

*Physiology & Pharmacology Departmental Steward*

- Representative for teaching assistants in Physiology and Pharmacology department
- Address concerns and draw feedback from departmental teaching assistants to Public Service Alliance of Canada

**University of Western Ontario** | London, ON, Canada

2008-2009

*Western Scholarship of Excellence*

### EMPLOYMENT AND RESEARCH EXPERIENCE

---

**University of Western Ontario** | London, ON, Canada

2013-Current

*Teaching Assistant*

- Teaching assistant for Dr. Angela Nissen in course Pharmacology 2060B: Introductory Pharmacology and Therapeutics

**Mount Sinai Hospital – Centre for Fertility and Reproductive Health** | Toronto, ON, Canada

2012-2014

*Research Intern*

- Interned as research assistant for Dr. Ellen Greenblatt at Mount Sinai Hospital – Centre for Fertility and Reproductive Health, primarily focused on improving aspects of reproductive technologies in cases of infertility
- Manuscript submitted for publishing in February 2014

**Hannam Fertility Center** | Toronto, ON, Canada

2012-2013

*Data Management*

- Completed statistical analysis on clinic data as requested by Dr. Thomas Hannam and Dr. Carol Redmond

**Sunnybrook Hospital/First Steps Fertility** | Toronto, ON, Canada

2009

*Research employment with Dr. Sony Sierra*

- Assisted Dr. Sierra with personal research specifically focusing on the effects of Polycystic Ovarian Syndrome (PCOS) on recurrent miscarriages in pregnant women

## **PUBLICATIONS, PRESENTATIONS, AND ABSTRACTS**

### **Anti-Mullerian Hormone, using the Generation II assay, and prediction of response to ovarian hyper-stimulation**

*Manuscript for publishing submitted, February 2014*

**6<sup>th</sup> Annual Developmental Biology Research Day** | London, ON, Canada      May 2014

*Poster presentation*

- Abstract selected for poster presentation on *Integrin-linked kinase modulates stress-induced apoptosis in keratinocytes*

**7<sup>th</sup> Canadian Developmental Biology Conference** | Mont Tremblant, QB, Canada

*Poster presentation*

March 2014

- Abstract selected for poster presentation on *The role of integrin-linked kinase on cell survival of keratinocytes*

**Annual Department of Physiology and Pharmacology Research Day** | London, ON, Canada

November 2013

*Poster presentation*

- Abstract selected for poster presentation on *The role of integrin-linked kinase on cell survival of keratinocytes*

**The Canadian Fertility and Andrology Society 59<sup>th</sup> Annual Meeting** | Victoria, BC, Canada

September 2013

*Poster presentation*

- Abstract selected for poster presentation on *Anti-Mullerian Hormone (Generation II assay) in assessment of ovarian reserve and prediction of IVF outcomes*

**Oncology Research and Education Day** | London, ON, Canada

June 2013

*Poster presentation*

- Abstract selected for poster presentation on *The role of integrin-linked kinase on cell survival of keratinocytes*

**Developmental Biology Research Day** | London, ON, Canada

May 2013

*Poster presentation*

- Abstract selected for poster presentation on *The role of integrin-linked kinase on cell survival of keratinocytes*

**Mostly Mammals in Montreal** | Montreal, QB, Canada

March 2013

*Poster presentation*

- Abstract selected for poster presentation on *The role of integrin-linked kinase on cell survival of keratinocytes*